

Faculdade de Engenharia da Universidade do Porto



FEUP

**Biomechanical study of pelvic organ prolapse
and correction under application of
urogynecologic surgical meshes**

Gonçalo Henrique Lourenço Sá Rios

PROVISIONAL VERSION

Dissertation performed under the Integrated Master Degree in
Bioengineering
Biomedical Engineering Field

Coordinator: Prof. Dr. Renato Natal
Co-coordinator: Prof. Dr. Marco Parente

20th of September, 2013

© Gonçalo Rios, 2013

Abstract

The main goal of this dissertation was to, through the study and refinement of a previous pelvic floor three-dimensional model, perform a biomechanical analysis of normal conditions and pathologic scenarios using impaired endopelvic connective tissue (uterosacral ligament and pubocervical fascia) structures. Simultaneously, restoration of ligament-like and fascia-like structures was achieved by the placement of polypropylene-like surgical meshes (used in minimally invasive techniques) within rectovaginal and vesicovaginal space, respectively. The surgical reconstructive procedure followed carefully the scientific guidelines of new tension-free soft vaginal meshes manufactured by Gynecare, Prolift® technique, for anterior and posterior isolated repair with uterine preservation. Three distinct synthetic propylene meshes, (Ultrapro - lightweight, ProLite - midweight and Trelex - heavyweight) with evident non-linear hyperelastic behavior were applied and compared during the experiments.

Moreover, the three-dimensional mathematical model of the pelvic organs, as well as uterine/vaginal wall repair, firstly settled in a computer-aided design program (*Rhinoceros* software), was feasibly acquired by application of finite element model. Besides, all material properties, associations (ties and contact pairs) between structures and intrapelvic load sets were employed by *ABAQUS*, considered nowadays a very precise and powerful tool for the resolution of complex biomechanical engineering problems. *FEMAP*, another essential tool, used in mechanical finite elements, was also assessed in this work after mesh acquisition, for the initial placement and positioning of each new structure within the previous pelvic floor model.

The model was able to predict clinical scenarios for uterine/vaginal pelvic wall injury through a wide range of specific intrabdominal pressures (from 0,00024 to 0,00529 MPa) when stiff properties of the ligaments and fascia were lowered progressively, 75%, 50%, 25%, until absence of the supportive tissue. On the other hand, clinical and surgical mesh repair was rigorously compared, in order to evaluate the displacement behavior of the anterior and posterior uterine/vaginal wall. In the simulated surgical procedures, incremented pressures had lower magnitudes than intrabdominal pressures (ranging from 0,00005 to 0,00024 MPa).

Given the fact that this was a pioneer study, no validation model was used due to lack of information of such a specific procedure. Data was only compared between injured tissues and vaginal/uterine reconstructive surgery. Therefore an exhaustive study based on numerical analyses of the structures was carried, defining the uterine cervix (supported

mainly by uterosacral ligaments), and the cervical ring (created by healthy pubocervical fascia) as meaningful sections to perform final mechanical analysis.

Concerning the study using vassalva pressure applied on the posterior surface of the uterus, it was found that the magnitude of displacements of the uterus fundus (in XX axis), and anterior and posterior vaginal/uterine wall (in YY axis) for non-weakened pelvic tissue was approximately: 25 mm, 4,30 mm and -1,70 mm. For uterosacral ligaments with 50% of the initial stiffness the same sequence of displacements was: 29 mm, 4,7 mm and -3,20 mm. For pubocervical ligaments with 50% if the initial stiffness: 28 mm, 4,7 mm and - 7,47 mm. On the other hand, about cervical ring nodal displacement, absence of pubocervical fascia lead to an increase of 0,6737 mm, in XX axis, comparing to healthy fascia.

Applied pressures (lower than vassalva pressures) in the absence of uterosacral ligaments support, the magnitude of displacements of the anterior/posterior vaginal wall, in the XX axis, ranged between 0,765 - 1,75 mm. After vaginal reinforcement, with Prolift Posterior, this range was lowered to 0,34 - 1,41 mm. Concerning, uterine cervix there were no evidences of pronounced displacements before and after Prolift Posterior placement, even if it was used three different propylene materials. In the absence of pubocervical fascia the displacements of the anterior and posterior vaginal wall, in the XX axis, ranged between 0,180 - 0,415 mm and after Prolift Anterior placement this range was lowered to 0,096 mm. Regarding YY axis, this range was initially 0,077 - 0,158 mm and after anterior vaginal wall reinforcement with Prolift Posterior the range was 0,098 - 0,179 mm.

Among the three polypropylene meshes, ProLite™ presented the best results, lowering the displacement of the cervical ring, in the XX and YY axis, in magnitudes of 0,0220 mm and 0,0302 mm, respectively. Trelex also presented a great supportive behaviour, although magnitude of displacements was half of the presented by ProLite™.

Therefore, results obtained in the study were relevant to understand pathophysiological conditions of vaginal and uterine suspension. Besides, this optimized approach in biomechanical modeling enabled a better understanding of computer-based simulation applications. It was proved that, nowadays minimally invasive surgical techniques, which employ urogynecologic meshes, within recto or vesicovaginal space, present interesting support and suspension of genital organs under specific pelvic floor clinical scenarios.

Acknowledgements

I would like to express my sincere gratitude to Prof. Renato Natal for accepted me and letting me participate in this incredible master thesis.

I would also like to thank to Prof. Marco Parente for all the guidance, suggestions and knowledge passed during the working time.

It was a great pleasure to develop such a multidisciplinary research work and contribute to optimize new approaches in biomechanical modeling.

I dedicate this master thesis to my parents, Paula and Joaquim Rios, who have always given me the strength and wisdom to work hard during these last years. Besides, without their education and financial support it would be impossible to finish my college and graduation in Faculdade de Engenharia da Universidade do Porto.

I also want to express my gratitude for my girlfriend for all the patient, dedication and love given during these last months. You were crucial during the research work and master thesis writing. Without your help this was not possible. I am a really lucky guy.

Moreover, I am very grateful to my friends, mainly to those who studied and worked with me side to side these last months.

Additionally, I am also thankful to MEDSIMLAB for letting me finish all the academic duties before starting the internship in Coimbra.

“ O homem que tem presunção de si próprio só sente a verdadeira alegria ao vencer as grandes dificuldades. As pequenas dificuldades não pesam na vida dos homens e não podem dar-lhes a consciência, a alegria plena do cumprimento do dever” - António Oliveira Salazar

Index

Chapter 1	1
Introduction.....	1
Chapter 2	5
Female Pelvic Anatomy	5
2.1 Pelvic Bone	6
2.2 Pelvic Cavity.....	9
2.2.1 Pelvic Wall	9
2.2.1.1 Ligaments of the pelvic wall	10
2.2.1.2 Muscles of the pelvic wall	11
2.2.2 Pelvic Floor	12
2.2.2.1 Muscles of pelvic floor	12
2.2.2.2 Connective tissue of pelvic floor	15
2.2.3 Pelvic Organs	17
Chapter 3	20
Female Pelvic Floor Disorders	20
3.1 Pelvic Organ Prolapse.....	20
3.1.1 POP classifications: nomenclature and anatomical deformity stages	20
3.1.2 POP pathophysiological conditions	23
3.1.3 POP etiology.....	24
3.1.4 UI and FI.....	26
3.1.5 Epidemiology - POP, UI and FI.....	28
3.1.6 Diagnostic of pelvic dysfunctions	29
Chapter 4	20
Female Pelvic Floor Disorders	20
Chapter 5	54
Biomechanics of Pelvic Floor and Surgical Meshes	54
5.1 Pelvic Floor Mechanical Structures	54
5.2 Morphological and Biomechanical Properties of Pelvic Tissues	56
5.3 Mechanical Properties of Urogynecologic Surgical Meshes	60
5.4 Three-Dimensional Modeling of the Pevic Floor.....	63
5.4.1 Finite Element Model	63
5.4.2 ABAQUS	64
5.4.3 Three-Dimensional Numerical Models of the Pelvic Floor	64
Chapter 6	68

Biomechanical Simulation of Pelvic Floor Impairment and Repair	68
6.1 Construction of 3D pelvic structures	68
6.1.1 Pelvic Organs	69
6.1.2 Sacrospinous Ligament	70
6.1.3 Urogynecologic Surgical Meshes.....	71
6.2 Construction of Finite Element Model	73
6.2.1 Pelvic Organs and Sacrospinous Ligament.....	74
6.2.2 Urogynecologic Surgical Meshes.....	74
6.3 Simulation of the 3D FEM	75
6.3.1 Materials Mechanical Properties	76
6.3.2 Boundary Conditions	78
6.3.3 Constraints.....	79
6.3.4 Contact Pairs	80
6.3.5 Loads Set	80
6.4 Results and Discussion	81
6.4.1 Analyses of vaginal and uterine wall displacements during normal and clinical conditions.....	81
6.4.2 Analyses of vaginal and uterine wall displacements during clinical conditions after urogynecologic surgical mesh placement	86
Chapter 7.....	91
Conclusion and Future Perspectives	91
7.1 Conclusion	91
7.2 Future Perspectives	92

List of Figures

Figure 1 - Anterior view of female pelvic bone (left) and male pelvic bone (right) (Adapted from [73])	5
Figure 2 - Anterior view of the female pelvic bone with main components properly identified [72]	6
Figure 3 - Medial projection of the right innominate pelvic bone [72]	8
Figure 4 - Lateral projection of the right innominate pelvic bone [72]	8
Figure 5 - Functional representation of sacrospinous and sacrotuberous ligaments [61]	9
Figure 6 - Medial projection of the right side of the bony pelvis comprehending the pelvic wall ligaments [61]	10
Figure 7 - Medial projection of the right side of bony pelvis comprehending the obturator internus and piriformis muscles [61]	11
Figure 8 - Medial projection of the right side of the pelvic diaphragm and coccygeous muscles [61]	13
Figure 9 - Illustration of the muscles of the deep perineal space with perineal membrane in the horizontal plane in the standing position [61]	14
Figure 10 - Detailed representation of fascial and ligament-like structure of the pelvic floor. In addition, three integrated levels of uterus/vagina support are presented for female standing position [65]	15
Figure 11 - 3D sagittal representation of connective tissue support levels concerning the pelvic organs and their relation with bony pelvis [78]	16
Figure 12 - Representation of the pelvic organs (bladder, uterus and rectum) and pelvic floor in a sagittal view [79]	18
Figure 13 - Sagittal representation of POP involving different injured sites and respective pelvic viscera falling into the vagina (Adapted from [85])	21
Figure 14 - Coronal plane of POP map with main elements of pelvic support (on the left) and representation of Baden-Walker half way system with four grades of prolapse (Adapted from [82])	22

Figure 15 - Points and landmarks for POP-Q system examination. Aa - point A anterior; Ap - point A posterior; Ba - point B anterior; Bp - point B posterior; C - cervix or vaginal cuff; D - posterior fornix; gh - genital hiatus; pb - perineal body and tvl - total vaginal length [82] ... 22

Figure 16 - Graphic of a study revealing percent of women with POP or UI care-seeking in each age group. Mature women reveal higher percentage of care-seeking comparing younger aged groups [96] 25

Figure 17 - The images present assessment of stress incontinence and cystometrogram through video study. On the left is shown a videourodynamics frame of a female patient with stress incontinence: mobility of the urethra and bladder base, presence of leakage and the cystometrogram is flat, indicating detrusor pressure component. On the right image is shown a videourodynamics frame in an elderly woman with stress and motor urge incontinence symptoms. There is lateral detachment-type small cystocele and gross leakage with stress is seen (Adapted from [103]) 30

Figure 18 - MRI with high resolution coronal T2 weight image in female without defective tissue (left) and MRI with high resolution axial T2 weight image in female patient with recurrent prolapse (right). In the normal female, the ICM (black arrows), PRM (white arrows) and EAS (arrow heads) are anatomically well positioned within the surrounding pelvic fat. In the clinical case the right pubovisceralis muscle has been completely avulsed (arrow head), with no remaining muscle in its usual position (white heads) and the opposite side shows an intact muscle (black arrow) [114] 31

Figure 19 - Sagittal FISP images through the midline of the pelvis in a female patient during MRI proctography. On the left image is shown a large rectocele (black arrows). On the right image is demonstrated a loop of a small bowel has descended anterior to the rectum to form a large enterocele (black arrows). Additionally, is noted a presence of cystocele (white arrows) and small collapsed rectocele (arrow head) 31

Figure 20 - Sagittal T2-weighted MR images of the pelvis obtained with the patient at rest (left) and straining (right). It is possible to observe prolapse of the vaginal vault during straining movement (solid black arrow). Given this, cul-de-sac (open black arrow) also descends. As well, bladder descent occurs with straining [110] 32

Figure 21 - Sagittal T2-weighted MR image (left and center) and coronal MRI (right) of urethral hypermobility with funnelling in a female patient with SUI and stress urinary frequency. Left MR image shows the urethra in its normal vertical orientation (solid arrow). The bladder (open arrow), cervix (*) and rectum are also seen. Central MR image obtained with the patient straining presents urethra approximately horizontal in orientation and lying inferior to the pubis. There is presence of SUI with the proximal part of the urethra (arrow) being inferior to the distal portion (double arrows). The entire urethra appears shortened due to funnelling or dilation of the proximal urethra and the presence of urine in the lumen. On the coronal MR image obtained with the patient straining, the urethra (arrow) is seen en face below the pubic symphysis because it is now horizontal in orientation. The striated outer muscle layer in the wall of the urethra is seen as a circular hypointense band [110] .. 33

Figure 22 - Demonstration of transducer placement in translabial/perineal US (left) and respective schematic representation of imaging in midsagittal plane [115] 33

Figure 23 - Standard acquisition screen of 3D pelvic floor ultrasound. A - Midsagittal, B - coronal, and C - axial planes and D, rendered axial plane of female pelvic floor. Region of interest is represented in the transparent box [115] (A, anal canal; P, puborectalis; R, rectal ampulla; S, symphysis pubis; U, urethra; V, vagina) 34

Figure 24 - 3D US images of female patient after TVT division due to de novo urgency, urge incontinence, and chronic mild obstruction. A - Midsagittal plane with arrow indicating most likely tape location. B and C - Coronal and axial views, respectively, with 2 free tape ends (arrows). The gap between 2 tape ends is also evident in D - axial plane rendered volume [115] (A, anal canal; B, bladder; R, rectal ampulla; S, symphysis pubis; U, urethra) 34

- Figure 25** - Types of support (first line) and space occupying pessaries (second line) [4] 37
- Figure 26** - Sagittal representation of abdominal sacrocolpopexy. Polypropylene mesh is placed over the anterior and posterior vaginal walls and then sutured to the anterior sacrum [12] 38
- Figure 27** - Sagittal representation of transvaginal uterosacral ligament suspension. The uterosacral ligaments are re-attached to the vaginal vault using specific sutures [12] 39
- Figure 28** - Medial view of right pelvis regarding sacrospinous fixation (left) and iliococcygeus suspension (right). In the sacrospinous surgical procedure vaginal vault is suspended by both sacrospinous ligaments with stiches. The right suspension is coloured and left suspension appears transparent. In the iliococcygeus procedure vaginal vault is fixated by stiches to both sides of iliococcygeus muscle [74] 39
- Figure 29** - Table with percentage of female undergoing POP surgical interventions in Germany, France and England. The respective costs in each country are considering for public and private hospitalization [1] 42
- Figure 30** - Schematic representation of Prolene sling with TVT for midurethra support. Sling is placed posteriorly in the midurethra (left) and both arms pass endopelvic fascia and rectus sheath (right). Arms are then pulled emerging through the obturator membrane (top) [153] 50
- Figure 31** - Representation of tension-free vaginal mesh supports of different brands (Gynecare, AMS and Bard). It is presented from an anterosuperior view meshes precise placement within respective pelvic anatomic sites and corresponding to each repair method. In the first line are displayed the anterior support systems and in the second line there are displayed the posterior support systems [156] 51
- Figure 32** - Table presenting main characteristics of each tension-free vaginal repair system [22] 51
- Figure 33** - On the top image there is represented the Prolift™ System with all treatment options (anterior, posterior and total) and surgical objects (insertion guide, cannula and retrieval device) [29]. On the bottom image there is represented the concept of the tension-free vaginal mesh procedure of the Prolift™ System. Mesh is placed to support and reinforce both the vaginal wall and vaginal canal. In the anterior procedure (TVM-A), four arms are passed through the obturator foramen to the arcus tendineus fascia pelvis to restore fascial and lateral support of the vagina. In the posterior procedure (TVM-P), two arms are passed to the sacrospinous ligament to reinforce uterosacral and cardinal ligament complex [155] 52
- Figure 34** - Schematic representation of urethral (top and bottom-left) and anorectal (bottom-right) opening and closing mechanisms. It is displayed three different urethral configurations: closed during tissue relaxation (top-left); closed during strength efforts (top-right); and opening during urine expel (bottom-left). (Bv - bladder-vagina fixation, LMA - transverse muscle, LP - levator ani muscle, PCM - pubococctgeus muscle, PUL - pubourethral ligament, and USL - uterosacral ligaments) [78] 55
- Figure 35** - Representation of 72-year-old cadaveric female pelvic diaphragm with respective landmarks (right image) and 3D geometrical computer-based anatomy (left image) of the pelvic floor muscles based on the experimental data set measurements from the 3D palpator device (designed for these type of measurements) [37] 57
- Figure 36** - Biomechanical properties of pelvic ligaments studied by Rivaux et al. Mechanical response of uterosacral, round and broad ligaments to tension loading. Representative stress-deformation curves show the non-linear and hyperelastic behaviour of the tissues [53] 58

- Figure 37** - Experimental data acquired in [59]. Biomechanical testing stress-deformation curves of 8 specimens of vaginal prolapsed tissue. Bold line represents the average data ... 59
- Figure 38** - Experimental data acquired in [52]. Biomechanical stress-deformation behaviour of vaginal, rectal and bladder tissues. Vaginal tissue is clearly the most rigid tissue followed by rectum and bladder 59
- Figure 39** - Experimental data acquired in [19]. Representation of typical load-deformation curves for eight tested non-absorbable mesh-like materials (white dotted lines indicate the displacement at which failure occurred 60
- Figure 40** - Representation of the load-displacement curve postulated in [172]. The curve shows the definitions of stiffness quantities E_I and E_{II} 61
- Figure 41** - UltraproTM (lightweight type I macroporous) mesh in longitudinal (left) and transverse (right) orientations [176] 62
- Figure 42** - On the left, is exposed the 3D geometrical experimental data set from MRI measurements, with representations of pelvic bone in images (A) and (B) and muscle levator ani in images (C) and (D). On the right, is exposed the 3D geometrical model of pelvic floor muscles based on the experimental data set from the palpator measurements: on the left are the points measured during palpator approach and on the right is presented the final rendered surface muscular floor [37] 65
- Figure 43** - From left to right: The first presents mesh FEM generation and the last is a representation of pelvic bone fused with pelvic floor mesh [42] 66
- Figure 44** - Final fitted meshes from Visible Woman data set [43] 66
- Figure 45** - Generated realistic geometry of a 20-year-old female subject's pelvis. The model consists of 35 anatomical parts including 10 pelvic muscles, 10 pelvic ligaments, 6 pelvic bone, skin, fat tissues, bladder, urethra, uterus, vagina and colon, rectum and anus. The ambulatory model was used on the participants to characterize their specific landing impact parameters [46] 67
- Figure 46** - Final 3D FEM developed in [69] containing the pelvic organs (bladder, uterus and rectum), levator ani main musculature, key pelvic support ligaments (uterosacral, pubourethral, arctus tendineus and posterolateral retal), pubocervical fascia and pubic bone 69
- Figure 47** - Representation of uterus (top), bladder (center) and rectum (bottom) obtained in Rhino. B-splines and surfaces network used in the design process are shown 70
- Figure 48** - Sacrospinous ligaments obtained in *Rhino* with designed B-splines and respective network surfaces 71
- Figure 49** - Four perspectives of the final job of the posterior surgical mesh design. The mesh arms were carefully aimed to reproduce their real design. The top segment has an approximate shape and width for suitable attachment to the posterior face of the uterine isthmus (about 2cm above the cervix) 73
- Figure 50** - Four perspectives of the design complexity of the 2 bilateral arms and top segment of the anterior surgical mesh. It is possible to observe that the top surface presents a suitable size and shape for suitable attachment of the anterior face of the uterine isthmus (about 2 cm above the cervix) 73
- Figure 51** - Final 3D FEM of the pelvic floor containing the new organs and sacrospinous ligaments. It is possible to observe new smoothed organs with precise elements definition (top) and placement of the meshes within vesicovaginal and rectovaginal space (bottom)... 75

Figure 52 - Representation of the stress-strain curves of uniaxial experimental data obtained for Trelex® and respective representation of three constitutive models.	77
Figure 53 - Representation of the stress-strain curves of uniaxial experimental data obtained for ProLite™ and respective representation of three constitutive models.	77
Figure 54 - Representation of the stress-strain curves of uniaxial experimental data obtained for Ultrapro™ and respective representation of three constitutive models.	78
Figure 55 - Schematic representation of static non-pathologic pelvic structure (top) and nodal displacements in the XX (bottom left) and YY (bottom right) axis after valsalva pressures.	82
Figure 56 - Schematic representation of pathologic pelvic structure 50% USL. There are presented nodal displacements in the XX (bottom left) and YY (bottom right) axis after valsalva pressures.	83
Figure 57 - Schematic representation of pathologic pelvic structure 50% PCF. There are presented nodal displacements in the XX (bottom left) and YY (bottom right) axis after valsalva pressures.	83
Figure 58 - Schematic representation of pathologic pelvic structure 0% PCF. There are presented nodal displacements in the XX (bottom left) and YY (bottom right) axis after valsalva pressures.	84
Figure 59 - Graphical representation of the cervical ring displacement (U, U _x , and U _y , respectively) regarding the stiffness variation (0% PCF to 100% PCF).	85
Figure 60 - Graphical representation of the cervix uterine displacement (U, U _x , and U _y , respectively) regarding the stiffness variation (0% USL to 100% USL).	86
Figure 61 - Schematic representation of nodal displacement, in XX (left) and YY (right) axis, for pathological 0% USL condition (top) and Prolift-like posterior support (bottom), under pressures of 0,00024 MPa. Ultrapro was the surgical mesh's material used in this simulation	87
Figure 62 - Graphical representation of the uterine cervix displacement (U, U _x , and U _y , respectively) for 0% USL with and without different polypropylene-like meshes reinforcement.	88
Figure 63 - Schematic representation of nodal displacement, in XX (left) and YY (right) axis, for pathological 0% USL condition (top) and Prolift-like anterior support (bottom), under pressures of 0,00024 MPa. Ultrapro was the surgical mesh's material used in this simulation.	89
Figure 64 - Graphical representation of the cervical ring displacement (U, U _x , and U _y , respectively) for 0% PCF with and without different polypropylene-like meshes reinforcement.	90

List of Tables

Table 1 - Traditional anatomical site of prolapse classification [82]	21
Table 2 - Stages of POP-Q system measurement [82]	23
Table 3 - Case study of prevalence of selected pelvic floor disorders by birth group (nulliparous, caesarean delivery or vaginally parous) [91]	25
Table 4 - Types of synthetic mesh used in urogynecology for POP and stress incontinence treatment (including description of mesh properties and main benefits, accordingly to information provided by the different brands)	45
Table 5 - Categories of biologic graft materials used in urogynecology for POP and SUI treatment (including composition, device and respective brand)	48
Table 6 - Main characteristics of meshed pelvic surfaces based on extrusion (single or double).....	74
Table 7 - Main characteristics of triangular shell and membrane meshed surfaces of urogynecologic surgical meshes	75
Table 8 - Constraints considering master and slave surfaces and correspondent type of ties defined in the simulation.....	77
Table 9 - Contact pairs surfaces defined between pelvic floor, bony tissue and refined pelvic organs	78
Table 10 - Intraabdominal pressure values for each type of maneuver. Magnitude of four pressures submitted in the first study [67]	79
Table 11 - Magnitude of four pressures submitted in the second study	79

Abbreviations

AMS	American Medical Systems
ATFP	Arcus Tendineus Fascia Pelvis
ATLA	Arcus Tendineus Levator Ani
ASC	Abdominal Sacrocolpexy
AUS	American Urogynecologic Society
CAD	Computer-Aided Design
CL	Cardinal Ligament
EAS	External Anus Sphincter
FDA	Food and Drug Administration
FI	Fecal Incontinence
FISP	Fast Imaging with Steady Precession
HDMI	Dicyclohexylmethane-4, 4-Diisocyanate
ICM	Iliococcygeus Muscle
ICS	International Continence Society
ISD	Intrinsic sphincter deficiency
LA	Levator Ani
MMP	Matrix Metalloproteinase
MRI	Magnetic Resonance Image
PCM	Pubococcygeus Muscle
PFD	Pelvic Floor Dysfunction
POP	Pelvic Organ Prolapse
POP-Q	Pelvic Organ Prolapse Quantification system
PVL	Pubovesical Ligament
PRM	Puborectalis Muscle
PUL	Pubourethral Ligament
PP	Polypropylene
SGS	Society of Gynecologic Surgeons
SPL	Sacrospinous Ligament
SPLS	Sacrospinous Ligament Suspension
STL	Sacrotuberous Ligament

SUI	Stress Urinary Incontinence
TFT	Tension Free Technique
TVM	Tension-Free Vaginal Mesh
TVT	Transobturator Vaginal Tape
UI	Urinary Incontinence
UIS	Uterine Isthmus
US	Ultrasonography
USL	Uterosacral/Cardinal Ligament
USM	Urogynecologic Surgical Mesh

Chapter 1

Introduction

Pelvic floor dysfunction (PFD) is a common disorder affecting about 30-40% of parous women [1]. This dysfunction has severe physiological, social and financial impact, interfering directly in women's quality of life [2]. In the complex range of pelvic floor disorders are included the following pathologies: urinary incontinence (UI), fecal incontinence (FI) and pelvic organ prolapse (POP). Pelvic floor disorders usually demand for a multidisciplinary care and derive from a wide age range of women (30-90-years-old). Although mature age groups (≥ 60) are more likely to seek care. These findings are also related with the increase of average life expectancy, being predicted that, in 2030, is expected that 1 billion women worldwide can present dysfunction regarding the pelvic floor [3].

Prolapse (from the Latin *prolapsus*) refers to the falling or sliding out of place of a part or viscus. Given this, genital prolapse is known, by the specialist medical practitioners, as the falling of intrapelvic organs (into the vagina): vaginal wall, uterus, bladder, urethra and rectum. Hence, there is a loss of support of coupled organs, by interaction of weakened pelvic bones, endopelvic connective tissue and pelvic floor musculature. Although prolapse can occur in different compartments (anterior, mid and posterior) the pelvic floor should be evaluated as a singular unit [4].

POP is often an asymptomatic disorder. Usually, bulging is the main symptom that correlates with prolapse severity but other symptoms are manifested as vaginal bleeding, abdominal pain or discomfort, obstructive constipation, heaviness of genitalia and urinary stress [5]. A wide range of POP's risk factors can be assumed, from aging to menopause, pregnancy, childbirth, obesity, smoking, genetic factor, collagen abnormalities, prior surgery, and chronic constipation [6]. Nowadays conservative treatment of genital prolapse consists mainly on pelvic muscle exercises [7], hormone administration [8] and the use of pessaries [9]. Although these approaches can limit the progression of low-grade genital prolapse, surgery remains the most appropriate approach for high-grade prolapse [10]. The lifetime risk of undergoing an operation for prolapse or incontinence is 11% but this probably grossly underestimates the true figure. Reoperation is required in 29% of cases, although the time interval reduces between each successive operation [11].

Abdominal sacrocolpopexy (ASC) remains the "gold standard" surgical technique with high patient satisfaction and cure rate higher than 90%. However, open approach is associated with longer operation time and hospital stay with clear potential for postoperative complications. Additionally, this time-consuming procedure and slow patient recovery is associated to high clinical costs [10, 12 -13].

Nowadays, the use of urogynecological meshes in pelvic floor surgery has become increasingly popular. Over the last decades, engineers and surgeons have been developing and employing meshes, respectively, in abdominal defects (hernia surgeries) which started to be adapted and designed for gynecologic procedures [14 - 15]. These graft materials have been applied to avoid an additional fascial-harvesting procedure or to use materials that are stronger than the patient's own fascial tissue [15].

Regarding the loss of supporting and mechanical functions in the anterior and posterior compartments, the use of a graft material (sling and mesh) appears to be effective in the improvement of anatomical outcomes and longevity of repairs [16]. While there are clear differences between naturally occurring and synthetic graft materials, the most widely used are synthetic macroporous polypropylene (PP) meshes. This type of non-absorbable implants provides strong knitting, replacement of defective ligament and fascias, inert reaction (minimal inflammatory response), new connective tissue ingrowth and well-defined low stiffness followed by great tensile strength. However, these prosthetic-reinforced repairs are associated with particular postoperative complications like mesh extrusion, symptomatic retraction and/or persistent pain [17 - 21].

Given the need to minimize morbidity, invasiveness and recovery time of abdominal sacrocolpopexy and laparoscopic techniques, novel transvaginal meshes have been developed to vaginally place PP graft material [18, 22 - 27]. Tension-Free Vaginal Mesh (TVM) is a minimally invasive surgical technique which addresses midline, paravaginal, and apical defects through specific mesh kits such as Gynacare Prolift® system (Ethicon, Sommerville, NJ), Tension-Free Tape Obturator System (TVT) (Ethicon, Sommerville, NJ) or Perigee/Apogee® (American Medical Systems Inc., Minnetonka, MN) [22, 29-30]. In these procedures mesh or sling arms are delivered, in paravesical or pararectal spaces, through the obturator membrane and/or ischiorectal fossa, via trochars. Positioning of the mesh is performed tension-free passing the mesh in the respective anatomic attachment points (muscles or connective tissue) to reinforce the suspensor ligaments and/or pubocervical and/or the rectovaginal fascia [22, 30]. The safety and effectiveness of the vaginal kit approaches is carefully evaluated by Food and Drug Administration (FDA) [31].

Clinical studies reveal high anatomical success rates, ranging from 80% to 100% (short-term follow-up), for the treatment of POP (stages \geq II) with TVM kit techniques. Although the quality of life is meaningfully improved, without bulge symptoms, surgical intervention and long-term complications are quite significant (approximately 15% mesh erosion and prolapse recurrence) with subsequent reoperation [22, 32-35].

Furthermore, pathogenesis of POP and requirements for a successful surgical outcome vary from one person to another. To carry out an augmented repair, surgical objectives, movement dynamics and functional anatomy must be taken into account at the implantation site. Thus, anatomical three-dimensional (3D) modeling and simulation of the pelvic cavity can be a major approach for specific evaluation of pathologic and biomechanical deficiency, in a realistic way, of pelvic floor soft tissues.

The Finite Element Method (FEM) is a well-known numerical technique for solving mechanical engineering linear and non-linear complex problems that can be applied to assess 3D anatomical models and perform biomechanical experiments. This experimental tool allows the approximation of several geometric models into precise 3D and two-dimensional (2D) sub-regions called elements, approximating solutions for the whole domain by enforcing certain relations among the solutions of all elements. Nowadays, FEM is applied on high-speed

computation. There are numerous commercially available FEM programs, like *ABAQUS*, *NASTRAN* and *DYNA3D* [36].

Recently, anatomically realistic female pelvic floor finite element models have been developed based on live subject magnetic resonance image (MRI) and computer-based reconstruction using female cadaveric bodies. Regarding the importance of space, position and anatomical ratios between the pelvic organs, geometrical rebuilding is usually performed by Computer-Aided Design (CAD) models (SolidWorks, NURBS, Rhino, etc) [37-49]. Posterior generation of FEM implements 3D solid or 2D shell elements, taking into account ligaments, pelvic floor muscles and organs (vagina, bladder and rectum) as deformable bodies with best real-like geometrical parameters, precise anatomical associations, reliable supportive functions and distinct mechanical properties (hyperelastic) [50-66]. On the other hand, 3D computer-based programs allow the modeling of pelvic floor structures, as well as simulation of pathogenic scenarios in a non-invasive way with low cost-effectiveness. Thereby, to study the complex biomechanical behavior of pelvic floor structures and to investigate the effectiveness of reconstructive surgery, is compulsory to simulate realistic conditions (i.e: valssalva maneuver, coughing, continence mechanism, etc) [67].

Accordingly, a previous representative 3D model of pelvic cavity, with computer-generated organs and pelvic floor structures, was accessed and optimized in this research work [68, 69]. The main goal of this experimental work was the refinement of meshed pelvic floor organs followed the by simulation of clinical fault scenarios of pelvic floor tissue during intra-abdominal daily loads (valssalva, rest, sit and stand). At the same time, customized Prolift surgical mesh commonly employed in TVM techniques for POP treatment, were designed using CAD software (*Rhino*) and meshed in computer-based programs (*ABAQUS CAE* and *FEMAP*) to reinforce defective genital supportive connective tissue (uterosacral and cardinal ligaments, and pubocervical fascia). Therefore, biomechanical characterization was carried by *ABAQUS* applying specific loads to pelvic organs of healthy and impaired modeled tissues, with and without shell-based urogenital meshes placed within the rectovaginal (posterior vaginal wall support) and vesicovaginal spaces (anterior vaginal wall support).

Chapter 2

Female Pelvic Anatomy

The maintenance of continence and prevention of female POP relies on the support mechanisms of the pelvis. Therefore, effective management of UI, FI and POP requires knowledge regarding pathophysiologic mechanisms behind specific impairment of the pelvic cavity floor organs support [70].

Primarily, the pelvis acts as the main support for the upper part of the body. It transmits body weight to the legs, which enables mobility (walking and running) and flexibility of movement during stand upright postures [71].

Anatomically, the pelvis is composed of a bony ring (part of appendicular skeleton of the lower limb) with cartilaginous ligaments, and tendon attachments. Some of these arise from inside the pelvis and some originate from adjacent structures. On the other hand, muscles and fascia from the lumbar spine and hip bone play an important role in providing mobility and stability to the pelvis [71]. Proper functioning of bone and articular joints are essential for the transmission and absorption of energy and forces through the musculoskeletal system (from the spine and lower limb) [70]. The female pelvis is uniquely shaped, typically larger than men, with a wider diameter, more circular shape and less deep than that of the male (Figure 1). The wider inlet is adapted for the parturition but the wider outlet leads to subsequent pelvic floor and soft tissue weakness [70, 72].



Figure 1 - Anterior view of female pelvic bone (left) and male pelvic bone (right) (Adapted from [73]).

The pelvis comprehends two distinctive regions: major (false) and minor (true) pelvis. The first one affords protection to inferior abdominal viscera similar to the way the inferior thoracic cage protects superior abdominal viscera. The second one has the important role of providing skeletal framework for both the pelvic cavity (enclosed by the lesser pelvis contains elements of the urinary, gastrointestinal and reproductive system) and the perineum (inferior to the floor of the pelvic cavity and extended from the coccyx to the pubis, contains the external genitalia and external openings of the genitourinary and gastrointestinal systems). These two compartments of the trunk are separated by the musculofascial pelvic diaphragm [61, 71-72].

The physiological changes, mainly due to the course of pregnancy, cause alterations in the composition of the pelvis, its shape, and the plane of inclination and internal dimensions of the true pelvis. All of these changes serve to support the pregnant uterus throughout the term of pregnancy and assist with the normal mechanisms of childbirth.

The walls of the minor pelvis consist mostly of bone, muscle and ligaments, with the sacrum, coccyx and inferior half of the pelvic bones forming much of them [61].

2.1 Pelvic Bone

The bony pelvis is the rigid foundation to which all of the pelvic structures are ultimately anchored. The female pelvis comprises four bones - two innominate (or 'hip') bones, the sacrum (forming the rear of the pelvis) and the coccyx (forming the base of the spine and pelvis). Each innominate bone has three components: ilium, ischium pubis (or pubic bone) (Figure 2) [65, 72].

In daily standing positions the bony pelvis is oriented such that forces are dispersed to minimize the pressures on the pelvic viscera and musculature, transmitting the forces to the bones that are better suited for a long-term cumulative stress. Much of the weight of the abdominal and pelvic viscera is supported by the bony articulation inferiorly. Besides, variations in the orientation and shape of the bony pelvis have been associated with the development of POP. These variations are also an important factor concerning maternal soft-tissue damage and nerve injury during parturition [65].

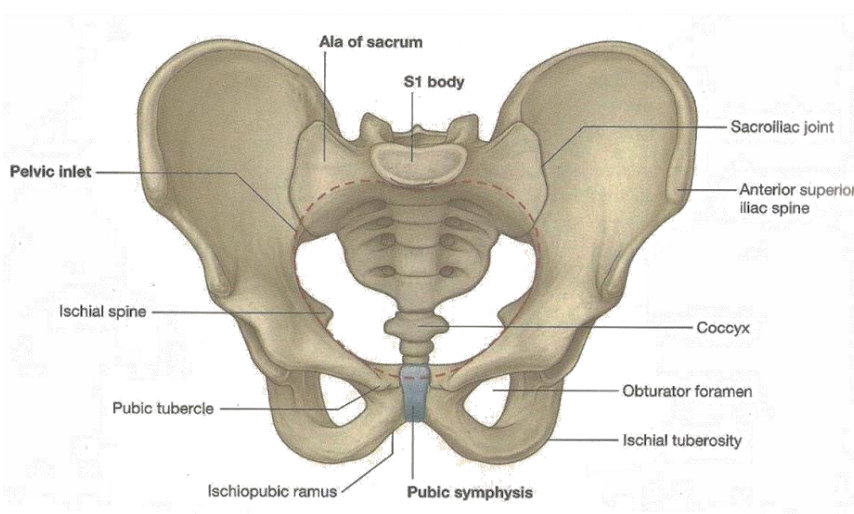


Figure 2 - Anterior view of the female pelvic bone with main components properly identified [72].

Sacrum

The sacrum has an inverted-triangle appearance and is composed by five merged sacral vertebrae forming a single bone (Figure 2). The base articulates with the vertebra of lumbar region and its apex articulates with the coccyx. The transversal vertebrae apophyses merge to form the sacrum wings which assemble the sacrum to the pelvic bones. The anterior border of the body of the first sacral vertebra makes a salience to form the sacral promontory. The apophyses of first four vertebrae merge partially to form protrusions, located on the posterior dorsal surface of the sacrum, which aggregate is called sacral crest. In the fifth vertebra the apophysis does not form, leaving a sacral hiatus [61].

Posterior to the large L-shaped facet of lateral surfaces, there is a large roughened area for the attachment of ligaments that support the sacro-iliac joint. Anteriorly, the sacrum surface is concave and the posterior surface is convex [72].

Coccyx

The coccyx is a small triangular-shaped bone, comprising four fused vertebrae that form a non-functional tail that articulates with the lower end of the sacrum (Figure 2). This bone provides attachment points for pelvic ligaments, anal sphincter fibers and ischiococcygeus muscle [61, 72].

Ilium

The ilium is a large broad bone, the top of which (the 'iliac crest') is felt when a woman rests her hands upon her hips (iliac crest). In this iliac thick prominence there are located key fixation points of important abdominal muscles and fascia.

Posteriorly the bone, with L-shaped facet, articulates with the sacrum and a roughened area is responsible for the strong attachment of the ligaments. Anteriorly it shows a rounded area forming the arcuate line. In the inferior line of the anterior superior iliac spine of the crest is found the anterior inferior iliac spine, which is responsible for attaching the rectus and femur muscles and the iliofemoral ligament through bond to the lower limb (Figure 3) [61].

Pubis (or pubic bone)

The pubis, commonly referred to as the pubic bone, is a smaller bone that forms the front, or anteroinferior aspect of the pelvis. It has a main body and two arm-like structures which protrude out. These structures, called rami, are positioned on either side (Figure 2). The pubis bone is flattened on the ventral part of the pelvic bone and forms one medial cartilaginous pubic symphysis. The body presents a rounded pubic crest on its superior surface. The suprapubic angle needs to be at least 90°, in order to allow the baby to pass underneath it during a vaginal birth. The triangular-shaped space enclosed by the body of the pubic bone, rami and ischium is known as the obturator foramen (Figure 3) [61, 72].

Ischium

The ischium represents the posteroinferior part of the pelvic bone, presenting a body one single ramus [61]. The body possesses superior and inferior limits and femoral, dorsal and pelvic areas (Figure 2).

Structurally this bone is elongated, larger on the top, narrowing towards the inferior surface and it allows the insertion for posterior femoral muscles [73].

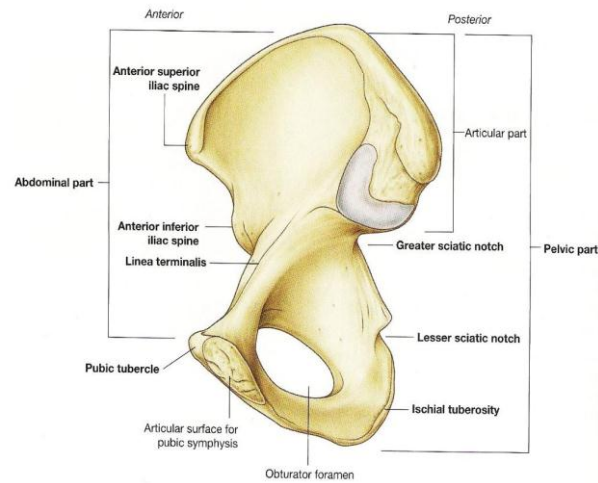


Figure 3 - Medial projection of the right innominate pelvic bone [72].

Structurally this bone is elongated, larger on the top, narrowing towards the inferior surface and it allows the insertion for posterior femoral muscles [73].

Upwards, it forms the inferior and posterior part of the acetabulum [73]. On the bottom the ramus projects anterior and medially to join with the inferior ramus of the pubis, forming an acute angle and completing the foramen obturator [71, 73].

The posterior margin of the bone is marked by a prominent ischial spine (Figure 4) [61]. On the other hand, it protrudes down and slightly medially. On its border it is inserted the sacrospinous ligament, which separates the superior and inferior ischiatic foramen. The ischial tuberosity is a big rough area in the inferior dorsal face and in the inferior border of the ischium bone [73].

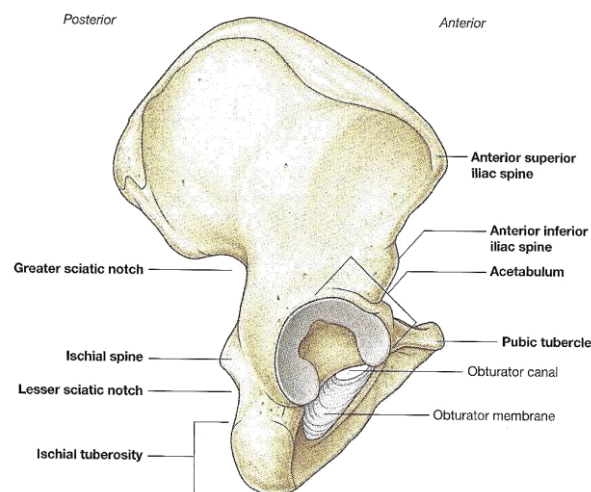


Figure 4 - Lateral projection of the right innominate pelvic bone [72].

2.2 - Pelvic Cavity

The female pelvic cavity is anatomically defined as the body abdominopelvic space that is well protected by bony tissue. Its space contains all the pelvic organs. The superior oblique and roof-like boundary is the pelvic inlet (opening) and it is closed by the sacrum on the superoposterior part (Figure 2). The cavity is inferiorly limited by the musculofascial pelvic floor suspended above the pelvic outlet, forming the bowl-like shape of the pelvic floor which is enclosed by coccyx.

The anteroinferior part is much shorter than the posterosuperior one and it presents a merging of pubic bones and pubic symphysis (Figure 1). By these facts, the axis of the pelvis is curved, pivoting around the pubic symphysis facilitating the fetal passage mechanism, through the pelvic cavity, during the birth [71-72].

2.2.1 - Pelvic Wall

Throughout the pelvic wall (circular opening wall) it is possible to pass from the abdomen to the pelvic cavity. This configuration is well surrounded by external bones and ligaments.

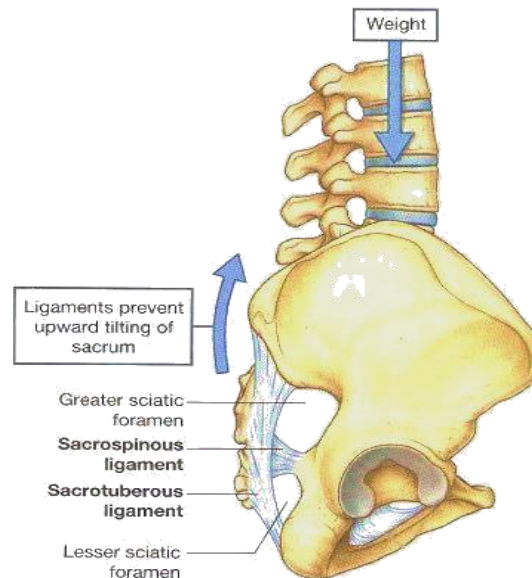


Figure 5 - Functional representation of sacrospinous and sacrotuberous ligaments [61].

In the pelvic wall, it is possible to observe the sacrum and coccyx of the section. Besides, there are two main ligaments comprehending this region - sacrospinous and sacrotuberous ligaments - and two structural muscles - obturator internus and piriformis (Figure 5, 6 and 7) [61].

2.2.1.1 - Ligaments of the pelvic wall

The ligaments that support the bony architecture of the pelvis are among the strongest in the body. The posterior sacrospinous ligament complex and sacrotuberous ligament are composed of interosseous and dorsal segments. The interosseous segments are short and strong, connecting the iliac tuberosity to the adjacent posterior sacral cortex. The unique

structure, of this posterior ligament complex, forms a dense mass of connective tissue that strongly resists displacement of the underlying joint.

Furthermore, both ligaments are responsible for joining the sacrum to the ischium, providing assistance on the apertures between the pelvic cavities and preventing upward tilting inferiorly of sacrum on the coupled pelvic bones (Figure 5 and 6) [61, 73].

Sacrospinous Ligament (SPL)

The SPL is a triangular-shaped ligament superficial to the sacrospinous ligament [61]. The base is inserted in the posterior iliac spine and extends along the dorsal aspect and the lateral margin of the sacrum and also to the dorsolateral surface of the coccyx (Figure 6) [61, 73]. The ligament oblique fibers descends laterally, converging to a narrowed and compact strip which enlarges again to fix down on medial fixing point of the ischial tuberosity. In the posterior facet of the ligament are inserted the inferior fibers of the gluteal muscle [73]

Sacrospinous Ligament (SPL)

The SPL is a narrowed, thin and triangular ligament. Its apex fixes on the ischial spine and extends until the lateral borders base of the sacrum and coccyx, anterior to STL with which it mixes (Figure 6) [61, 73].

Although the main role of SPL is to prevent rotation of the ilium respecting the sacrum, when the musculofascial tissue becomes weakened this ligament is requested to deliver a constant and effective support for the fixation of vaginal apex. Nowadays, this ligament is widely requested in surgical procedures. Sacrospinous ligament suspension (SPLS) is a technique performed in invasive surgeries regarding the prevention and repair of vaginal vault and uterine prolapse [12, 74-75].

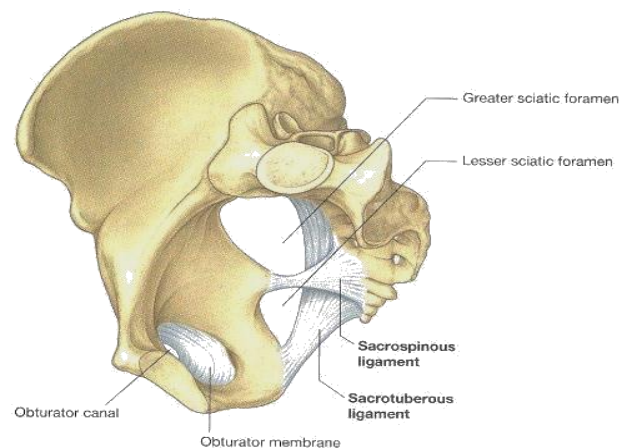


Figure 6 - Medial projection of the right side of the bony pelvis comprehending the pelvic wall ligaments [61].

2.2.1.2 - Muscles of the pelvic wall

Concerning the musculature of pelvic wall the two main important muscles are the obturator internus and piriformis. Functionally both are responsible for assisting the lateral stresses and solicitations induced on the pelvic cavity [61].

Obturator Internus

The obturator internus is a flat, fan-shaped muscle located in the lateral boundary of the pelvic wall and is composed by strong interlacing fibers which fills the obturator foramen (Figure 7). This muscle originates proximally from the deep surface of the obturator membrane, on the pelvic surfaces of the ilium and ischium, and fixes itself distally on the greater trochanter of femur. Their fleshy attachments cover and pad most of the lateral pelvic walls. The muscle fibers of each obturator internus converge posteriorly to form a tendon that leaves the pelvic cavity, making a 90° bend around the ischium between the ischial spine and ischial tuberosity, crossing the hip joint to finally be inserted in the greater trochanter of the femur [61, 71].

The main action of this muscle is to tightly and laterally rotate the extended hip joint, assisting in the holding of the head of the femur in the acetabulum [71].

In addition, recently, obturator internal muscle has been used for outside-in passage of synthetic meshes, during new surgical procedures for the reconstruction of pelvic floor compartments. These minimally invasive procedures bring into play cannulas and retrieval devices for a harmless placement of meshes and tapes through the transobturator space with preservation of the muscular tissue [23, 29-30, 76].

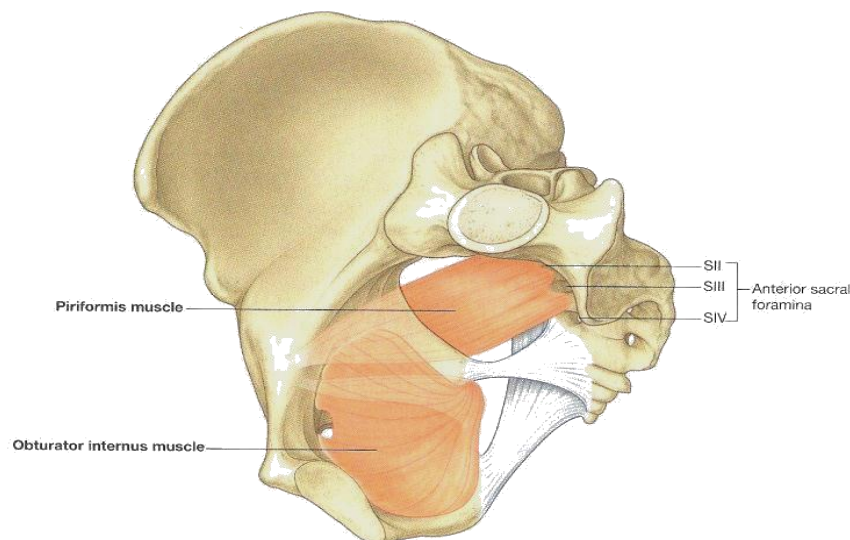


Figure 7 - Medial projection of the right side of bony pelvis comprehending the obturator internus and piriformis muscles [61].

Piriformis

The piriformis is a triangle-shaped muscle which arises from the superior sacrum, lateral to its pelvic foramina (Figure 7). The muscle passes laterally through the greater sciatic foramen, crossing the posterosuperior aspect of the hip joint, to attach to the superior border of the greater trochanter of the femur (above the insertion of the obturator internus muscle) [61, 71].

On the other hand, this muscle is responsible for separating the greater sciatic foramen into two distinct regions [61].

The main role of this muscle is to provide tight lateral rotation of the extended hip joint, tightly abducting and assisting in the holding of the head of the femur in the acetabulum, like the obturator muscle [71].

2.2.2 - Pelvic Floor and Structural Support

The pelvic floor is an arrangement of striated muscles, composed by ligaments and fasciae in a dome-shaped sheet and it is often described as a sling that encloses the pelvic viscera through midline defects. These defects are closed by connective tissue anterior to the urethra, anterior to the rectum, and posterior to the rectum. Together with the viscera, the pelvic floor has an important role regulating storage and evacuation of urine and stool. This complex structure is also fundamental for an active sexual life and dynamic vaginal delivery during labour [61, 64, 71, 77].

Moreover, the accurate support function required by the floor, due to the gravitational force (opposite direction to the pelvic force) and intra-abdominal pressure exerted during solicitation of mechanical movements on the lower limbs [70]. Likewise, increasing the rest state of the muscles of the pelvic floor can result in increased pressure within posterior bony pelvis [77].

2.2.2.1 - Structural Musculature of Pelvic Floor

The pelvic floor is formed by the bowl-shaped pelvic diaphragm and, in the anterior midline, the perineal membrane and deep muscles [61, 64]. The pelvic diaphragm separates the pelvic cavity from the perineum within the lesser pelvis [71].

On the pelvic diaphragm are found to distinct muscles: the levator ani and the coccygeus muscles and respective fasciae, which cover the inferior and superior surfaces of the muscles (Figure 8) [61, 71]. These muscles are attached peripherally to the pubic body (anterior fixation), the ischial spine (posterior fixation), and to the arcus tendinus (lateral fixation).

Functionally, the pelvic floor muscles act as a dynamic backstop, absorbing most of the expulsive load placed on the pelvic organs by intra-abdominal forces. The muscular tonus, during low exertion activity, narrows the gap through which the urethra, vagina and anus exit the abdomen. Furthermore, rapid reflex contractions occur from the fast twitch fibers, neutralizing any sudden increase in Valsalva forces. The renewal capacity of skeletal muscles fibers is advantageous since they can heal by hypertrophy and become stronger [61, 71].

Pelvic Diaphragm

The levator ani (LA) is the largest and most important component of the pelvic floor. Both the LA, from each side of the pelvic wall course medially and inferiorly and join together in the middle line [61]. The muscles are attached to the pelvic wall, following the circular contour of the wall. . This muscle is fixated anteriorly to the pelvic bones through a U-shaped gap (urogenital hiatus), posteriorly to the ischial spines through the anacoccygeal ligament and to a thickening in the obturator fascia between the two bony sites on each side [61, 71].

The LA consists of three distinctive parts, based on site of origin, course of its fibers and relationship to viscera in the middle line (distal to proximal):

- ***Puborectalis Muscle (PRM)***

This medial muscle is the second major collection of muscle fibers of LA. PRM presents a U-shaped structure passing posterior to the anorectal junction and form a sling around the

vagina, rectum, and perineal body, resulting in the anorectal angle (perineal flexure) and promoting closure of the urogenital hiatus [61, 71]. Besides, urogenital hiatus refers to the space between the LA musculature through which the urethra, vagina, and rectum pass (Figure 8) [65].

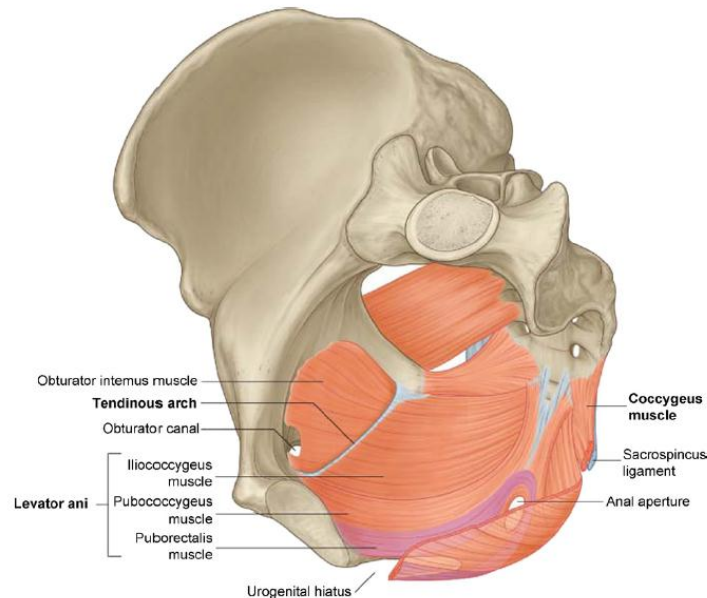


Figure 8 - Medial projection of the right side of pelvic diaphragm and coccygeus muscles [61].

- ***Pubococcygeus Muscle (PCM)***

This intermediate muscle is the wider but thinner part of LA, arising from the back of the pubis body and anterior portion of the arcus tendineus ligament levator ani (ATLA), a linear thickening of the fascial covering of the obturator internus that runs from the ischial spine to the posterior surface of the ipsilateral superior pubic ramus [65, 70]. PCM is inserted in the midline-visceral organs and its medial fibers merge with those of the contralateral muscle with the aim to form a fibrous tendinous plate (levator plate), between the anus and the coccyx (Figure 8) [65, 71]. The levator plate shelf provides an effective horizontal support to the rectum and to the upper two thirds of the vagina above it, when the body is in a standing position [70].

- ***Iliococcygeus Muscle (ICM)***

This thin postolateral muscle arises from the ATLA to the ischial spine. Posteriorly ILM attaches to the last 2 segments of the coccyx (Figure 8). The fibers from both sides fuse to the anococcygeal ligament [70].

Coccygeus

This triangular shaped muscle, one on each side of the pelvis, overlies the sacrospinous ligaments [24]. It extends from the ischial spine (apices) to the lateral surfaces of lower sacrum and coccyx (bases), forming the posterior part of the pelvic diaphragm [23, 24].

The main action of coccygel muscle is to form, as well as in the case of LA, part of the pelvic diaphragm, supporting the pelvic viscera but with a reduced approach [71].

Perineal Membrane (Urogenital Diaphragm)

The perineal membrane is a thick musculofascial sheet, triangularly shaped and presented over the anterior pelvic outlet below the diaphragm (Figure 9).

The superficial perineal space contains the ischiocavernosus and bulbocavernosus muscles inferiorly and superficial transverse perineal muscle superiorly. The deep perineal space is located inferiorly to the LA muscles. In this space lie the external urethral and the urethrovaginal sphincters, compressor urethrae and deep transverse perineal muscles [65].

The structure bridges the gap between the inferior pubic rami bilaterally and the perineal body. Besides, the membrane is involved in the vaginal and urethral distal region suspension and provides fixation of the distal urethra, distal vagina and perineal body to the pubic arches. Therefore it behaves like a contractible sphincter to provide continence [65, 70].

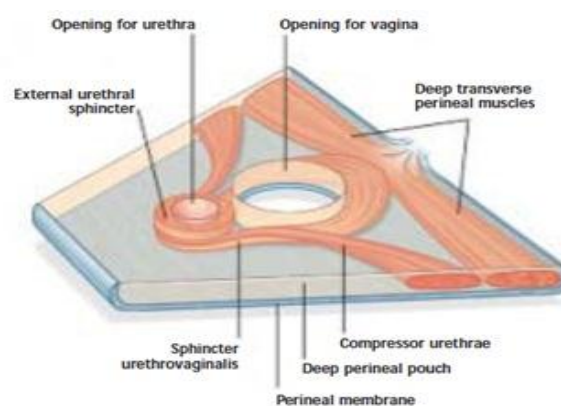


Figure 9 - Illustration of the muscles of the deep perineal space with perineal membrane in the horizontal plane in the standing position [61].

Perineal Body

The perineal body is a pyramidal fibromuscular structure in the midline between the anus and vagina (Figure 10). Inferiorly, muscles and fascia converge and interlace. This structure is attached to the rectum, vagina, perineal muscles and anal sphincter [70].

The perineal body plays an important role in the support of the distal vagina and in normal anorectal function [65].

2.2.2.2 - Connective Tissue of Pelvic Floor

The structure and strength of the pelvic organs are directly dependent on the properties and regular function of surrounding connective tissue. This exclusive tissue is rich in fibrotic components (fibroblasts, collagen type I and III and elastin), smooth muscular tissue and vascular structures. The endopelvic fascia is continuous with the visceral fascia, which provides a capsule containing the organs and allows displacements and changes in volume. The distinct regions of this structure are given individual names, specifically ligaments and fascia, with variable internal structure [70].

This layered complex creates a synergic action of ligaments, muscles and bones. Besides, their collagenic and elastic fibers have the important role to resist tissue stretching and

conferring stable support to daily mechanical solicitations (i.e. vaginal delivery, heavy lifting, sexual life, continence, etc). In contrast, certain dysfunctional changes may weaken the ligaments and fascia, thereby affecting the structural integrity of the pelvic floor. This may result in POP [72, 78].

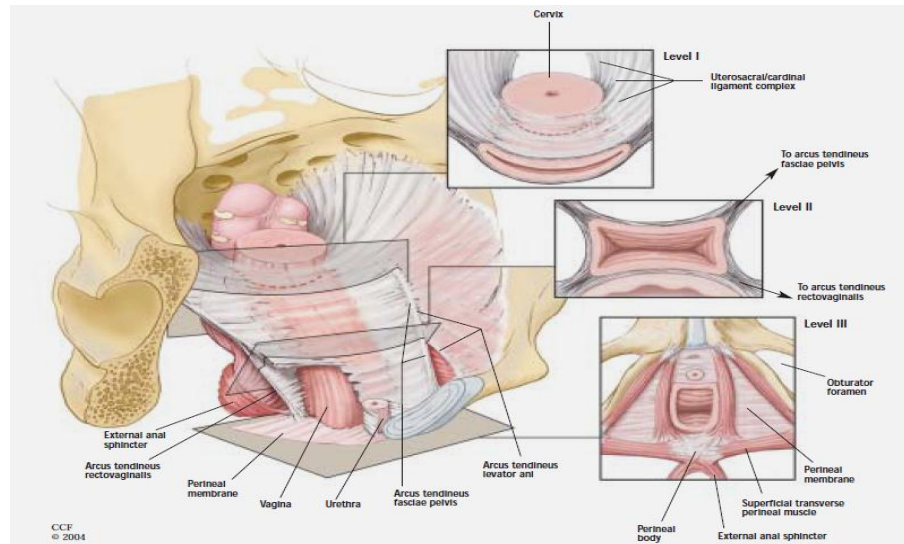


Figure 10 - Detailed representation of fascial and ligament-like structure of the pelvic floor. In addition, three integrated levels of uterus/vagina support are presented for female standing position [65].

By this fact, to understand the performance of the pelvic floor connective tissue, it is important to describe the anatomic and physiological characteristics of the endopelvic fascia and key pelvic floor supportive ligaments (pubourethral, pubovesical, arcus tendineus fasciae pelvis, and the cardinal and sacral ligaments).

Endopelvic Fascia

The endopelvic fascia is the loose connective tissue network that envelops all of the organs of the pelvis and connects them loosely to the supportive musculature and bones of the pelvis. It occupies the space between the perineal membrane and the muscular pelvic walls and floor which is not occupied by the pelvic viscera (Figure 10). Histologically, it is composed of collagen, elastin, adipose tissue, nerves, vessels, lymph channels, and smooth muscle [65].

Generally, this fascia is described as having two distinct parts: fascia parietal and fascia visceral. The parietal pelvic fascia covers the pelvic surfaces of the obturator internus, piriformis, coccygeus, levator ani and part of the urethral sphincter muscles. The visceral pelvic fascia respects to the membranous fascia that involves the pelvic organs, forming an adventitial layer of each organ [71]. Concerning the visceral fascia, endopelvic network tethers the vagina and uterus in their normal anatomic local due to inferoanterior attachment of pubocervical fascia (PCF). It forms a strategic cervical ring anteriorly to the uterine cervix providing mechanical resistance to vaginal/uterine forward displacements. In addition, rectovaginal fascia (RVF), is located in the inferoanterior wall of the rectum, preventing anatomic displacements towards uterus posterior wall [65, 77].

Moreover, the pelvic connective tissue is classified in three levels of vaginal support by a superficial growing order (Figure 10 and 11). These levels comprehend the apical support (level I), mid-portion of the anterior vaginal wall support (level II) and distal support (level III). Thus, loss of level I support contributes to prolapse of the uterus and/or vaginal apex (vaginal vault prolapse), loss of level II support can lead to prolapse of the anterior vaginal wall and loss of level III support anteriorly leads to urethral hypermobility and stress incontinence and posteriorly to rectal and/or perineal descent [65].

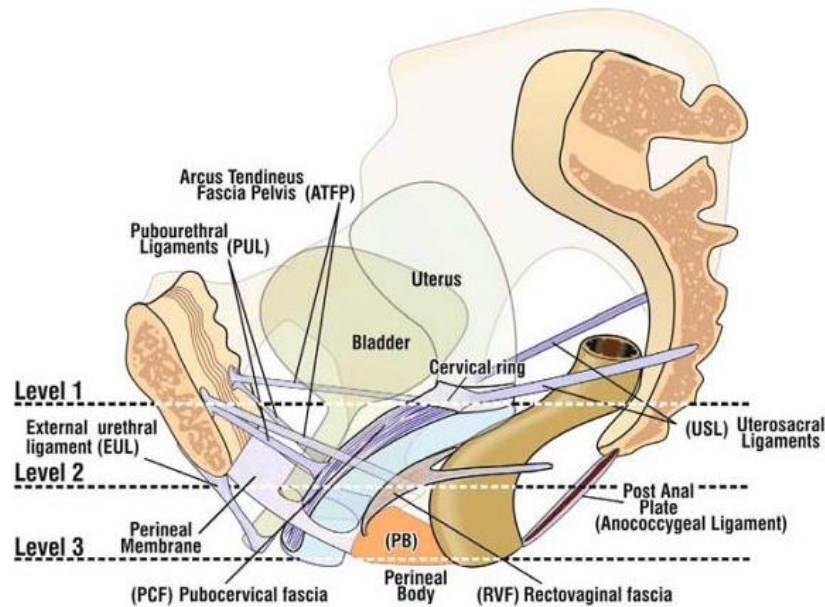


Figure 11 - 3D sagittal representation of connective tissue support levels concerning the pelvic organs and their relation with bony pelvis [78].

Pelvic Floor Ligaments

The ligaments of pelvic fascia result from the condensations of the fascia that extends from the cervix to the pelvic walls. These ligaments, together with perineal membrane, the levator ani muscles and the perineal body, prevent mainly their misplacement from anatomical natural standing position and are thought to stabilize three-dimensionally the pelvic viscera structures [61, 78].

To understand the role of the different pelvic floor ligaments it is important to analyze each ligament regarding relations with each support level (I, II and III) [65-66, 70, 78]:

- ***Uterosacral/Cardinal Ligament (USL)***: arises from the sacral vertebrae S2, S3 and S4 and attaches to the cervical ring posteriorly and laterally. The USL provides level I support, suspending the apex of the vagina and has effective insertion points of the downward muscle forces (Figure 10 and 11). Additionally, it serves to maintain vaginal length and keep the vaginal axis nearly horizontal in a standing woman.
- ***Pubovesical Ligament (PVL)***: connects the fundus (base) of the bladder to the pubis. The PVL provides level II support, suspending the anterior wall of the bladder and has effective insertion points of the precervical arc of Gilvernet (a

stiff fibromuscular structure on the anterior bladder wall). Moreover, PVL confers rigidity to the anterior wall of bladder (Figure 10 and 11).

- ***Pubourethral Ligament (PUL)***: extends from the urethra to the pubis. The PUL provides level III support, suspending the urethra and keeping the vesical neck closed. Because there is an attachment of the lower third of the urethra to the pubis, it is postulated that there are two separate structures, one for support at the mid- or distal urethra and one near the bladder neck that may open it during voiding (Figure 10 and 11).
- ***Arcus Tendineus Fasciae Pelvis (ATFP)***: originates on the ischial spine and inserts on the inferior aspect of the pubic symphysis. It fuses with the PCF superiorly, and the RVF inferiorly. The ATFP is a thickened condensation of fascia overlying the ICM that provides II support. This paravaginal ligament suspends the vagina bilaterally like a trampoline between the two arcus (Figure 10 and 11).

2.2.2.3 Pelvic Organs

Bladder and Urethra

The bladder has the main role of temporarily reserve urine with capacity to change in size, shape and position, according with its content and respective viscera states. Anatomically the bladder is a balloon-shaped organ that is located in minor pelvis, when is empty, but when starts to distend it expands anterosuperiorly towards the abdominal cavity.

This distend organ, is the most anterior element of the pelvic viscera, separated from the pelvic bone by the retropubic space, lying mostly inferior to the peritoneum. It presents a three-sided pyramid shape in the pelvic cavity, containing an apex, a base superior face and two inferolateral surfaces (Figure 12). The apex is the most superior part, coated externally by the peritoneum and directed towards the top of the pubic symphysis when empty. The base is inverted-triangle shaped and posteroinferiorly faced, presenting a smooth mucosal firmly attached to the underlying smooth muscle coat of the wall. The inferolateral surfaces of the bladder are between the pelvic diaphragm and the LA muscles above the attachment of the diaphragm.

In women, the bladder fundus (triangular and posteroinferior) is deeply related with the anterior wall of the vagina. There are two main muscular tissues - detrusor and trigone. The first is responsible for the concentric distention capacity of the bladder. The second is located inferoposteriorly in a triangular shape communicating with two ureteral orifices and internal urethral orifice [73].

The female urethra is a muscular-membranous channel which begins at the base of the bladder and ends with an external opening in the perineum. It is approximately 4 cm long and passes inferiorly through the pelvic floor into the perineum. The urethral opening and external orifice are anteriorly placed to the vaginal opening. Besides, two small paraurethral mucous glands are merged with the lower end of the urethra [73].

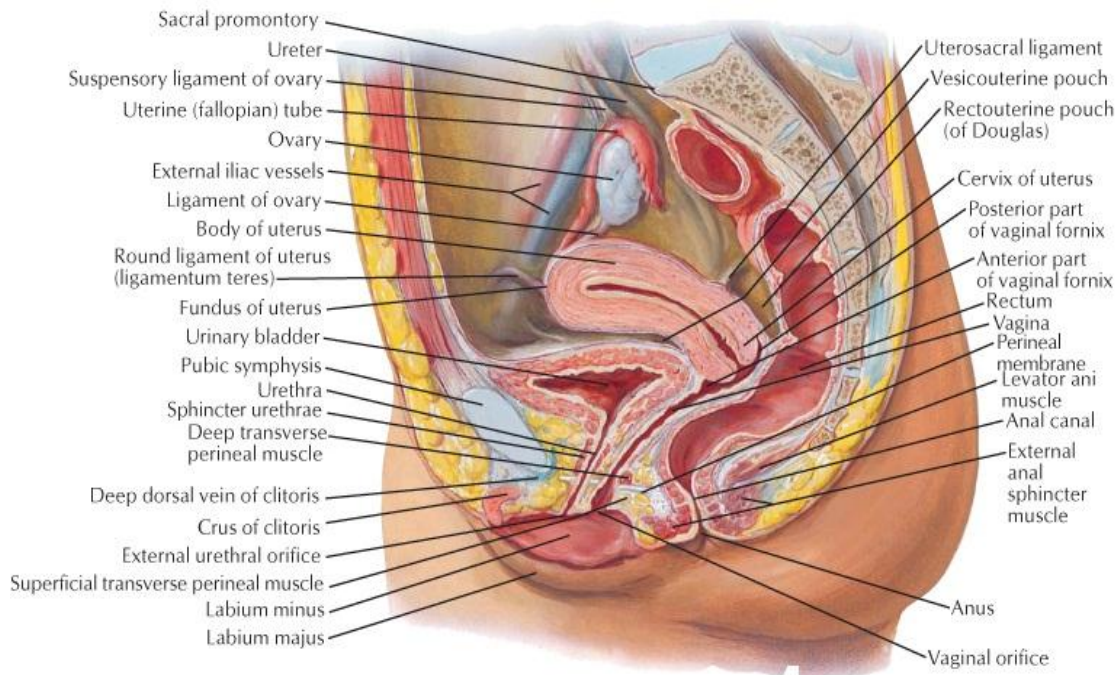


Figure 12 - Representation of the pelvic organs (bladder, uterus and rectum) and pelvic floor in a sagittal view [79].

Uterus and Vagina

The uterus is a thick-walled, pear-shaped, hollow muscular organ. It is responsible for the pregnancy and childbirth, leading to a muscular adaption of the walls during the growing of the fetus and in its expulsion. Usually, the normal non-pregnant adult uterus is anteverted and anteflexed, standing in the lesser pelvis, with its body lying on the urinary bladder and the rectum. It is estimated that the uterus is 7.5 cm long, 5 cm wide and 2 cm thick, weighs approximately 90g and is divided in two distinct parts, body and cervix.

The body of the uterus is responsible for two thirds of the organ. It includes the fundus of the uterus, respecting the rounded part that lies superior to the orifices of the uterine tubes and having great mobility. The cervix is cylindrically shaped, inferiorly narrowed, approximately 2.5 cm long in non-pregnant adult woman and has two main parts: supravaginal and vaginal. The first lies between the isthmus (constricted segment) and the vagina and the second protrudes into the vagina (Figure 12).

The wall of the uterus body is divided in three distinct coats: perimetrium, myometrium and endometrium. The perimetrium is the outermost layer that consists in peritoneum coated by a thin layer of connective tissue. The myometrium is the middle coat, consisting in smooth muscle which allows the distension of the uterus during the pregnancy. The endometrium is the inner mucous coat, well firmied to the myometrium and is responsible to regulate the menstrual cycle [73].

The vagina is a copulatory organ in women, distensible, fibromuscular tube with rugal folds that extend from the vestibule (perineum) to the uterine cervix (pelvic cavity). The anterior vaginal wall is 7,5 cm long and is embedded with the urethra. It presents a longitudinal shape that resembles a trapezoid, growing progressively wider as it approaches the cervix [61, 65]. The final enlarged region is called vaginal vault. In the sagittal view, it is observed that two thirds are directed towards the third and fourth sacral vertebrae through a

distinct angulation (Figure 12). In the standing position the vaginal wall is practically horizontal. On the other hand, the lower third is almost vertical as it passes through the perineal membrane to the vestibule. It is estimated a mean angle between the upper and lower vaginal axes approximately of 130° [61, 65, 73].

The vaginal wall is composed of three main layers: mucosa, muscularis and adventitia. The first one is the most superficial layer, possessing stratified squamous epithelium and a lamina propria. The second one is a well-developed fibromuscular layer that consists of interdigitating smooth muscle, collagen, elastin and vascular tissue. The final layer is the most superficial one and possesses a layer of collagen, elastin and adipose tissue containing blood vessels, lymph and nerves. In addition, the final layer is visceral endopelvic fascia, found on the adjacent pelvic organs, allowing independent expansion and contraction [65].

Rectum

The rectum, a 12cm to 15cm long structure, is the most posterior structure of pelvic viscera and is located immediately anterior to the concave contour of the sacrum (Figure 12). Below it has an anal canal where lie important contractible muscles, for the fecal expelling, rich in longitudinal muscle that interlaces with the underlying circular muscle. The canal penetrates the pelvic floor and passes through the perineum to the superficial orifice, the anus [71].

Chapter 3

Pelvic Floor Disorders

Pelvic floor disorder (or dysfunction) is a general term that describes a wide range of functional clinical problems that are anatomically grouped regarding failure of pelvic floor complex structural and supportive system. They are associated with weakness of the skeletal and striated muscles, support and suspensory ligaments, fascial coverings and also fail of neural network [80-81].

The pathophysiology relies on the three pelvic compartments (anterior, mid and posterior). It can affect one or all the three compartments, often resulting in POP and functional disturbance of bladder (UI and voiding dysfunction), rectum (FI), vagina and/or uterus (sexual and pregnancy dysfunctions) [80]. There is a recent consensus among physicians that the segments of pelvic viscera should not be singly evaluated and treated. More commonly, UI and FI are thought to co-exist with POP [70].

Moreover, these lower limb dysfunctions form an extensive problem for individual women, deeply interfering with their life quality. To fully understand this global burden is necessary to study in detail etiologic factors, epidemiologic distribution, preventive diagnostic techniques and best suited treatment (non-invasive or surgical).

3.1 Pelvic Organ Prolapse

Pelvic organ prolapse is a common and distressing condition that occurs due to a weakness in the supporting structures of the pelvic floor, allowing the descent of the pelvic organs into the vagina, often accompanied by urinary, bowel, sexual, or local pelvic symptoms [82].

Clinical observations and scientific data indicate that pelvic organ support is affected due to pelvic bones, muscles, nerves and connective tissue functional disorder and the process generally occurs over many years [63].

3.1.1 POP Classification: Nomenclature and Anatomical Deformity Stages

In the past three decades, the medical community, the International Continence Society (ICS), American Urogynecologic Society (AUS) and Society of Gynecologic Surgeons (SGS) have been proposing many schemes for evaluating POP and they are in the forefront of the standardization of terminology systems [82-84]. The goal of this issue is to provide an easy understanding evaluation system to clinicians and researchers.

The terminology system more commonly used to classify the anatomical deformity in POP (Table 1) refers to fall of specific pelvic viscera: urethrocele, cystocele, uterovaginal prolapse, enterocele and rectocele (Table 1 and Figure 13).

Table 1 - Traditional anatomical site of prolapse classification [82].

Urethrocele	Prolapse of the inferoanterior vaginal wall involving the urethra
Cystocele	Prolapse of the superoanterior vaginal wall involving the bladder and usually leading to an urethrocele
Uterovaginal	Prolapse of the uterus, cervix and also accompanied by vault prolapse
Enterocele	Prolapse of superoposterior wall of the vagina
Rectocele	Prolapse of the inferoposterior wall of the vagina involving the rectum bulging forwards into the vagina

Baden-Walker Halfway Scoring System proposed in 1992, by Band and Walker, simplified the 3D anatomy in a 2D dimensional coronal plane. The vaginal support profile is divided in six main mapping sites (urethral, vesical, uterine, cul de sac, rectal and perineal) and extent of the prolapse is recorded by using a scale from 0 to 4 (0 no prolapse and 4 maximum prolapse) (Figure 14). For all sites except for the perineum, the hymen is used as a fixed anatomic reference point, also called the half-way system. The patients are evaluated during maximal straining by using a bidigital method or inserting the speculum or tenaculum into the vagina. Although this type of notation encodes much information in a small space, no specific location of fascial defects is included and is not well validated by the medical community [82, 84].

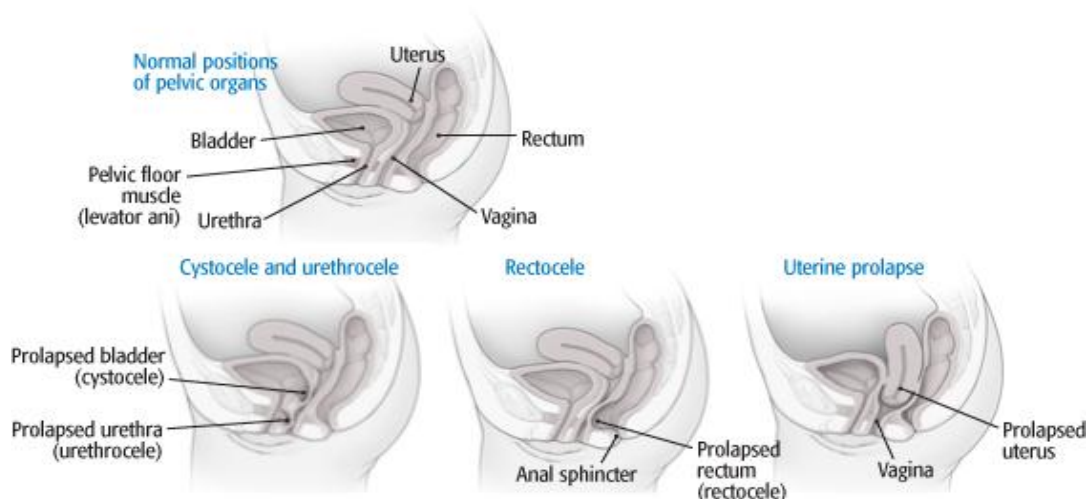


Figure 13 - Sagittal representation of POP involving different injured sites and respective pelvic viscera falling into the vagina (Adapted from [85]).

Therefore, in 1996 the Pelvic Organ Prolapse Quantification system (POP-Q) gained attention of the specialists and was validated by the collaboration of ICS, AUGS and SGS. The system relies on specific measurements of defined points in the midline of the vaginal wall [82].

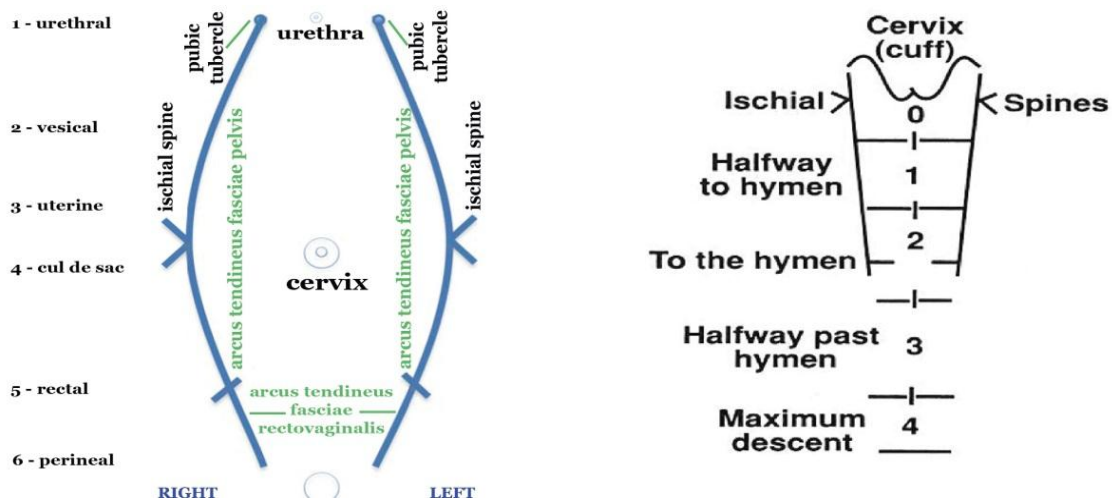


Figure 14 - Coronal plane of POP map with main elements of pelvic support (on the left) and representation of Baden-Walker half way system with four grades of prolapse (Adapted from [82]).

This system emphasizes that the criteria for the end point of the examination and the full development of the prolapse should be specified. Normally the criteria to consider a maximum prolapse should include at least of the listed topics; a) any protruding of the vaginal wall became tight during straining by the patient, b) traction on the prolapse causes no further descent, c) the size of the prolapse and the extent of the protrusion seen by the examiner are as extensive as the most severe protrusion that she has ever witnessed, or d) a standing, straining examination confirms that the full extent of the prolapse was observed in the other positions used. On the other hand, the stage of the POP can be assessed through maximal Valsalva maneuver [83].

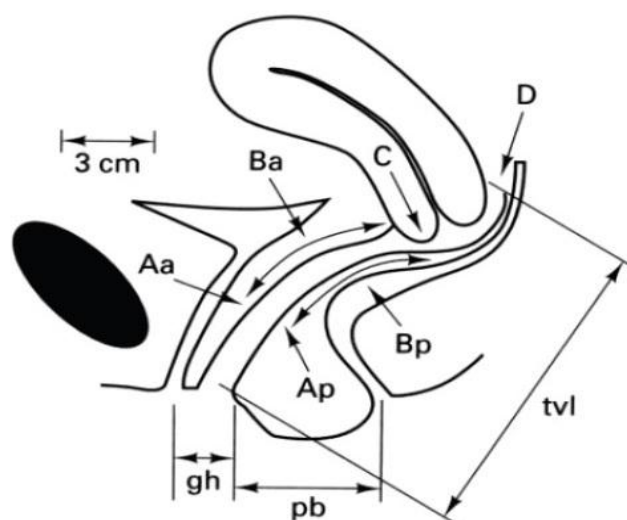


Figure 15 - Points and landmarks for POP-Q system examination. Aa - point A anterior; Ap - point A posterior; Ba - point B anterior; Bp - point B posterior; C - cervix or vaginal cuff; D - posterior fornix; gh - genital hiatus; pb - perineal body and tvl - total vaginal length [82].

The terminology avoids assigning a specific type of prolapse as in the traditional classification such as cystocele or enterocele. There are six defined points considered in the POP-Q system, three concerning the anterior part (Aa, Ba and C) and other three concerning the posterior one (Ap, Bp and D) as it is represented in Figure 15.

Special attention is given to point C and D after hysterectomy, since the first is taken as the vaginal cuff and the second is omitted. In addition, exist another three landmarks (gh, tvl and pb). Besides, the hymen ring remains the reference point of the system and small increases in POP are recorded as small increases in measurement. Once the measurements are taken, the patients are assigned to the corresponding stage of prolapse as it is shown in Table 2.

Table 2 - Stages of POP-Q system measurement [82]

Stage 0	No prolapse is demonstrated
Stage 1	The most distal portion of the prolapse is more than 1 cm above the level of the hymen
Stage 2	The most distal portion of the prolapse is 1 cm or less proximal or distal to the hymenal plane
Stage 3	The most distal portion of the prolapse protrudes more than 1 cm below the hymen but no farther than 2 cm less than the total vaginal length
Stage 4	Maximum vaginal eversion

3.1.2 POP Pathophysiological Conditions

Functionally when the LA muscle complex (pelvic diaphragm) relaxes or is damaged, the genital wall opens and an additional support is required by the suspensory ligaments (USL, PVL and PUL) constrained to the pelvic organs and connective tissue. As well, it is known that the ligaments can physically sustain these extra loads for short periods, the connective tissues of endopelvic fascia will stretch and eventually fall in the case of latter or weak closing of pelvic floor by the key pelvic floor muscles [63, 85-86].

Respecting visceral support, vaginal anterior and posterior support were extensively studied in this pioneer work since vaginal anterior, posterior and vault and uterine prolapse are within the most recurrent and harmful types of POP.

Concerning the vaginal wall, it is mechanically supported by connection points between the vagina and bony pelvis and LA muscles. The lower one-third of the vagina is attached between the perineum, preventing downward descent of the rectum in this region. In case of muscle fibers weakening, with posterior rupture, the bowel may protrude downward resulting in a posterior vaginal wall prolapse. Defects in the support at the level of the perineal body most frequently occur during vaginal delivery and are the most common type of posterior vaginal wall support problem. In the mid vagina, the wall is connected to the inside of the LA muscles (PRM) by sheets of endopelvic fascia, more precisely PCF. These connections prevent the ventral movement of the vagina during intensifications in abdominal pressure. In contrast, detachment of PCF and respective impairment of cervical ring, may lead up frontward irregular movements of the anterior vaginal wall and respective prolapsed state.

In the upper one-third of the vagina, the vaginal wall is connected laterally and dorsally by the cardinal and vaginal portion of the uterosacral ligament forming USL complex. Structurally, there are no attachments on the anterior or posterior wall. USL complex prevents downwards movement of the vagina and uterus. Therefore, when these key suspensions present damaged tissue, a descent of uppermost area of vagina and uterine cervix occurs. Additionally, it is generated a progressive clinical problem: uterine and/or apical prolapse. These unstable states may be boosted due to strength decrease of arcus tendineus local fixation points for muscles and connective tissue.

The multiple connections of the perianal body to the LA and the pelvic sidewall prevent a low anterior and posterior prolapse from descending downward through the opening of the vagina (the urogenital hiatus and the LA muscles) [65].

Alternatively, it may well present that POP is related to abnormal repair of the injured tissue after the stress of delivery. Thus, the increased flexibility, dispensability and decreased tensile strength (associated with an increase in collagen III), together with a decrease in elastin levels, will be very likely to contribute to the progression of POP [86].

On the other hand, there are some biochemical corroborations for pelvic floor muscular tonus and endopelvic fascia weakness. Regarding the connective tissue, collagen is the endopelvic fascia constituent with greater concern and abnormalities in the quantity, type and quality of collagen have been observed in both stress incontinence and in genitourinary prolapse [87]. Based on Jackson et al findings, it is suggested that genitourinary prolapse is associated with a reduction in total collagen content and a decrease in collagen solubility. They also found that collagen turnover, as indicated by matrix metalloproteinase (MMP) activity, was four times higher in prolapsed tissue. Therefore collagenolytic activity causes loss of collagen from prolapse tissue [88]. Histochemically, there may also be other associated findings about the alteration in MMP, which affects various components of the extracellular matrix system and consequently the muscular tonus of the pelvic floor [89].

Evidence of neuromuscular injury has been proposed as an important factor in predisposing to pelvic floor dysfunction. Progressive pelvic floor denervation, mainly through ageing and childbearing, is thought to lead to sagging of the levators, widening of the levator hiatus with loss of urethral and vaginal support leading to stress urinary incontinence (SUI) and genital prolapse [87].

3.1.3 POP Etiology

POP is a complex multifactorial defect [90]. Most of the literature regarding risk factors for POP is based on epidemiological studies, case control studies and observational studies [6, 91-93].

The few studies that examine the association of POP with pregnancy implicate vaginal delivery as an important risk factor. A study proved that there were no significant differences in the prevalence of disorders between cesarean delivery and nulliparous groups, with both showing 27% prevalence for any pelvic floor disorder. These groups had a protective effect when compared to vaginal route of delivery. Vaginal parous women presented a rate of 8, 18 ad 28% for POP, UI and FI (a total of 42% for any pelvic floor disorder) (Table 3) [90]. In other study higher vaginal parity was associated with prolapse when defined as stage II POP-Q or greater [93]. Additionally, it have been indicated that there are associated factors which add co-morbidity in vaginal parous women, such as birth weight, duration of second stage of labor, as well as instrumentation [94].

Table 3 - Case study of prevalence of selected pelvic floor disorders by birth group (nulliparous, caesarean delivery or vaginally parous) [91].

	Nulliparous (N=787)		Cesarean Delivery (N=389)		Vaginally Parous (N=2,927)	
	%	n/N	%	n/N	%	n/N
POP	4	29/774	4	16/386	8	223/2,883
SUI	8	64/771	11	43/387	18	505/2,885
OB	9	70/773	9	36/381	15	427/2,852
AI	19	143/766	16	60/365	28	786/2,823
APFD	27	201/750	27	98/369	42	1,153/2,767

POP, Pelvic Organ Prolapse; SUI, Stress Urinary Incontinence; OB, Overactive Bladder; AI, Anal Incontinence; APFD, Any Pelvic Floor Disorder
n, number of women with the specific floor disorder; N, total number of women of each studied group

As mentioned earlier, the studies done by Olsen et al, examining prolapse or surgery for prolapse showed an increased prevalence with aging. In this study the lifetime risk to undergo a pelvic organ or stress incontinence intervention with 80 years old was 11% [11]. Additionally, Nygaard et al presented a random study showing that in a population of 270 women with a mean age of 68.3 years, 64.8% of total women were stage II-III POP-Q [94].

In a Swedish study it was evident the progressive decrease in pelvic floor muscle strength with increasing age and parity [95]. Morrill M. et al assessed 4392 women to identify characteristics that were associated with seeking care for pelvic floor disorders. Women who sought care were significantly older (Figure 16) [96].

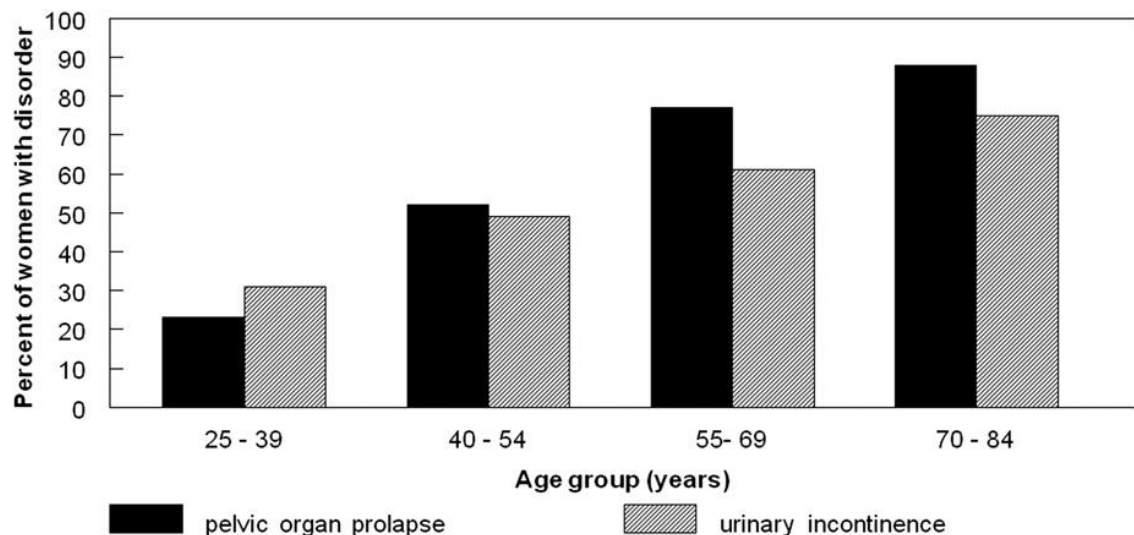


Figure 16 - Graphic of a study revealing percent of women with POP or UI care-seeking in each age group. Mature women reveal higher percentage of care-seeking comparing younger aged groups [96].

The aging is largely accompanied with menopause. More than 75% of women that have undergone treatment of POP, are post-menopausal [97]. An estrogen deficiency in menopause

decreases the urogenital vascularization, leading to a manifestation of several syndromes in the urinary tract.

Obesity is another condition that is associated with the increase of chronic abdominal pressure. Some studies have been proving that body mass index (BMI) increases the risk of pelvic floor support damaging. Kappor et al. found that obesity clearly had a negative impact on UI and POP [92]. On the other hand obesity was associated with sexual dysfunction and Ramirez et al verified an increase of operative failures in women after anti-incontinence procedures. In these cases they were likely to leak urine with activity and experience difficult rectal evacuation [98].

POP can also be associated to prior hysterectomy or prolapse surgery. Marconi et al demonstrated that after 13 years, 11.6% of the women who had undergone hysterectomy for prolapse had occurrence of vaginal vault prolapse. Certain procedures have higher risk of specific pelvic support defects, such as “gold standard” surgeries using native tissue (colposuspension and sacrospinous ligament fixation) for reconstruction of the pelvic floor [90]. Outcome data from Olsen et al showed that in primary and in recurrent repair cases, with suturing of native tissues, there was a high rate of failure; 41% and 67%, respectively [11, 99].

There is evidence of other type of abnormalities like congenital syndrome, such as bladder exstrophy, collagen defects (principally collagen type III) and congenitally short vagina. This is still an area in need of intensive study and research [90, 100]

In general, younger age at first delivery, ageing (>65), higher BMI, vaginal delivery, ageing and history of gynecologic surgery are significantly associated with subsequent development of pelvic floor disorders, more precisely POP [90 - 92, 101].

3.1.4 UI and FI

Urinary genuine incontinence is a common problem among older women, with an estimated prevalence of 42% to 57% among women older than 40 years of age in the United States of America [102].

Women with anterior vaginal wall support defects often have bladder neck hypermobility with stress incontinence, as well as concurrent defects of uterine and posterior wall support. However with greater degrees of anterior vaginal wall prolapse (stage III and IV) fewer women have symptoms of stress incontinence [90].

Besides, involuntary urine loss can be associated with an increase in abdominal pressure which develops the symptom of stress incontinence. Most persons with this problem experience leaking with coughing, sneezing or vigorous effort. However, in some cases , minimal efforts is required to induce involuntary urine loss, which be more or less continuous but still classified as stress incontinence [103].

In normal bladders, bladder wall tension is in part a passive phenomenon related to the distensibility or visco-elastic properties of the bladder wall itself, and in part an active phenomenon due to the contractility of the detrusor muscle and its neurological control. It is thought that the mid-urethra at rest, closure is largely maintained through the intrinsic striated muscle of the rhabdosphincter; however, the extrinsic striated muscles of PCM and compressor urethrae may be significant in maintaining urethral closure with increased intra-abdominal pressure. [87].

In urodynamic terms, stress continence is maintained when the maximum urethral pressure exceeds the intravesical pressure. Therefore, in any case when abdominal pressure causes leakage and detrusor pressure at time is minimal, true stress incontinence is present [87, 103].

There is a well-conceived theory of urethral support, the 'hammock hypothesis', in which it is thought that the urethra is supported posteriorly and inferiorly by the anterior vaginal wall. The vaginal sulcus represents the two lateral insertion of the vaginal 'hammock' for portions of PCM attachment within the pelvis that can produce elevation during voluntary contraction. Immediately anterior to the proximal urethra is found endopelvic fascia support. The PUL is shown as the most prominent sufficiently condensed to form distinct support. However, it is suggested that elongation or damage of any of these structures may be responsible for the loss of urethral support in stress incontinence.

Emerging concepts of urethral weakness conceive the idea of UI independent of vaginal weakness. Intrinsic sphincter deficiency (ISD) is focused on the urethral independency from the vaginal position and mobility. It comprehends the pudendal innervation, striated sphincter mass and function, and urethral smooth muscle, mucosa and submucosal cushions damage. Normally muscle mass and function is measured through electrophysiological studies of pudendal nerve and sphincter function. MRI and sonography estimates the muscle mass. The typical patient with ISD presents symptoms low urethral closure pressures, a "stovepipe" appearance on cystoscopy, and opening or funneling of the urethra under resting or minimal increase in intra-abdominal pressures on radiographic images.

Thus, it is important for incontinence specialists to have well-grounded understanding of POP in order to provide optimal patient continence re-functionalization and urethral restore. It is the area of functional understanding of urethral anatomy that the greatest progress is likely to be made [94].

FI occurs when the normal anatomy or physiology that maintains the structure and function of the anorectal unit is disrupted. Incontinence usually results from the interplay of multiple pathogenic mechanisms and is rarely attributable to a single factor [104]. In United Kingdom the prevalence of FI in women with 64 years old is approximately 13.3 % [105].

In normal females, the anus is normally closed by the tonic activity of internal anal sphincter, which is reinforced by voluntary squeeze of external anal sphincter (EAS). Besides, PRM forms a flap-like valve that creates a forward pull and reinforces the anorectal angle. In pathologic cases the pudendal nerve, main nerve, innervates the EAS for a functional rectal contractile reflex response. Other key physiological fact is the rectal distention, directly associated a rectoanal inhibitory reflex, respecting the fall in anal resting pressure. This phenomenon facilitates the flatus discharge and the amplitude and duration of this relaxation increases with the increase of rectal distention [95].

In terms of pathophysiologic mechanisms underlying FI, disruption or weakness of the EAS muscle causes urge-related or diarrhea-associated fecal incontinence. In contrast, damage to the IAS muscle or the anal endovascular cushions may lead to a poor seal and an impaired sampling reflex. Generally after vaginal delivery, 35% of primiparous women present anal sphincter disruption [105]. Other risk factors include forceps-assisted delivery, prolonged second stage of labor, large birth weight and occipito posterior presentations.

In the pelvic floor excessive perineal descent, aging and trauma can lead to PRM damage causing obtuse anorectal angle sphincter weakness.

The innervation of the pelvic floor is essential for maintaining continence. The most relevant innervation dysfunction concerns the pudental nerve. The damage of pudental nerves occurs during the childbirth due to stretching and elongation of nerves. Higher damage happens when fetal head is large or heavy, when the second stage of labour is prolonged and when high forceps are applied [95, 106].

Rectal accommodation can be also affected by previous hysterectomy, radiation proctitis, ulcerative colitis or infiltration of the rectum by tumor. In these cases the rectal wall compliance is impaired and consequently a determinate volume of stool material can generate high intrarectal pressure that can overwhelm anal resistance and cause incontinence. Some medicaments are also responsible for inhibiting the sphincter tone (i.e; anticholinergics) [105].

3.1.5 Epidemiology - POP, UI and FI

Until now there are no epidemiological studies of POP, UI and FI in community-based populations. The majority of published studies are from clinical populations, especially from registers of surgical procedures that are specific for prolapse in the most severe degrees [107].

The prevalence of prolapse at hymen's level (I-IV) varies from 2% to 48%. This broad range is likely to result from differences in sources of study populations, age, race, parity and examination techniques [90].

In Women's Health Initiative proposed by ICS, which used a non-validated physical exam to measure prolapse in post-menopausal women, the overall presence of prolapse was 41% and 38% for women with uterus and after hysterectomy, respectively [106].

In the Swedish study, mentioned earlier, 44% of parous women of studied ages (20 - 59 years old) had some form of prolapse [95]. As stated previously there are many aspects of childbirth to consider in assessing risk: vaginal delivery, instrumented delivery, episiotomy, birth weight, time and management of second stage, type of anesthesia and others [60].

A designed study with 4458 completed surveys in significantly older women, approximately 64 years old, showed that 13% of respondents had POP (29% and 19%, UI and FI, respectively), clarifying that older populations or countries with aged populations can show higher potential to develop multidimensional pelvic floor diseases. Nowadays these disorders may be prevalent due to the increase of average life expectancy [96]. The annual incidence of surgery for POP varies between 0.4 per 10,000 in women aged between 20-29 and 34.3 per 10,000 in women aged from 70 to 79 [107].

The prevalence of prolapse based on the absence of symptoms is also controversial. Normally the prevalence of symptomatic prolapse varies between 7% and 23%. This is easily explained by both asymptomatic anatomic changes and the lack of correlation between prolapse symptoms and measured pelvic prolapse [107]. In contrast, for prolapsed women in the posterior compartment, symptoms of low back and groin pain are very common among women with any degree of support or prolapse. In one study 33% of subjects (range of 18-82 years old) reported that as a bothersome symptom [108].

However, 'bulging' is the main symptom that correlates with prolapse severity and also this well-known symptom (by 'feeling' and 'seeing') is correlated moderately to the greatest extent of prolapse. In one study, when prolapse reached 1 cm outside the hymen, 84% - 87% patients reported symptoms of bother, and once the prolapse reached 3 cm outside the

hymen, more than 90% of subjects reported bother [5]. Besides, the prevalence of prolapse measured by physical exam is higher than the prevalence of symptoms of prolapse [107].

It has been postulated that the incidence of POP may be affected by race and ethnic. It has been suggested that black women may be less susceptible to prolapse than white women, but the majority of few studies reveals inconsistent findings [109 - 110]. In 2003, 199,698 women underwent prolapse surgery and racial disparities between caucasian and black women appeared to exist. Rates of prolapse surgery per 10,000 women were 14.8, 5.6 and 8.7 for caucasian, black and other races, respectively [109].

Regarding pelvic floor compartments, the anterior compartment is usually more affected due to high abdominal pressure done on the coupled muscles and fascia. It was found that cystocele and uterine prolapse was 15.3% and 3.1%, respectively, among 509 45-year-old women [95]. Prolapse occurs most frequently in the anterior compartment, next most frequently in the posterior compartment, and least in the apical compartment. The majority of prolapse degree in affected women is mild to moderate measured as I and II, respectively [98, 107].

3.1.6 Diagnostic of Pelvic Dysfunctions

The examination and investigation are normally done to identify POP and any concomitant SUI. Traditionally prolapse has been defined as first degree if it descends within the vagina but above the introitus and second degree if it descends outside the introitus. Currently, most clinical care worldwide is given following simple physical examination. However, additional tools are useful in the clinical care of complex patients and essential for describing patients participating in research studies. These additional tools include speculum observation, various digital assessment modalities (i.e. MRI, 3D Ultrasound, etc) and urodynamic tests (i.e. videourodynamics, etc) [4, 110-116].

Cystometry and uroflowmetry are recommended in women with genital prolapse to evaluate potential stress incontinence, UI, and emptying phase dysfunction. In general, potential stress incontinence may be masked by prolapse, so urodynamic studies should occur before any surgery [4]. Almost half of women with advanced POP experience incomplete bladder emptying undergone specific multichannel urodynamic testing [111]. Proper patient evaluation, including videourodynamics and measurement of Valsalva leak point pressure, is the key to making the best treatment decisions and obtaining optimal patient outcomes (Figure 17). Stress leakage tests are sufficiently accurate to measure stress incontinence: any case when abdominal pressure causes leakage and detrusor pressure is minimal (coughing or straining), true stress incontinence is present [103].

If prolapse is visible at the vaginal introitus or 'bulging' is noted during the Valsalva maneuver, a systematic examination should be performed. With the patient in a supine position and the head of the examination table elevated to 45 degrees, an appropriately sized vaginal speculum is placed in the vagina to view the cervix to vaginal cuff. While the patient is performing the Valsalva maneuver, the speculum is slowly removed. The extent to

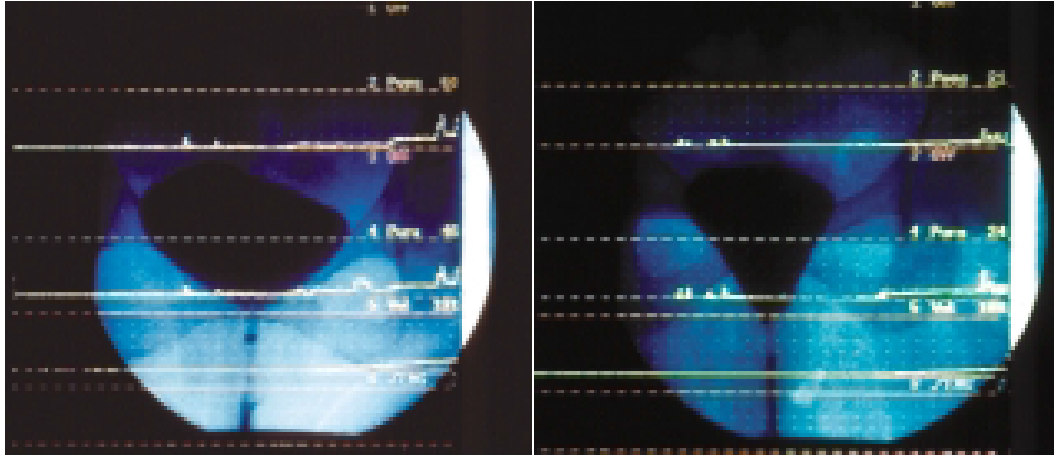


Figure 17 - The images present assessment of stress incontinence and cystometrogram through video study. On the left is shown a videourodynamics frame of a female patient with stress incontinence: mobility of the urethra and bladder base, presence of leakage and the cystometrogram is flat, indicating detrusor pressure component. On the right image is shown a videourodynamics frame in an elderly woman with stress and motor urge incontinence symptoms. There is lateral detachment-type small cystocele and gross leakage with stress is seen (Adapted from [103]).

which the cervix or the vaginal vault follows the speculum through and out the vagina is noted. The speculum is dissembled and the posterior or fixed blade is used for examination.

Regarding anterior wall examination, the posterior wall is retracted with the fixed blade and the extent of any anterior vaginal prolapse during the Valsalva maneuver is noted. During posterior wall examination, the fixed blade is inverted, the anterior wall is retracted, and the patient is instructed to repeat the Valsalva maneuver. Any resulting prolapse is noted [113].

As it was stated early, the anatomical and functional anatomy of the pelvic floor is highly complex, and imaging techniques are becoming increasingly sophisticated in order to provide the clinician the necessary structural and functional information to optimize patient care management [114]. Since the advent of multiplanar high resolution MRI techniques, considerable insight has been made into etiology and functional significance of injury to the muscle and tissues of the pelvic floor. MR images allow the visualization and identification of a 3D anatomy, showing: average width of functional levator hiatus at the level of the transverse urethral ligament; levator plate nearly parallels the pubococcygeal line in continence women; bladder base lying above the pubococcygeal line in healthy volunteers; mean anorectal junction position lying on the pubococcygeal line; and/or pelvic floor muscles contraction. In a normal anatomy of the pelvic floor the PRM is seen as a separate structure on MRI lateral to the pubovisceralis. The PRM and pubovisceralis are best imaged in the axial and sagittal planes, whereas the larger ICM of the LA complex is better seen coronally. When the pelvic floor muscles present defects MRI plane allows an easy identification and interpretation of the impaired areas (Figure 18). However these techniques have high cost limitations [102]. Most commonly, MR images are acquired in axial, sagittal and coronal planes angled to the pelvic floor muscles using a surface coil placed on the pelvis of the patient. It is possible to acquire detailed high resolution of the anal sphincter complex using an endoluminal approach (usually endoanal coil) [114].

Most commonly defaecography or cystocolpodefecography are used to image the pelvic floor and provide assessment of anorectal function which may help the evaluation and choice of

technique especially in those patients with concomitant bowel dysfunction or to distinguish an enterocele from a high rectocele or sigmoidocele [113].

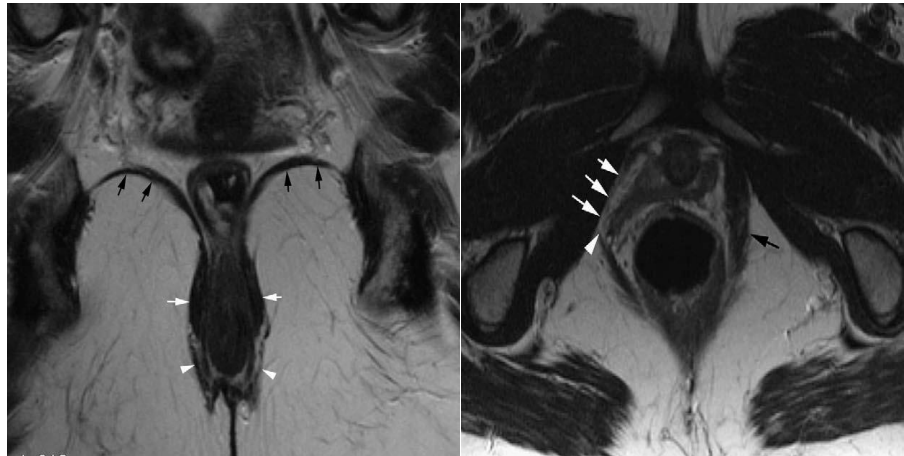


Figure 18 - MRI with high resolution coronal T2 weight image in female without defective tissue (left) and MRI with high resolution axial T2 weight image in female patient with recurrent prolapse (right). In the normal female, the ICM (black arrows), PRM (white arrows) and EAS (arrow heads) are anatomically well positioned within the surrounding pelvic fat. In the clinical case the right pubovisceralis muscle has been completely avulsed (arrow head), with no remaining muscle in its usual position (white heads) and the opposite side shows an intact muscle (black arrow) [114].

Dysfunction fluoroscopy has been used as the most important fluoroscopic technique, in opposition to evacuation proctography or defecography, which involves imaging of rectal expulsion of a barium paste enema. This is a specific test for volunteer muscles. However, where available, MRI will likely replace functional dynamic fluoroscopic imaging of the pelvic floor, giving a relatively non-invasive global assessment of pelvic floor function without the use of ionising radiation. Besides, MRI has many intrinsic advantages over fluoroscopic techniques, like non-using ionize radiation and inherent high contrast such that pelvic organs are easily seen without the need for opacification (Figure 19).

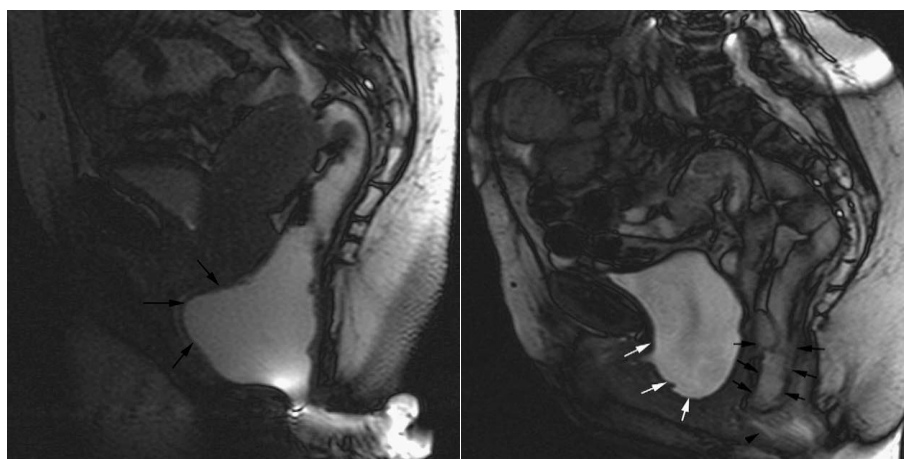


Figure 19 - Sagittal FISP images though the midline of the pelvis in a female patient during MRI proctography. On the left image is shown a large rectocele (black arrows). On the right image is demonstrated a loop of a small bowel has descended anterior to the rectum to form a large enterocele (black arrows). Additionally, is noted a presence of cystocele (white arrows) and small collapsed rectocele (arrow head) [114].

Furthermore, imaging in any anatomical plane is easily achievable. Many authors described the use of MRI as the most feasible and precise technique for assessment of pelvic floor structure and function. Likewise, development of sequences such as fast imaging with steady state precession (FISP) and single shot fast spin echo reduce the overall procedure time and allow rapid images acquisition (around one image every second) [102, 114].

To isolate and evaluate prolapsed states, dynamic MRI multiplanar capability together with patient straining, in some cases, is preferable because prolapse may be visible only with increased abdominal pressure. Thus, the variation between resting and straining images helps to define the severity of the support defects regarding different types of prolapse (i.e. cystocele, vault prolapse or rectocele) (Figure 20 and 21) [110, 115].

Nevertheless, there are some limitations regarding MRI techniques used in urogynecology and female urology: high cost, access limitations, and generally static.

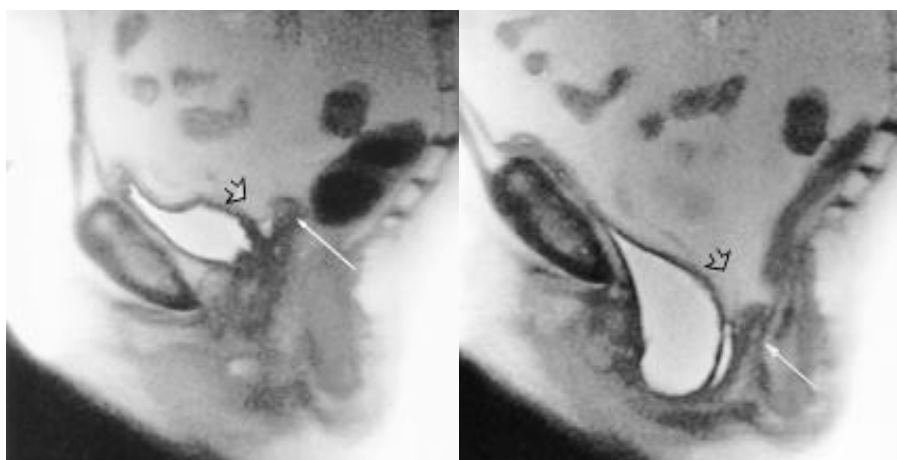


Figure 20 - Sagittal T2-weighted MR images of the pelvis obtained with the patient at rest (left) and straining (right). It is possible to observe prolapse of the vaginal vault during straining movement (solid black arrow). Given this, cul-de-sac (open black arrow) also descends. As well, bladder descent occurs with straining [110].

Therefore, ultrasonography (US) for the investigation and management of women with gynecological problems is now well established. Both transabdominal and transvaginal scanning allow the identification of the uterus and annexes with excellent resolution to direct appropriate management. However, transabdominal US provides poor imaging of the lower

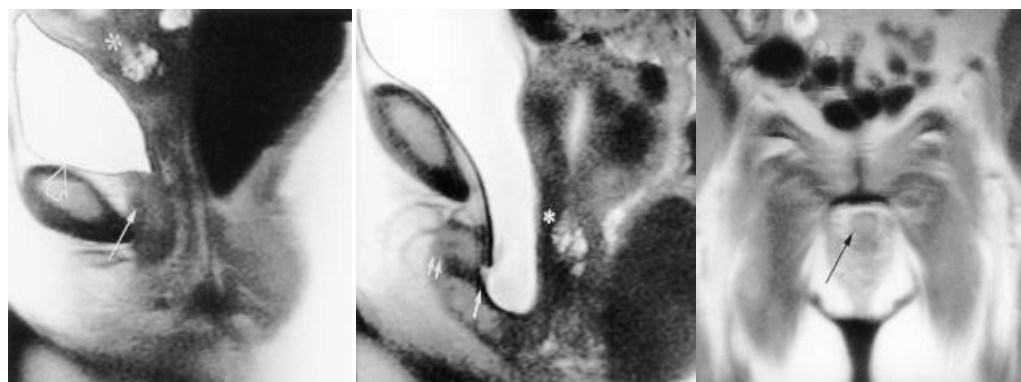


Figure 21 - Sagittal T2-weighted MR image (left and center) and coronal MRI (right) of urethral hypermobility with funnelling in a female patient with SUI and stress urinary frequency. Left MR image shows the urethra in its normal vertical orientation (solid arrow). The bladder (open arrow), cervix(*)

and rectum are also seen. Central MR image obtained with the patient straining presents urethra approximately horizontal in orientation and lying inferior to the pubis. There is presence of SUI with the proximal part of the urethra (arrow) being inferior to the distal portion (double arrows). The entire urethra appears shortened due to funnelling or dilation of the proximal urethra and the presence of urine in the lumen. On the coronal MR image obtained with the patient straining, the urethra (arrow) is seen en face below the pubic symphysis because it is now horizontal in orientation. The striated outer muscle layer in the wall of the urethra is seen as a circular hypointense band [110].

pelvic structures, particularly the support structures of the vagina and LA muscle group, due to the depth of the tissues from the transducer. Transvaginal ultrasound US allows excellent visualization of the bladder, urethra and the posterior compartment but distorts the pelvis thereby precluding accurate assessment of POP [116].

In attempt to overcome this, engineers have been developing translabial or transperineal US. It involves the use of front-firing vaginal endoprobes placed in the introitus. Information is generally obtained with no discomfort to the patient. The transducer can be placed firmly against the symphysis pubis without causing significant discomfort, unless there is marked atrophy. Imaging is performed in dorsal lithotomy position, with the hips flexed and slightly abducted, or in the standing position. There is no agreement on image orientation options (Figure 22).

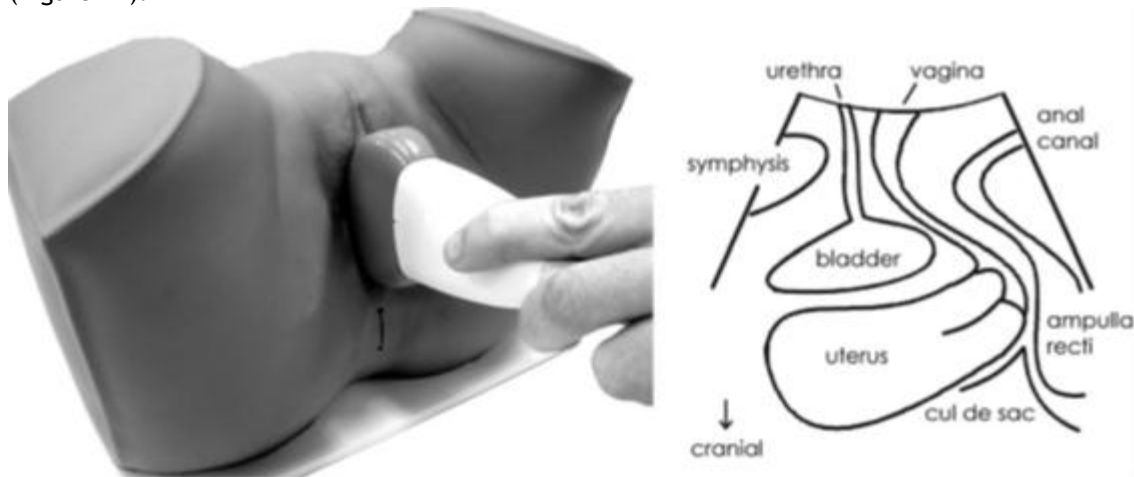


Figure 22 - Demonstration of transducer placement in translabial/perineal US (left) and respective schematic representation of imaging in midsagittal plane [115].

However conventional transvaginal US involves cranioventral aspects to the left and dorsocaudal to the right. Physicians and researchers have been proposing the addition of POP-Q system to US routine pelvic examinations. It is at least equivalent to other imaging methods in visualizing such diverse conditions as urethral diverticula, rectal intussusception, mesh dislodgment, and avulsion of the PRM. Besides, this image technique is helpful in determining residual urine; detrusor wall thickness; bladder neck mobility; urethral integrity; anterior, central, and posterior compartment prolapse; and LA anatomy and function (Figure 23) [115-116].

On the other hand, US is the only precise technique method able to visualize modern mesh slings and implants and may predict who actually needs such implants. It is also very helpful when assessing women with complications of suburethral slings such as voiding dysfunction and de novo symptoms of urgency, helping the surgeon to decide whether to cut a sling (Figure 24). In addition, 3D translabial US has been demonstrating that implanted mesh often is nowhere near as wide as it is supposed to be. This technique allows the

identification of mesh shrinkage, contraction, or retraction [115]. Another powerful tool in pelvic floor digital assessment is 4D US allowing data storage of volumes of information as opposed to single plane images, as well as offline analysis and independent audit [116].

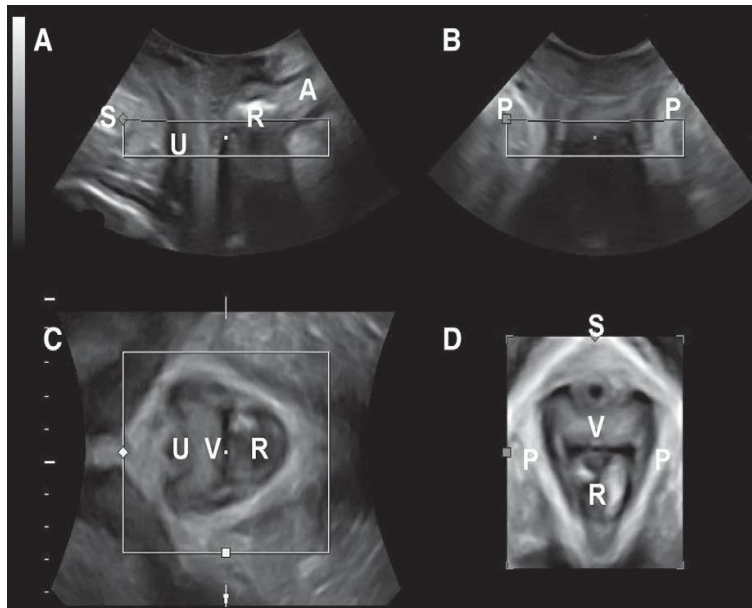


Figure 23 - Standard acquisition screen of 3D pelvic floor ultrasound. A - Midsagittal, B - coronal, and C - axial planes and D, rendered axial plane of female pelvic floor. Region of interest is represented in the transparent box [115].

A, anal canal; P, puborectalis; R, rectal ampulla; S, symphysis pubis; U, urethra; V, vagina.

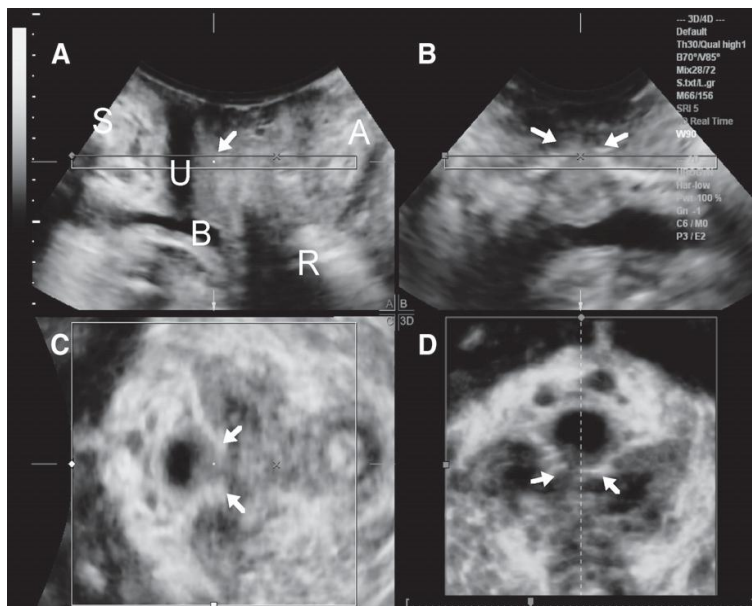


Figure 24 - 3D US images of female patient after TVT division due to de novo urgency, urge incontinence, and chronic mild obstruction. A - Midsagittal plane with arrow indicating most likely tape location. B and C - Coronal and axial views, respectively, with 2 free tape ends (arrows). The gap between 2 tape ends is also evident in D - axial plane rendered volume [115].

A, anal canal; B, bladder; R, rectal ampulla; S, symphysis pubis; U, urethra.

Chapter 4

Pelvic Organ Prolapse Treatment

Management options for women with symptomatic POP include observation, hormonal therapy, pelvic floor muscle training, conservative mechanical support, and several approaches of surgical intervention [4, 8-10, 12-35, 113].

The goal of conservative management is to improve symptoms, reduce progression, and avoid or delay surgical treatment in cases of mild or intermediate POP [67].

Regarding surgical reconstruction and invasive repair interventions, they are specially recommended by gynecologists and urologists in the cases of: post hysterectomy; notable comorbidities, severe vault prolapse with more than compartment affected; recurrent prolapse; failure of pessaries; prolapse combined with UI and FI; patient desire of definitive treatment; and/or no desire to maintain sexual function [10, 12, 15, 99, 111].

An ideal operation should reattach apical support to the pelvic skeleton, restore integrity within anterior and posterior suspensory hammock and re-distribute some of the expulsive load back onto pelvic diaphragm [99].

There are many approaches to the surgical correction of POP, which frequently reflect the nature and anatomical site of the defective support, but essentially the surgeon has to decide whether to perform this surgery vaginally or via the abdomen an open or laparoscopic procedure. The anterior colporrhaphy is still the most common procedure for anterior compartment prolapse with or without the use of synthetic graft; vaginal hysterectomy with uterosacral suspension is performed for uterine prolapse; posterior native tissue colporrhaphy is the most common for posterior compartment prolapse and post-hysterectomy apical prolapse is mostly repaired with abdominal sacrocolpopexy [12]. However, in surgical repairs using native tissue failure rates are as high as 30%, due to weakened pelvic structures and by definition qualitatively insufficient connective tissue [17]. As mentioned previously, Olsen et al. found that after 5 years 29% of patients who undergone traditional repairs had failures and reoperation was required [11].

In surgical interventions performed vaginally, further decisions regarding the use of synthetic or biological graft to reinforce the repair need to be made. Graft use for pelvic floor surgery is commonly accepted, mainly in the form of sacralcolpopexy and TVT both of which demonstrate longevity of successful repair [12,117-118].

Efforts are ongoing to find materials that achieve superior results while minimizing adverse graft-related effects. A variety of prosthetic materials have been developed for the provision of durable support to reduce also recurrence rates in traditional surgery for POP. Graft material can be naturally occurring (i.e. porcine-derived grafts, human cadaveric dermis, autologous fascia lata, etc) or synthetic (i.e. macroporous PP meshes, absorbable

polygalactin-910, polyester meshes, etc) to augment fascial repairs and prevent prolapse recurrence [14, 15, 17, 20].

More recently, PP macroporous meshes are placed tension-free through TVM and delivery vaginal kits (Perigee-Apogee and Prolift systems) have been developed in an attempt to make these surgeries minimally invasive, more standardized, easier to perform, and with low adverse events [22, 27, 29, 34].

4.1 Conservative Treatment

Observation

Regular lifestyle modifications can be employed in women with mildly symptomatic or stage I POP. Weight loss should be recommended as a preoperative measure and also to overweight women with the aim of reducing symptoms. Alternative modifications must be introduced such as smoking cessation, avoidance of heavy lifting and constipation [113].

Pelvic Muscle Exercises

Pelvic floor muscle training may improve pelvic function and limit the progression of mild prolapse, alleviating mild prolapse symptoms such as low back ache and pelvic pressure [4, 113]. This systematic conscious contraction of the muscles of the pelvic floor is commonly known as Kegel exercises (accomplished by electrical stimuli and biofeedback training). Moreover, to isolate pelvic floor muscles are used Kegel cones, being more effective on the prevention and treatment of POP [113]. However, they are not useful if the prolapse extends to or beyond the vaginal introitus [4].

Hormonal administration

It has been suggested that reduced oestrogen levels may affect periurethral tissues and contribute to pelvic laxity and stress incontinence. In addition, oestrogen-deficient vagina (hypoestrogenemia) may develop a less acid pH level and vaginal flora may predispose post-menopausal women to urinary tract infection.

In these critical cases, local hormonal therapy has been based in vaginal creams, tablets or suppositories. Topical and systemic oestrogen therapy increases the skin collagen content and maintains skin's thickness. Besides, they maintain the skin and urogenital territory moisture by increasing acid mucopolysaccharides and hyaluronic acid and maintaining the epithelial barrier function.

Both local and systemic administrations have been proved as effective in the maturation of the vaginal epithelium, and in the decrease of urinary symptoms such as frequency, urgency, dysuria, incontinence, and/or recurrent infections [8].

Pessaries

Pessaries are mechanical supportive devices which are placed in the vagina to restore prolapsed tissue organs to their normal anatomic position. Commonly medical-grade silicone or latex rubber pessaries are used due to their durability, ease cleaning, inertness and

decreased absorption of secretions and odor [113]. There are a variety of sizes and shapes of support and space occupying pessaries (Figure 25) [4].

This kind of non-invasive treatment is used for short-term symptom relief in women awaiting surgery or for long-term treatment in women with high stages of prolapse, who are poor surgical candidates or who have declined surgery.

However some intrinsic drawbacks limit the use of pessaries, such as arthritis, dementia and comorbidities including active pelvic inflammatory disease, vaginitis and endometriosis [4, 113].

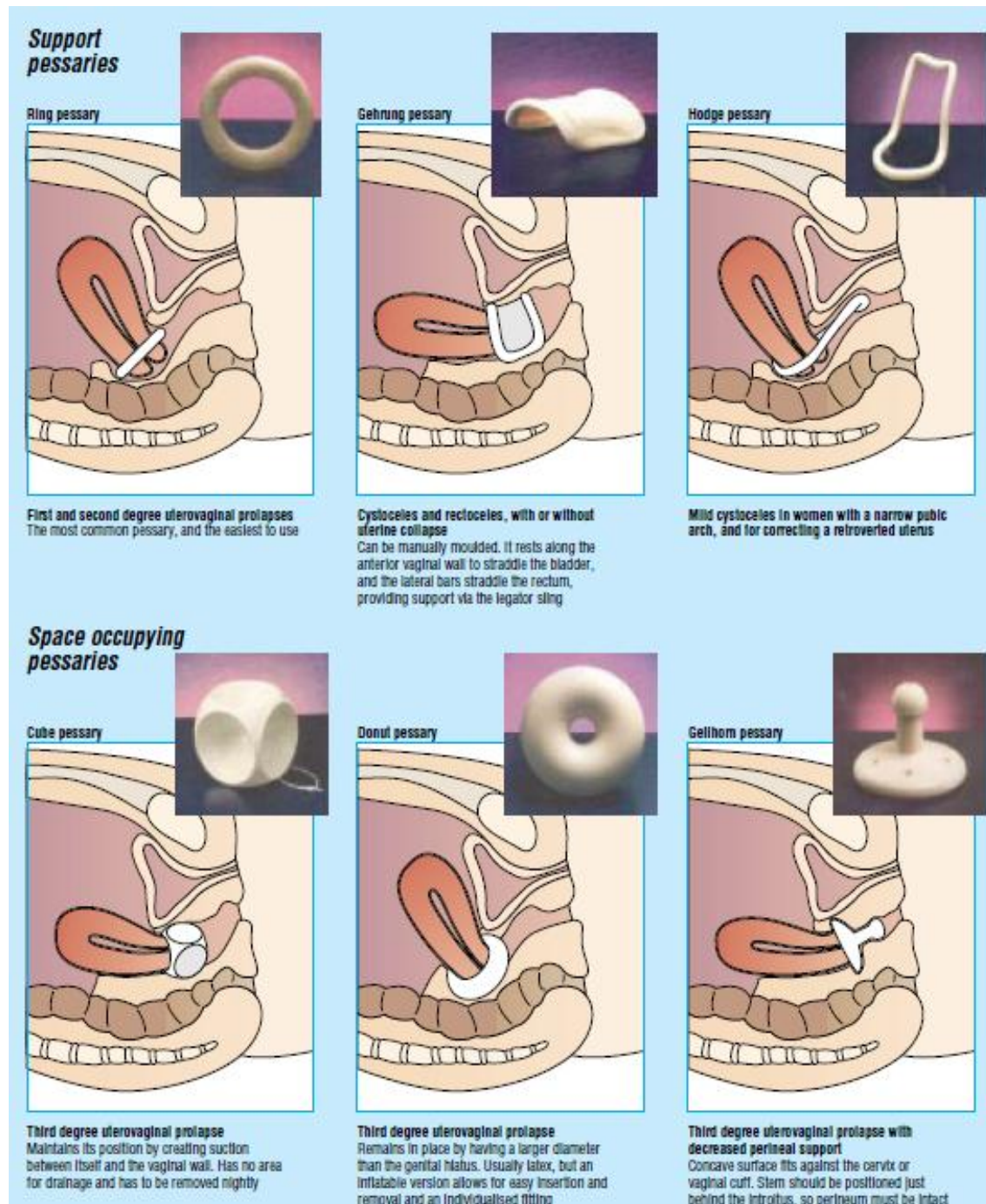


Figure 25 - Types of support (first line) and space occupying pessaries (second line) [4].

4.2 Invasive Treatment

Common vaginal and abdominal surgical procedures for POP repair according to the defective compartment:

Anterior compartment

- **Colposuspension:** approximation of paravaginal fascia on either side of the bladder to the pelvic wall by sutures placed through the ipsilateral and iliopectineal ligaments. The paravaginal repair is a site-specific repair that re-approximates the detached PCF to its attachment along the ATFP. This technique is indicated for urethral sphincter incontinence associated with cystourethrocele grade II or III [4, 12].

Middle/Apical compartment

- **Hysterectomy:** is the total removal of the uterus and can be combined with posterior and/or anterior repair. This technique is performed to treat uterine prolapse and usually involves repair or support of the vaginal vault [4, 111].
- **Sacrohysteropexy:** attachment of the uterus to the anterior longitudinal ligament. Usually is performed in women who want to retain the uterus and wish to bear children [4].
- **Sacrocolpopexy:** vaginal vault is attached by a mesh to the longitudinal ligament over the sacrum (Figure 26). This abdominal or laparoscopic technique is intended to address apical or vaginal vault prolapse in women. This procedure is considered the 'gold standard' of abdominal approaches with high anatomical cure rates ($\approx 90\%$) [4, 10, 12, 16].

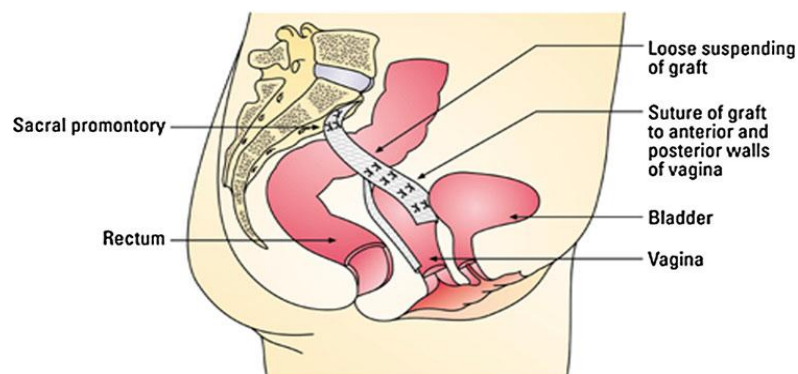


Figure 26 - Sagittal representation of abdominal sacrocolpopexy. Polypropylene mesh is placed over the anterior and posterior vaginal walls and then sutured to the anterior sacrum [12].

- **Uterosacral ligament suspension (McCall culdoplasty):** the McCall culdoplasty obliterates the Pouch of Douglas using a series of continuous sutures suspended to the USL (Figure 27). The procedure is usually employed in post-hysterectomy patients with or without an enterocele and/or vaginal vault prolapse [12, 16, 111].

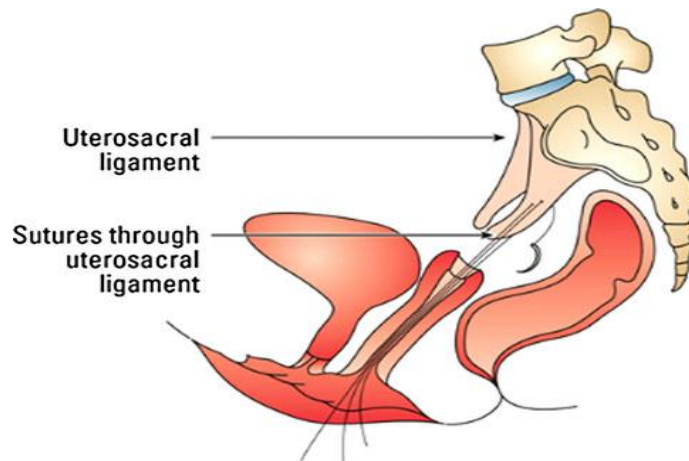


Figure 27 - Sagittal representation of transvaginal uterosacral ligament suspension. The uterosacral ligaments are re-attached to the vaginal vault using specific sutures [12].

- **Sacrospinous ligament suspension:** unilateral or bilateral sutures are placed into the SPL and attached to the vaginal vault. Each end of the suture is sewed underneath the surface of posterior wall. In order to avoid vascular and nerve structure, the sutures are placed 1-2 centimeters medial to the ischial spine. This surgery is often combined with a vaginal hysterectomy and/or surgery to treat prolapse of the bladder; bowel or SUI (Figure 28) [4, 12, 74-75].
- **Iliococcygeal hitch:** vaginal vault suspended bilaterally to the fascia of the ICM, just anterior to the ischial spine (Figure 28) [4, 74].

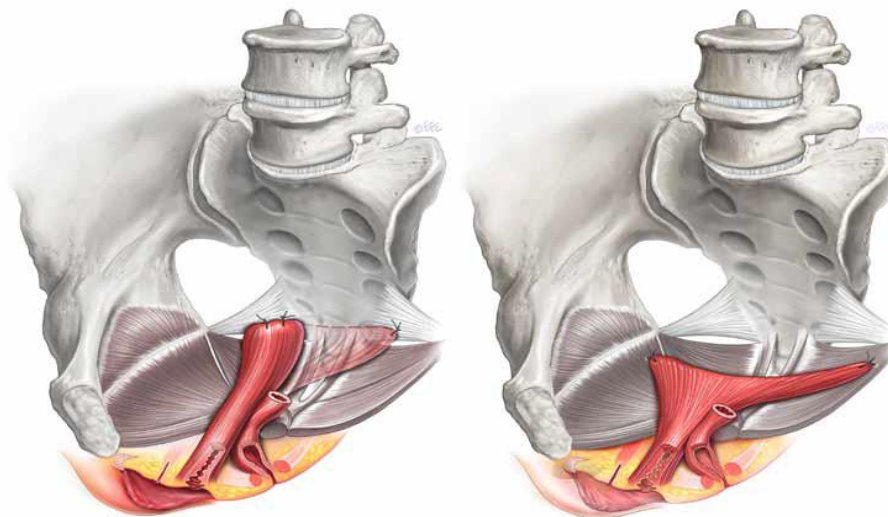


Figure 28 - Medial view of right pelvis regarding sacrospinous fixation (left) and iliococcygeus suspension (right). In the sacrospinous surgical procedure vaginal vault is suspended by both sacrospinous ligaments with stiches. The right suspension is coloured and left suspension appears transparent. In the iliococcygeus procedure vaginal vault is fixated by stiches to both sides of iliococcygeus muscle [74].

- **Intravaginal slingplasty:** open knit PP tape is passed using a specially designed intravaginal tunneler via the ischioanal fossa. Two small perineal incision are made laterally and below the anal margin, allowing the entrance to the fossa. The tunneler pierces the ICM below the SPL to reach the previously made vaginal

incision just below the vault. Then, tape is secured to the vagina and the remnants of the USL by delayed absorbable sutures [16].

Posterior compartment:

- **Sacropolpexy:** involving side-to-side plication without specific identification of fascial defects often combined with midline levator ani plication over the rectum [12].

4.2.1 Traditional reconstructive surgeries: Abdominal (open or laparoscopic) vs Vaginal approaches

Up to now, there is no standardized technique that presents perfect results through a particular route. Furthermore, patients are often older and have coexistence of other medical problems. There are several operations available in these circumstances, particularly for vault prolapse, as well as a variety of new materials that are on the market but not all are evaluated. It is important that proper evaluation is undertaken, as there is scope for both unnecessary expense but also the prevention of further surgery if recurrences can be avoided [16-17].

Concerning surgical strategies for vaginal vault prolapse treatment, both abdominal and vaginal approaches may offer to the patient an excellent cure rate higher than 90% [119].

The surgical intervention selection is dependent on the patients demands (maintenance of sexual activity and childbearing), as well as physiological factors (age, menopause, primary or recurrent prolapse, presence of uterus, site of prolapse, individualized risk for recurrence and pre-existing co-morbidities) [12]. Surgeons play an important role, since they must first identify and repair each defect, anticipate the development of future defects and take surgical steps to prevent their occurrence. On the other hand, it is required optimal experience regarding the surgical technique option [12, 120].

Vaginal hysterectomy is the second most common gynecologic procedure, with over 600 000 operations performed yearly in the United States of America. Uterus prolapse is the commonest indication for hysterectomy in postmenopausal women and patients with severe symptoms who consider the treatment before family completion. Key principles have been established as part of the procedure and technique of VG: namely attachment of the USL complex to the vaginal apex for vault support or high peritoneal closure to prevent enterocele formation [120-124].

However, the removal of the uterus or disruption of this complex, can lead to defects in the rectovaginal fascia, thus causing descent in the posterior vaginal wall and mobilization of the supporting tissues of the cervix. Therefore techniques with uterine preservation are adequate for premenopausal women [121].

In Hogston's review is mentioned that Manchester Repair - transvaginal cervical amputation, anterior colporrhaphy and fixation of the uterosacral ligaments anteriorly and a "wellformed" perineorrhaphy - had optimal long-term cure rates ranging from 87% to 96 %. Vaginal hysterectomy may increase the blood loss, surgical operation time, length of stay in the hospital and the period of convalescence. Generally 25% of women develop a pelvic haematoma following vaginal hysterectomy. It also results in stenosis of the cervical canal. In premenopausal women this can cause painful haematoma and in post-menopausal women in the event of post-menopausal bleeding it can make the physical assessment of the

endometrium very difficult [124]. In addition, some times this technique increases morbidity without evidence of increasing success rate, and shortens vaginal length [16]

A variety of other surgical procedures to conserve the uterus have been described and many show high rates of symptom improvement in a short term. Period fertility after conservative surgery for prolapse is unknown as very few pregnancies have been reported in the literature after such surgery [122]. The two most common modern techniques are vaginal sacrospinous hysteropexy and abdominal sacrohysteropexy [124 - 125].

Roovers et al. compared the effects of vaginal hysterectomy (with anterior and/or posterior colporrhaphy) and ASC surgical corrections in patients with uterine prolapse stages II to IV. They reported a re-operation rate, of 22% and 5% for the first and second mentioned procedures, respectively [125]. In another study, it was reported a long-term efficacy of 93.4% for ASC surgery in women of child bearing age (range, 29 - 34 years and 1 - 5 parity) [126].

In a review study performed by Nygaard et al. it was published data about ASC techniques in long-term treatment of vault prolapse. This study included the use of meshes for reconstructive treatment. In nearly all case studies, surgeons attached the mesh to the anterior longitudinal ligament with sutures, fixed to the promontory. The success rate, when defined as lack of apical prolapse postoperatively, ranged between 78-100% and when defined as no postoperative prolapse, between 58-100%. The median reoperation rates for POP and for SUI in the studies that reported these outcomes were 4.4% (range 0-18.2%) and 4.9% (range 1.2% to 30.9%), respectively [127].

The incidence of site specific POP defects following ASC is not clearly reported. Although, the most common are cystocele and rectocele grade II-III after a long-term follow-up [128]. Sacrocolpopexy provides good patient satisfaction, durable pelvic support and restores vaginal function. In addition, Burch colposuspension or pubovaginal sling is usually performed at the same time for those patients who suffer from stress urinary incontinence. Abdominal sacrocolpopexy with concurrent Burch colposuspension led to a success rate of 94% after a mean follow-up of 34 months and a total relieve of dyspareunia symptoms [129].

Laparoscopic sacrocolpopexy (LSC) is an alternative treatment option for patients with vaginal vault prolapse and multi-compartment defects. This technique via umbilical port, consists, generally, in mesh suturing posterolaterally to the distal LA muscles (rectal artery and recta nerve plexus carefully avoided). Anteriorly, the mesh is sutured to the anterior vaginal wall or cervical fascia. Meshes are trimmed and sutured to the anterior longitudinal ligament of the sacral promontory [129]. This alternative surgery is considered less invasive than abdominal route, with minimal post-operative pain, reduced recovery time and lower morbidity when compared to abdominal intervention treatments [128]. Higgs et al. verified good long-term support of the vault in 92% among women after a considerable follow-up of 66 months, although 42% of women had recurrence of vaginal vault after POP-Q examination. Besides, mesh erosion rate was lower comparing to vaginal route - 20% vs 6% for vaginal *versus* laparoscopic insertion. Relative drawbacks solve depends on surgeon's experience, due to the complexity of each case, since umbilical camera port, various trocars and more than one mesh are used [129-130].

After ASC or LSC or sacrohysteropexy, the vaginal epithelium retracts to a normal shape within a few days, keeping normal thickness, vascularization and innervations. Furthermore, keeping the whole vaginal wall avoids tension and dyspareunia [16]. In this context, open

approaches are preferred when vaginal capacity is reduced and ongoing sexual function is important, or when fertility and future pregnancies are desired [12].

Vaginal SSLS is the most commonly performed transvaginal suspension procedure for vaginal vault prolapse repair. The described advantages of vaginal route for pelvic reconstruction include avoiding the morbidity of an abdominal incision and the ability to repair concomitant anterior and posterior compartment defects using the same surgical site [131]. The SSLS can be accessed via an anterior or posterior approach, with similar reported anatomical success and results in an exaggerated posterior vaginal axis [12]. Surgical management of genital prolapse, and particularly anterior vaginal wall prolapse, is unsatisfactory, as recurrent or de novo anterior vaginal wall prolapse occurs in up to 40% of women after SPLS [75].

In one clinical study using SPLS technique to repair vault prolapse, during long-term follow-up, it was revealed that 3.25%, 8.1%, 0.8% and 0.8% of total women had recurrent prolapse, cystocele, rectocele and enterocele, respectively. It was found a significant difference between vaginal and abdominal approaches, for several surgical procedures in the cure of pelvic floor dysfunctions; women with cervical prolapse, vaginal vault prolapse and vaginal wall descent. In general, vaginal approach increased failure rate with 29% and 10.5% of total women re-operated for vaginal and abdominal group, respectively. Vaginal vault inversion recurred in 12% for vaginal approach and 2.6% for abdominal approach. The vaginal group had also more infections and predisposition for incontinence. This was explained due to two main factors: vaginal approach may predispose the anterior wall to greater pressure forces within the abdominopelvic cavity and neuropathies produced by vaginal dissection [132].

	Germany	France	England
Female population (2005)	42,122,628	32,242,213	25,707,800
Total number of admissions involving POP procedures	36,854	36,679	28,958
Rate of admissions involving POP procedures (per 1000 women)	0.87	1.14	1.13
Admissions for POP surgery as a percentage of total admissions for female genital therapeutic interventions	10.4%	16.7%	16.9%
Percentage of hysterectomies with POP as the primary indication	20.1%	21.4%	25.0%
Percentage of POP admissions that include the following ^a			
Hysterectomy	57.4%	44.5%	40.6%
Colporrhaphy (all types)	n/a	72.9%	93.9%
Anterior	n/a	14.1%	40.2%
Posterior (including enterocele repair)	n/a	15.9%	27.9%
Anterior and posterior	n/a	14.4%	25.8%
Not specified	n/a	28.5%	n/a
Vault repair (all types)	n/a	38.8%	10.3%
Sacropopexy	n/a	6.9%	5.9%
Sacrohysteropexy	n/a	14.9%	n/a
Sacrospinous ligament fixation	n/a	17.0%	n/a
Other	n/a	n/a	4.4%
Average costs ^b			
Hysterectomy	€3316 to €4310	€3404 to €4664	€3440
Other procedures	€2260 to €4759	€2968 to €3827	€2731
Total costs of admissions involving POP procedures ^c	€144,236,557	€83,067,825	€81,028,828

^a More than one procedure may be performed during a single hospital admission.

^b Public sector reimbursement rates in France.

^c Computed using public and private reimbursement rates for France.

Figure 29 - Table with percentage of female undergoing POP surgical interventions in Germany, France and England. The respective costs in each country are considering for public and private hospitalization [1].

It is crucial to outline that these clinical outcomes and recurrence rates associated with POP surgery have major implications on the current costs of POP. Interestingly these outcomes may vary depending on whether biological or synthetic mesh materials were used as part of POP repair. Burden and costs associated with POP surgery are substantial in

developed countries. Subak et al. estimated the direct annual costs in 1997 ranged between 1012 million dollars in USA. Concerning the costs, 49%, 28% and 13% were used in vaginal hysterectomy, cystocele/rectocele repair and abdominal hysterectomy, respectively [133]. An European survey performed by Subramanian et al. revealed the annual costs of traditional surgical procedures (hysterectomy, colporrhaphy, sacrohysteropexy, ASC and SPLS) for POP treatment. It was found that the costs were approximately 144, 83 and 81 million euros in Germany, France and England, respectively (Figure 29) [1]. Thus, programs aimed at reducing the burden of this disease are desirable. It is mainly necessary to decrease number of invasive interventions and reduce recovering time in severe cases of pelvic dysfunctions.

4.2.2 Graft Materials and Urogynecologic Meshes

The success of prolapse surgery may be compromised the excessive movement of the healing vaginal tissues and the increase of intrabdominal pressure increase with coughing, straining, and physical activity in the early postoperative period. Thus, it has become mandatory to improve surgical strategies to decrease the incidence of surgical failure and recurrent prolapse.

While general surgeons have had decades of experience using mesh in hernia surgery, the design and development of grafts in gynecologic procedures is still ongoing.

Nowadays, advances in pelvic reconstructive surgery are due in part to the availability of new biological (xen-, auto- or alloenxerts), synthetic (polypropylene, polyglactin 910, etc) and hybrid (collagen-coated polypropylene) graft materials that allow reinforcement and repair of large pelvic fascial defects in a manner that achieves anatomical and functional results that may be superior to traditional procedures. Efforts are ongoing to find materials that achieve superior results while minimizing adverse graft-related effects.

Recently, multidisciplinary studies involving urogynecology and biomedical engineering have proven advances in new physico-chemical mesh and techniques, and sutures and trocars for mesh insertion. Biomechanical properties have been studied in the last few years, since new materials used to replace support native tissues play a vital role in their in-vivo function. To date, little engineering testing has been considered regarding the choice of materials to be used in incontinence and prolapse surgery [16-17].

General requirements of an implant material for fascial augment repair [17]:

- Cause minimal or no foreign body reaction;
- Should be elastic and flexible;
- Possibility to tailor it easily to its desired size;
- Internal architecture should allow collagen and cellular tissue ingrowth to incorporate the native tissue;
- Provide a strong and permanent tissue repair with a high enough tensile strength;
- It should be inert or well tolerated;
- Local complication rate should be low;

Synthetic Meshes

Polypropylene mesh is a permanent material that is neither absorbable nor degraded and is currently the most commonly used synthetic graft material in gynecology [14 -17, 20].

These materials are made of synthetic filament. The mesh differs in several physical properties including the type of filament (mono or multifilaments), pore size (macroporous > 75 μm or microporous < 10 μm), porosity (defined as the difference between total fabric area and area covered by fabric), weight, architecture (knitted versus woven) and biomechanical properties (flexibility and stiffness) [17]. Amid suggested a classification which is based on mesh porosity and filament type [134]:

Type I: macroporous mesh. The pore size is in excess of 75 μm which is desired for the infiltration by macrophages, fibroblasts, new blood vessel formation (angiogenesis) and collagen fibres;

Type II: microporous mesh. The pore size is lower than 10 μm which presents barrier to new tissue formation;

Type III: macroporous/microporous due to multifilament component;

Type IV: submicronic pores.

Pore size influences not only the flexibility of the mesh but also determines migration and infiltration of macrophages (16 - 20 μm) and leucocytes (9 - 15 μm) into the graft site to prevent infection [14, 26]. The porosity or interstices of less than 10 μm may allow passage of bacteria (usually 2 μm or less), leading to infection triggering [16]. Potential for infection also depends on the chemical properties of the material. In hydrophilic materials, as PP, adherence of bacteria is initial reversible but the process becomes irreversible when the bacteria create an extracellular adherence [20].

Fibroblasts, new blood vessel formation and collagen fibers also require a large enough pore size to be able to migrate into the new materials [14]. Pore sizes > 75 μm allow for rapid ingrowth of fibroblasts and vascular elements necessary to anchor the implant within the native tissue.

Mechanical properties, such as flexibility and strength are dependent on individual stiffness of polypropylene yards, the knitting procedure and pore size. Meshes with large pores are more flexible than implants with smaller pores. Implants that are more interpoled have smaller pores and higher degree of stiffness [17]. Dietz et al, studied the mechanical properties of urogynecologic implant materials, and proved that new non-reabsorbable polypropylene suburethral slings (TVT and Sparc) and meshes (Prolene) demonstrated a non-linear behavior during load-deformation tests. On the other hand, they had lower mean resistance to deformation at forces below the elastic limit, when compared to other biomaterials made of nylon, polyester or polytetrafluoroethylene. The elastic limit for polypropylene implants was only reached at an elongation of almost 50% of their initial length, although at relatively low forces [19]. A stiff non-flexible implant may wrinkle and fold, which in turn causes local pressure, and eventually erosion or pain [17].

In addition, promotion of fibrous growth around the mesh without tissue infiltration is associated with the phenomenon called as 'encapsulation' which decreases the regenerative and biomechanical efficacy, increasing the risk of mesh shrinkage and erosion as the mesh is not being incorporated into the host tissue [97]

In response to the concerns regarding synthetic mesh erosion (10.3%), granulation (6.8%) and dyspareunia symptoms (8.9%), new absorbable alternative urogynecologic meshes have been developed [98]. The most well-known is Polyglactin 910 developed by ETHICON

available in Vycril™ mesh formulations. Additionally a combination of PP and Polygalactin 910 is also available in the market: Vypro™ II [20].

It has been suggested that macroporous tension-free vaginal meshes should be an important contribution to the techniques for the correction of pelvic floor defects since they provide great flexibility, low stiffness and less adhesion formation with underlying viscera [27, 137-138].

Thus, POP monofilament and macroporous implant materials have traditionally been preferred in clinical practice for POP repair. Many laboratories and companies (American Medical Society, Bard, Ethicon, Sofradium, Caldera Medical, American Medical Systems, TEI Bioscience, Atrium and Covidien) have been producing new urogynecologic non-absorbable meshes with safe, durable, great biomechanical and biocompatible properties, shown in Table 4.

Tabela 4 - Types of synthetic mesh used in urogynecology for POP and stress incontinence treatment (including description of mesh properties and main benefits, accordingly to information provided by the different brands).

<i>Devices (Brand)</i>	<i>Mesh type</i>	<i>Main benefits</i>
IntePro™ (AMS)	Lightweight polypropylene (50 g/m ²) and considerable porosity (> 10 µm)	Formulation commonly used in other meshes. High flexibility.
Intemesh™ (AMS)	Silicone-coated polyester. InhibiZone (rifampin and minocycline) impregnated in silicone.	High support for soft tissues and great regenerative capacity
Apogee™ (AMS)	Type 1 polypropylene mesh	Minimally invasive. Allows fixation of biologic material (InteXen™)
Anterior, Apical and Posterior Elevate® (AMS)	IntePro® Lite: Ultra-lightweight polypropylene (< 50 g/cm ²)	Low density allows extreme anatomic comfort and adequate vaginal mobility. Minimal invasive insertion kit and approach. Effective in cystocele and enterocele repair.
Perigee® (AMS)	IntePro® or IntePro® Lite	Tension-free mesh.
Straight-In™ (AMS)	IntePro®	Y-shaped mesh reduces surgical intervention time. Extreme comfort and high flexible support. Effective in cystocele repair.

Prolene™ (Ethicon)	Type 1 polypropylene mesh	Formulation well-used in other meshes.
Vycril™ (Ethicon)	Absorbable mesh of polyglactin 910 (90% glycolide and 10% lactide)	Non-antigenic and non-pyrogenic. Great polymeric absorption during tissue ingrowth
Vypro™ (Ethicon)	Lightweight polyglactin 910	Bigger pores and better biomechanical behaviour than Prolene™
Vypro™ II (Ethicon)	Lightweight multifilament mesh composed Prolene™ 50% and Vicryl™ 50%.	Long-term tissue integration. Effective formation of tissue connective scar.
Prolite™ (Atrium)	Macroporous polypropylene mesh. Monofilaments aligned parallel	Monofilaments well-spaced angles allow optimal material 2D flexibility
Prolite Ultra™ (Atrium)	Lightweight (50 g/cm ²) Litemesh™ with microfilaments and 25% less material than Prolite™	Softer and comfortable. Tensile strength reinforcement that is 83% stronger than the normal abdominal wall tissue.
Gynemesh™ PS (Gynacare)	Prolene™ Soft Mesh	70% more flexible than Prolene™. Lower density reduces the mesh wear.
Prolift® (Gynacare)	Gynemesh™ PS	High strength retention during surgical insertion

Information published in brand sites and brochures.

AMS - American Medical Systems, Inc., Minnetonka, MN, USA. Ethicon - Johnson & Johnson Medical, Somerville, NJ, USA. Gynacare - Ethicon Women's Health & Urology, Somerville, NJ, USA. AMA - American Medical Association (Distributed by Boston Scientific). CM - Caldera Medical, Inc. MM - Mpathy Medical (Acquired in 2010 by Coloplast).

Biologic Meshes

Several complications as mesh shrinkage, erosion and extrusion, translate into a variety of bothersome complains: dyspareunia, pelvic pain, infection and voiding dysfunctions. Regarding this, non-absorbable synthetic meshes have led to an increased use of biologic grafts in pelvic floor reconstructive surgeries, mainly because latter ones show histological and extracellular-matrix similarity, as well as adequate foreign body reaction [14, 17]. When implanted, biologic grafts show lower erosion rates (approximately 10%) than synthetic

implants [136, 138] However, biologic-derived meshes may have potential limitations, such as cost, inconsistent tissue strength and lack of long-term data [139].

Biologic grafts can be divided into three main groups: xenografts (animal donor), allografts (human donor) and autografts (self-donor) [14]. The used xenografts derive from porcine dermis (Pelvisoft®, Pelvicol®, InteXen®, etc), small intestine submucosa (Stratasis®, Surgisis® etc) or bovine pericardium (Veritas, etc). Generally these grafts derive from porcine dermis and have been used throughout the human body. The cellular components are removed, which leaves the three-dimensional architecture of dermal collagen (cross-linked or not) bundles and small amounts elastin fibers intact [20, 139 - 143]. Xenografts and the other two categories of biologic grafts are strictly controlled by the FDA guidelines, which include in this case knowledge of the animal herd, vaccination status, feed source, abattoir approval and bovine spongiform encephalopathy clearance [17].

The host response to xenografts depends mainly on chemical cross-linking and porosity [142]. Chemical cross-linking is intended to increase resistance to degradation by host collagenases, but the long-term fate of cross-linked xenografts in vivo is presently unknown [139-140]. Cross-linked xenografts (Pelvicol® or Pelvisoft®) are stabilized with dicyclohexylmethane-4, 4-diisocyanate (HMDI), to prevent collagenase and inflammatory cells destruction and render the nonresorbable collagen [142]. However, these grafts may be encapsulated without infiltration of connective tissue inside the implant. This encapsulation, as in the case of synthetic meshes, may prejudice the biomechanical behaviour and lead to seroma formation [17]. Other concern respects the prevention of cellular infiltration by crosslinking process which retards the remodeling, vascularization and graft breakdown [143].

Non cross-linked xenografts (InteXen® or PelviSoft®) are designed as scaffold for cellular ingrowth with strong graft material replacement by host connective tissue and fast remodeling of the implant. These scaffolds also avoid poor cytotoxic effects of crosslinking agents (HDMI or glutaraldehyde). On the other hand, there are great concerns about the use of non-cross-linked xenografts due to potential loss of strength at the repair site during graft remodeling [17, 142-143].

Autologous grafts include rectus fascia, fascia lata, and vaginal skin, usually inducing a limited foreign body reaction. They are well incorporated into native tissue and may in theory be used in an infected environment. Main disadvantages are the quantitative and qualitative availability, surgical morbidity at the harvested site and unpredictable durability of the repair which depends on many factors. Weak mechanical properties of connective tissue and poor reinforcement of absorbable fascia, may compromise the supportive and regenerative (Table 4) [16, 20].

Allografts are tissues harvested from a human donor, usually a cadaveric donor fascia lata (Tutoplast®, LifNet®, etc) and transplanted into a human recipient. They have been used in clinical practice for more than 30 years, considered excellent sling material as safe and stable with time. Universally, the local response to allogenic cadaveric fascia is not so widely different from autologous fascia [144-146]. These cadaveric grafts provide same advantageous of autologous fascia, but can overcome the usual complications and morbidity associated with their intraoperative repair (Table 4) [17, 144, 146]. Concerns respect the unpredictable absorption and integration. Usually histopathologic analysis of the grafts shows several failed processes. Grafts normally show areas of linear organization of collagen fibres, relatively low cellularity and low vascularity, similar to native tissue fascia with potential non-inflammatory scar tissue formation. On the other side it might be possible to observe

alternated high tensile strength extents with areas of graft degeneration and total tissue breakdown [147]. Table 5, presents a small resume of all biologic grafts used in urogynecological procedures for the treatment of POP and/or SUI.

Table 5 - Categories of biologic graft materials used in urogynecology for POP and SUI treatment (including composition, device and respective brand)

<i>Category</i>	<i>Composition</i>	<i>Brand - Device</i>
Xenografts	Porcine dermal cross-linked collagen	Bard: Pelvicol®; Pelvisoft® and Pelvilace
	Porcine dermal non-cross-linked collagen	Convien: Permacol®
	Procine non-cross-linked smallintestine submucosal collagen	AMS: Intexen; Cook:Surgisis
	Bovine dermal non-cross-linked	TEI Biosince: Xenform®
Autologous grafts	Fascia lata	*
	Rectus fascia	*
	Vaginal mucosa	*
Allografts	Fascia lata	Bard: Fasлата®
	Human dermis	LifeCel: Repliform®
		Alloderm®

AMS - American Medical Systems, Inc., Minnetonka, MN, USA

* Device not mentioned since graft is harvested from patients' tissue and used for posterior reconstruction of their own pelvic floor

Biosynthetic Meshes

More recently, biosynthetic meshes have been developed with the aim of combining the advantages of synthetic materials and biological grafts [148]. Generally it consists in a synthetic polypropylene mesh (i.e. Prolene) with an absorbable coating, such as porcine collagen (i.e. Pelvitex®) or hydrophilic film (i.e. Ugytex®, normally composed by atelocollagen, polyethylene glycol and glycerol) [149].

The absorbable coating protects the delicate pelvic viscera from the risk of acute inflammatory reaction during healing inflammatory peak. Regarding morbidity, it has been proven a low rate of vaginal erosion (6.3%) with new protected polypropylene mesh. This new formulation increases mesh-tissue integrity, higher biocompatibility and decrease in collateral effects (discomfort, severe pain and erosion) [148-150].

Respecting biomechanical properties, collagen-coated lightweight polypropylene mesh seems to be stronger than polypropylene and porcine dermal collagen alone. Collagen coating is absorbed allowing tissue ingrowth and neovascularization within polypropylene architecture. On the other hand, in the few studies, is noticed minimal fibrosis in which fibroblasts are organized linearly to give strength with low cell-to-connective tissue ratio and adequate vascularity to resemble that of native fascia. Still, significant low rates of clinical cell turnover remains to be determined [151-152].

4.2.3 Novel TVT and TVM procedures for POP repair

TVT procedure for treatment for female of SUI treatment was the first modern minimally invasive midurethra sling operation involving tension-free techniques (TFT) with the use of specific kits in the assessment of the pelvic floor. TFT are mainly used in urogynecology to treat incontinence and prolapse in order to avoid the blocking or stretching of the tissues. In TVT sling reaches from the sub-peri-urethral region to the suprapubic area through guiding probes. It is supported by the various tissue structures that it crosses and a blunt needle is used to place it in position (Figure 30). On the other hand this procedure is much simpler than traditional invasive surgeries, by having all of the necessary equipment, graft, and needles packaged together in one kit. The sling is effective in correcting urinary incontinence and urethrocele, but it cannot be used to correct cystocele. In addition, TVT is the only standardized implant-like procedure that to date has document surveys with long-term follow-ups. It is proved that TVT procedure has high cure rates (> 90%), even after 11 years of functional outcomes followed (93% continent and 97% recommended TVT operation) with no signals of efficacy decline, even when 62% of the population is more than 60 years old [117-118, 153-154]. When women are treated with concomitant vaginal hysterectomy or other pelvic floor reconstruction techniques, postoperative urgency and voiding disorders increase significantly (17.9% and 13% bladder perforation, respectively *versus* 5% of TVT alone) [117]. Throughout published data it is possible to infer that TVT is considered a safe and effective procedure. Prolene® is the most used polypropylene-like tape and studies emphasize no tape rejection. Since genital prolapse with or without SUI is a major health care problem, and even more with an aging population there is an crucial emergency to repair these defects and coupled damaged compartments.

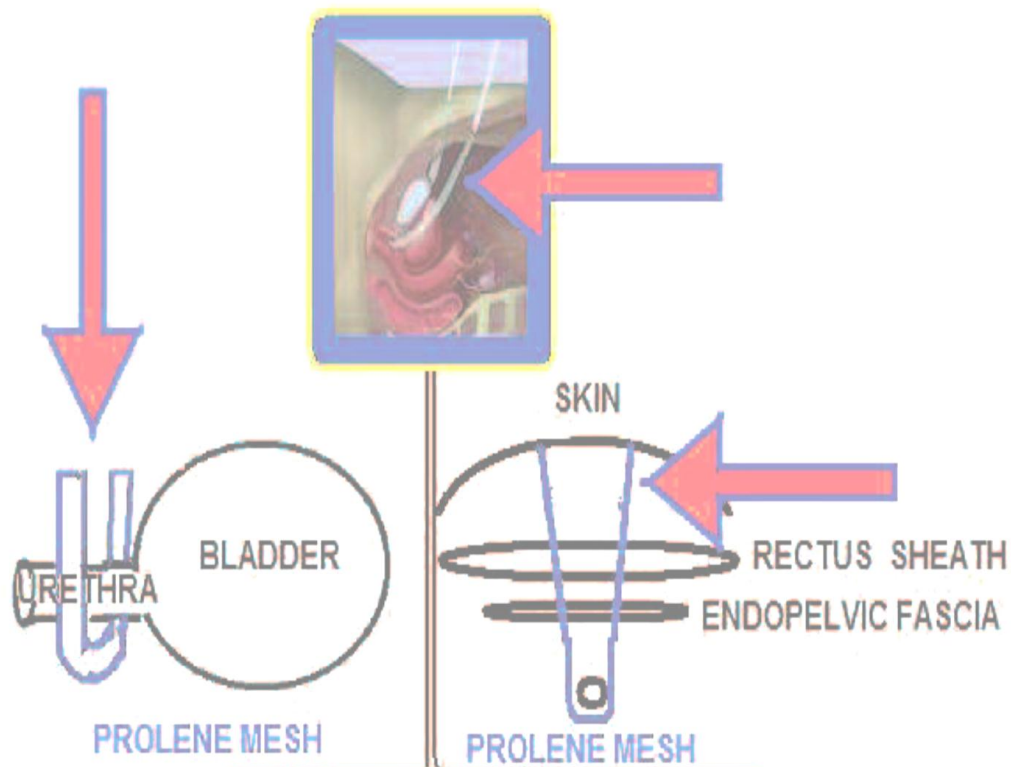


Figure 30 - Schematic representation of Prolene sling with TVT for midurethra support. Sling is placed posteriorly in the midurethra (left) and both arms pass endopelvic fascia and return sheath (right). Arms are then pulled emerging through the obturator membrane (top) [153].

Recently new mesh materials and medical devices have been designed by different companies in an attempt to reproduce standardized kits that have been developed for treatment of female SUI, such as the TVT. The Apogee/Perigee™ vaginal mesh kits (AMS) were the first kits to be released in the United States of America for treatment of POP in 2004. After that the Prolift™ and Avaulta™ vaginal mesh kits were released by Gynecare and Bard Urological, respectively (Figure 31) [29]. These different medical systems employ different types of implant material. However, as it was discussed above macroporous type I PP meshes are still the most feasible material to use in fascial repair. Characteristics of each TVM system can be observed in Figure 31.

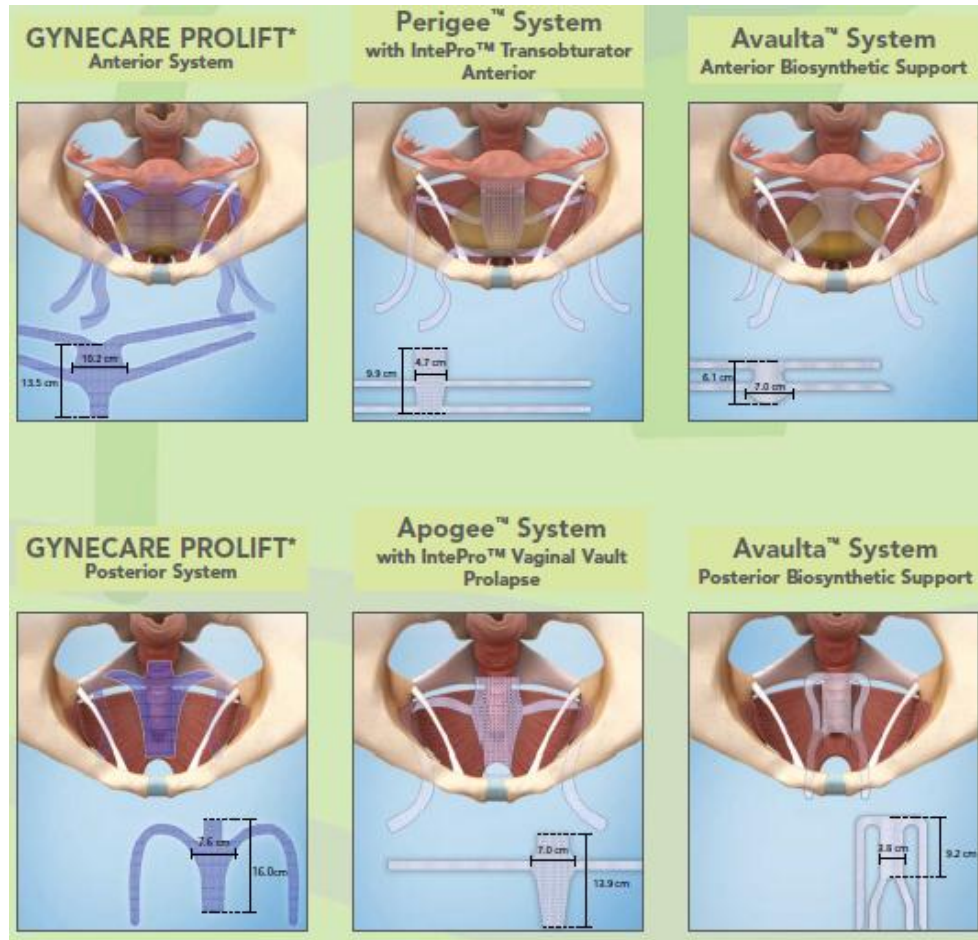


Figure 31 - Representation of tension-free vaginal mesh supports of different brands (Gynecare, AMS and Bard). It is presented from an anterosuperior view meshes precise placement within respective pelvic anatomic sites and corresponding to each repair method. In the first line are displayed the anterior support systems and in the second line there are displayed the posterior support systems [156].

Prolift® Gynemesh or Perigee/Apogee® are similar systems, which have been suitable used for anterior and posterior compartment support when pelvic floor collagenic and muscular structures are irreversibly damaged (Figure 32 and 33). Both use a transobturator approach through the arcus tendineus fascia pelvis. The first pierces to the SPL and the second pierces the ILM [26-27, 29, 30, 34, 155].

Device	Trocar	Anterior attachment	Posterior attachment	Retrieval device	Mesh material
Prolift	Straight + cannula	Proximal & distal ATFP	Sacrospinous ligament	Y	Type I polypropylene; Anterior/posterior/total
Apogee	Straight		Ileococcygeus muscle	N	Type I polypropylene or porcine dermis
Perigee	Helical	Proximal & distal ATFP		N	Type I polypropylene or porcine dermis
Avaulta-Plus	Straight & helical	Proximal & distal ATFP	Ileococcygeus + perineal body	Y (InSnare)	Type I polypropylene coated with porcine collagen; anterior/posterior

ATFP: arcus tendineus fascia pelvis

Figure 32 - Table presenting main characteristics of each tension-free vaginal repair system [22].

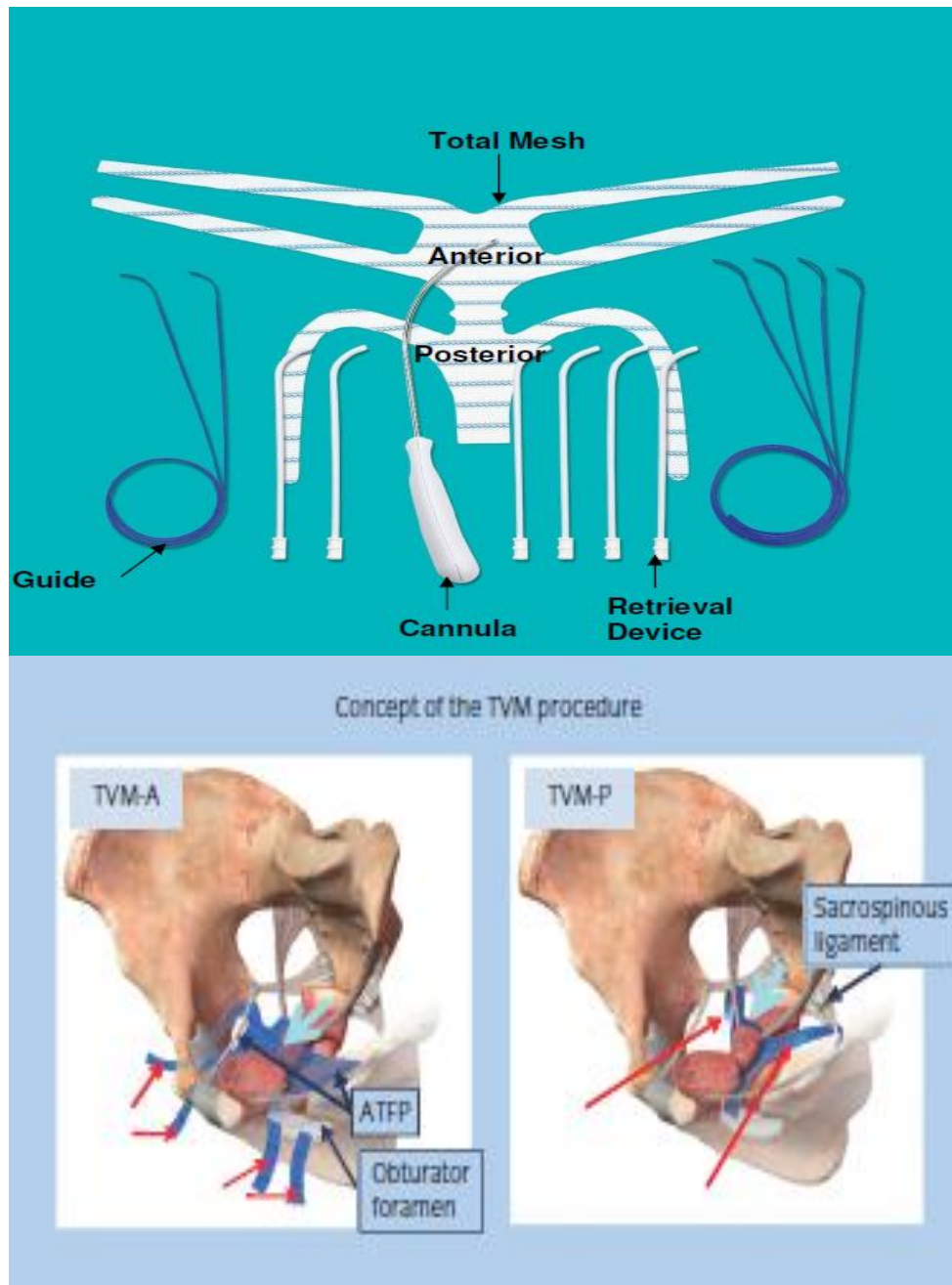


Figure 33 - On the top image there is represented the Prolift™ System with all treatment options (anterior, posterior and total) and surgical objects (insertion guide, cannula and retrieval device) [29]. On the bottom image there is represented the concept of the tension-free vaginal mesh procedure of the Prolift™ System. Mesh is placed to support and reinforce both the vaginal wall and vaginal canal. In the anterior procedure (TVM-A), four arms are passed through the obturator foramen to the arcus tendineus fascia pelvis to restore fascial and lateral support of the vagina. In the posterior procedure (TVM-P), two arms are passed to the sacrospinous ligament to reinforce uterosacral and cardinal ligament complex [155].

TVM and concomitant midurethral TVT sling operations have been showing an anatomic success rate and incontinence cure higher than 90% [157].

Vaginal approaches using synthetic mesh in TVM are effective and safe in vaginal vault, cystocele and/or rectocele support. Gynemesh PS used in Prolift™ procedure allows a 100%

cure rate for both cystocele and rectocele defects after short-term follow-ups (1 to 8 months) [95]. Regarding total Prolift™ vaginal mesh procedure, it has been proved a long-term anatomical correction with considerable success rate for patients with POP stage \geq II. Follow-up studies also revealed that success after 3 years did not differ with cure rates higher than 80% [158]. Interestingly, anterior Prolift™ procedure was tested for repairing lateral defects and turned to be a better surgical solution than the ‘gold standard’ anterior colporrhaphy technique. This is possible due to mesh covering and supporting of the central and lateral anterior vaginal wall [159]. Anterior vaginal wall repair with Prolift™ provides excellent support for impaired connective tissue. However small mesh exposure is still present (\approx 15%) [160]. Nguyen et al verified that 1 year after surgery, Perigee® mesh reinforcement had increasingly higher anatomical cure comparing to colporrhaphy using native tissue; 87% vs 55%, respectively. Besides, rates of dyspareunia for colporrhaphy were almost two times of the polypropylene mesh repair (16% vs 9%). Despite this mesh extrusion was found to be 5% [161].

Although these TVM techniques (Prolift and Apogee/Perigee) reduce intraoperative complications (\approx 0%) and have high anatomic cure rates ($>$ 85%), they introduce high rates of mesh exposure (5%), mesh shrinkage (\leq 17%) and dyspareunia (\leq 13%) [22].

ASC and LSC remains the “gold standard” technique with higher satisfaction rate and objective rate than TVM surgery. ASC performed with polypropylene continue to present high objective clinical rate success (\approx 93%) as well as LSC (\approx 95 %) [127, 130].

Given these facts, the use of TVM for POP repair is not yet definitively validated. However, comparison of TVM procedures with traditional techniques by adequately trained pelvic floor surgeons could greatly elucidate effectiveness and appropriateness of the use these novel surgical techniques in common urogynecologic practices. Despite this, until now Prolift™ anterior and posterior support is the preferred system for minimally invasive pelvic floor repair [22].

On the other hand, alternative replacement of non-absorbable meshes by porcine dermal matrix seems to be the most biocompatibility alternative, with feasible optimal host tissue response and potential regenerative due to its three-dimensional natural architecture. However, since the prolapsed tissue is weakened (even more in older patients), high genital prolapse recurrent rates are associated with porcine-derived scaffolds (19 - 25%). The high recurrence rate of genital prolapse with resorbable mesh suggests the importance of using a more permanent implant. This reinforces the use of PP even if the associated erosion rates are high [139, 162].

Long-term reduction of recurrent prolapse, mesh erosion and optimal host tissue, followed by one ideal support and reconstruction of pelvic floor, can be potentially achieved by new protected low-weight polypropylene. Ultra-lightweight mesh protected by hydrophilic absorbable film can reduce the mesh erosion ($<$ 7%), leading to better graft integrity and tensile strength. More precisely, Ugytex (Sofradium) has an almost perfect anatomic cure rate (93 - 97%), offering consistent tissue ingrowth and connective tissue differentiation. Randomized and controlled trials should be done confirm these promising results [149].

Chapter 5

Biomechanics of Pelvic Floor and Surgical Meshes

In the past decades meshes have been placed within vesicovaginal and rectovaginal space to replace impaired native tissue and to allow a feasible support of pelvic organs. Therefore a better understanding regarding biomechanical properties of normal and defective female pelvic floor could be crucial to enhance reconstructive surgery techniques and develop more functional surgical implants designed for the use of genital prolapse repair. As it was mentioned early, pelvic diaphragm (levator ani muscles) and connective tissue (support ligaments and endopelvic fascia) play a major role regarding pelvic organ support and mechanical management during standing and loading scenarios (daily abdominal pressures).

Accurate knowledge of complex properties and mechanical function of these tissues can be developed through the use of 3D computer-based models. Numerical mathematical models can be established to predict different states of complex systems through wide range of design (CAD) biomechanical (FEM) tools.

5.1 Pelvic Floor Mechanical Structures

Muscular Dynamics

As it was mentioned in Chapter 2, pelvic floor is made of innervated LA skeletal muscle. The LA is composed of elongate, multinucleate, cylindrical structures called fibers that bear alternating striations formed by the presence of intracellular fibrils. This unique structure allows voluntary contractile control. Together, the LA skeletal and smooth of pelvic viscera contribute to functional changes of the pelvic supporting tissues. Therefore, LA has the functional capability of supporting both pelvic and abdominal organs acting synergistically with the striated muscle of the anterior abdominal wall which generates several intra-abdominal pressures. Like any other soft tissue LA muscle as a non-linear mechanical behavior allowing large deformations but has the capacity to act dynamically depending on the firing rate of nerves [50].

Functionally, normal activity of LA keeps the urogenital hiatus closed against the opening action of the intra-abdominal pressure. On the other hand, this complex muscle exerts a key resultant force in a ventroencephalic direction, thereby helping to compress the rectum, vagina, and urethra, from back to front as it equilibrates intra-abdominal pressure. When standing it is exerted a 92% larger vaginal closure force comparing to supine position. The capacity to maximal contraction of the LA leads to an increase of vaginal closure force of 46%

by pubovesisceral and puborectalis muscles. Posterior to this, rectum, distal vagina and urethra are compressed behind the pubic bone distally and against intra-abdominal pressure more proximally. In the mid and dorsal iliococcygeus portion of LA, maximal contractile forces contribute to move the central region of the posterior pelvic floor upward [62].

LA muscle together with pubococcygeus and transvers muscle have also an important role in the opening and closure of urethral and anorectal orificies.

When urethral orifice is closed in relaxed scenarios the elastic tissue of the vagina is exposed to pressure from proximal LA muscle, inferior part of pubococcygeus muscle and longitudinal part of the transverse muscle. When urethral orifice is closed during mechanical efforts distal vagina and urethra are moved posteriorly by pubococcygeus muscle action. Then, vaginal tissue transfers enough dynamic response to close proximal urethra and vesical cervix (Figure 34).

During anorectal closure the LA muscle pushes anteriorly the rectum in the direction of the anus. At the same time the transversal muscle is stretched and originates an inferior force downward helping to form an anorectal angle to finally close the orifice. Contrarily, during evacuation is necessary a relaxation by the puborectal muscle [78].

In the case of defect of the natural hyperelastic properties or if the LA muscle is relaxed, the pressure on the side of pelvic organ may become greater permitting the organ to descend [50]. It is known that LA defects occur during vaginal birth. It results in reduced pelvic floor muscle strength, enlargement of the vaginal hiatus and consequent prolapse of the pelvic organs [163].

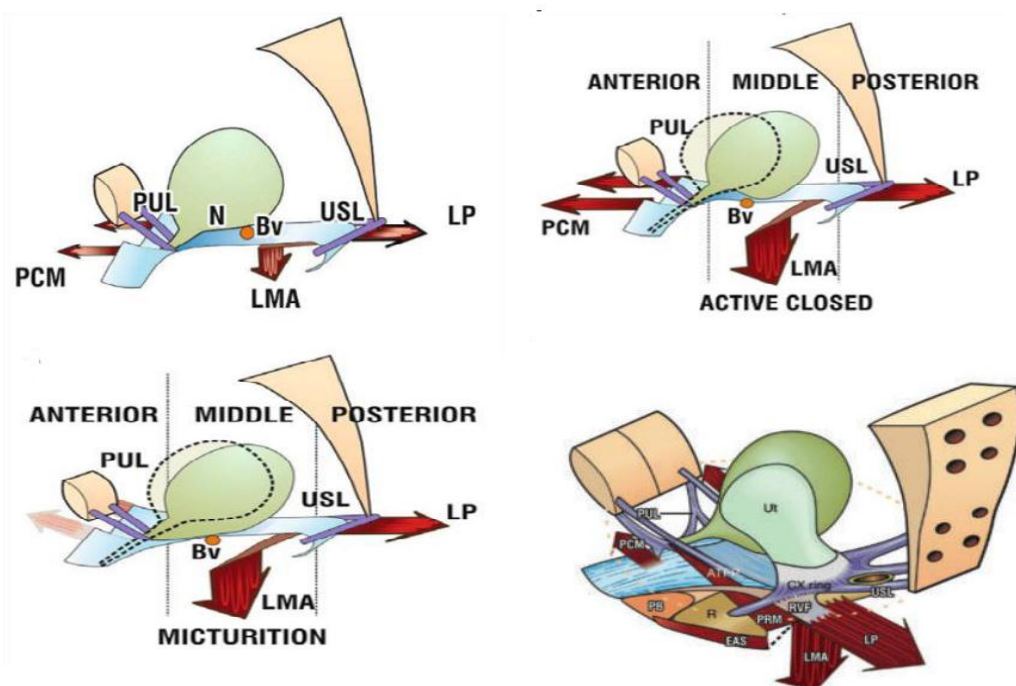


Figure 34 - Schematic representation of urethral (top and bottom-left) and anorectal (bottom-right) opening and closing mechanisms. It is displayed three different urethral configurations: closed during tissue relaxation (top-left); closed during strength efforts (top-right); and opening during urine expel (bottom-left). (Bv - bladder-vagina fixation, LMA - transverse muscle, LP - levator ani muscle, PCM - pubococcygeus muscle, PUL - pubourethral ligament, and USL - uterosacral ligaments) [78].

Connective Tissue Dynamics

It was discussed in previous chapters that pubocervical fascia and vaginal/uterine ligaments are key components for a stable support of pelvic organs. Mechanically, these passive tissues are capable of transferring physiological forces. Their mechanical ability can be analyzed regarding biomechanical compositions and spatial organization. Connective tissue consists primarily in collagen (I and III) with smaller amounts of elastin and smooth muscle. Collagen confers a rigid matrix during intra-abdominal loads and a designed-support structure for ligaments and fascia. It provides feasible network to resist compressive forces. On the other hand, elastin provides tissue resilience - passive recoil without much energy loss following high degrees of deformation. This property is crucial to normal dynamic function of the connective tissue attached to the vagina. These elastic fibers are designed to maintain their elastic function for a lifetime. However, in the female reproductive floor these structures can be degraded and re-synthesized following vaginal delivery. The MMP, collagen and elastin degrading enzymes, have been found to be up-regulated in women vaginal tissue [164].

In general, pelvic support ligaments are recognised as being the strongest element of the pelvic assembly unlike the vaginal tissue being the weakest. Significant failure of these passive structures may lead to vaginal tissue descent. Difference in resistance of the anterior (pubocervical fascia), posterior (uterusacral ligament) and paravaginal (arcus tendineus) mechanical support can result in genital prolapse [55].

It is suggested that the USL are the least deformable and most rigid structures among pelvic ligaments. Thus, it seems appropriate to use USL as strong anchoring element in pelvic floor reconstruction. When their structural integrity is affected, quantity and quality of collagen in the pelvic support tissues is inferior to women with normal support [53, 60, 164].

5.2 Morphological and Biomechanical Properties of Pelvic Tissues

In order to understand physiopathological characteristics (3.1) and progressive changes in different muscular and fascial tissues, it is strictly important to perform adequate mechanical tests together with biochemical investigations of living tissues. Research work has been proving that biomechanical weakness of the supportive tissues, either at the systemic or local level, may predispose women to POP. The structural components of female pelvic floor include, as it was mentioned in 5.1, multiple classes of collagen and elastin which when affected lead to pelvic organ injury and prolapse [60].

In a first attempt to study the biochemical changes in connective tissue, in 1987 Ulmsten et al. found that women suffering from SUI had 40% less collagen in the connective tissue when comparing to normal female [165]. Despite this, Falconer et al. have found that the concentration of collagen was higher in women suffering from SUI [166]. Another research work proved that changes in the quantity of type III collagen in with SUI were relevant. Liapis et al. findings suggested that connective tissue that supports the uterus at the USL and paravaginal fascia had significantly less type III collagen regardless of the degree of pelvic relaxation. However, the mechanism by which collagen metabolism is altered remains unknown [167].

In 2003 Janda et al. performed an experimental measurement of pelvic muscle structures in a 72-year-old cadaveric female. It was used MRI to describe the geometry of muscle fibers.

By the use of several reference landmarks it was obtained morphological data concerning fibre directions and optimal fibre length onto the geometrical data based on segmentation from MRI scans. Therefore, the complete diaphragm was divided into 8 muscles parts and each part was segmented to 22 muscle elements (Figure 35). This data was used for a posterior construction of a numerical-like model using finite elements [37]. De Lancey et al. found that women with POP were more likely to have LA defects than women with normal support - 55% vs 16%, respectively. They also compared vaginal closure force at rest and during maximal pelvic muscle contraction with an instrumented vaginal speculum. Women with prolapse generated less vaginal closure force during pelvic muscle contraction than controls - 2.0N vs 3.2N, respectively. Additionally genital hiatus of female patients was 50% longer than in case controls [168].

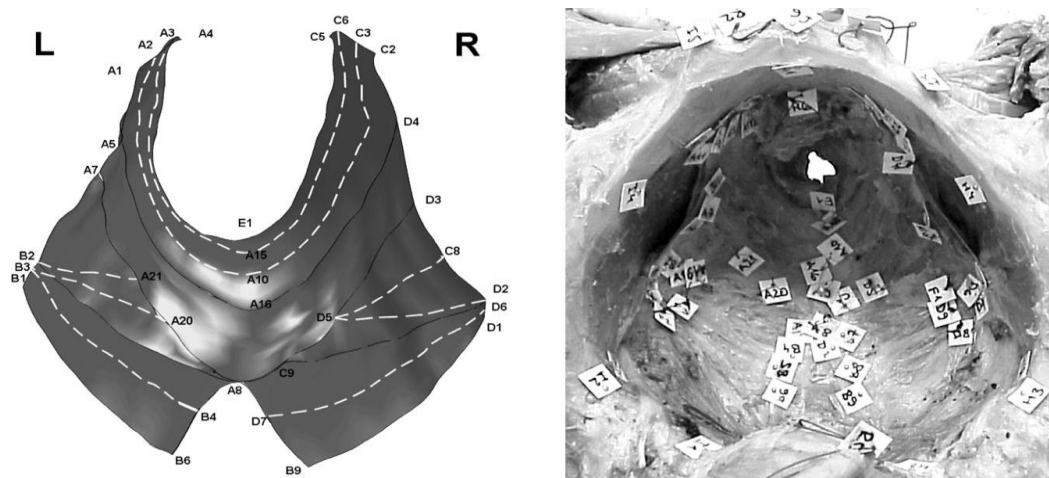


Figure 35 - Representation of 72-year-old cadaveric female pelvic diaphragm with respective landmarks (right image) and 3D geometrical computer-based anatomy (left image) of the pelvic floor muscles based on the experimental data set measurements from the 3D palpator device (designed for these type of measurements) [37].

In 2006, Janda developed a deep research during his thesis. The main research goal was to understand the complex biomechanical behaviour of pelvic floor muscles. He found that biomechanical mechanisms determining the behaviour of the diaphragm pelvis (pelvic floor muscles as well as connective tissue) are not yet understood. It was considered that the major problems are caused due to 3D complexity of the pelvic floor, the relation between active muscle tissue and connective tissue, and the complex loading by the intra-abdominal pressures and organs acting perpendicularly to the muscle fibers. At the same time a FE model was developed to predict the effect of surgical interventions and to give insight into the fundamental behaviour of the diaphragm complex [50].

Cosson et al. studied the strength at tearing of pelvic ligaments used in the cure of prolapse and urinary incontinence. There was a great variability between values - minimal values at around 20N and maximal values at 200N. The SPL and ATRF, usually requested for pelvic floor repair, presented lower values when compared to prevertebral ligaments - 20-30N vs 180-200N. This could explain the 10-30% surgical intervention failure described elsewhere, on the outside of technical problem, particularly for the SPL or the ATRF [55]. Later, Rivaux G. et al. hypothesized differences in the strength of various pelvic ligaments and evaluated their biomechanical behaviour. Uniaxial tension tests were performed in fresh female cadavers without prolapse to obtain stress-strain curves. They observed a non-linear

stress-strain relationship and a hyperplastic mechanical behaviour of the tissues (Figure 36). Besides authors concluded that USL was the most rigid ligament comparing to round and broad ligaments [53].

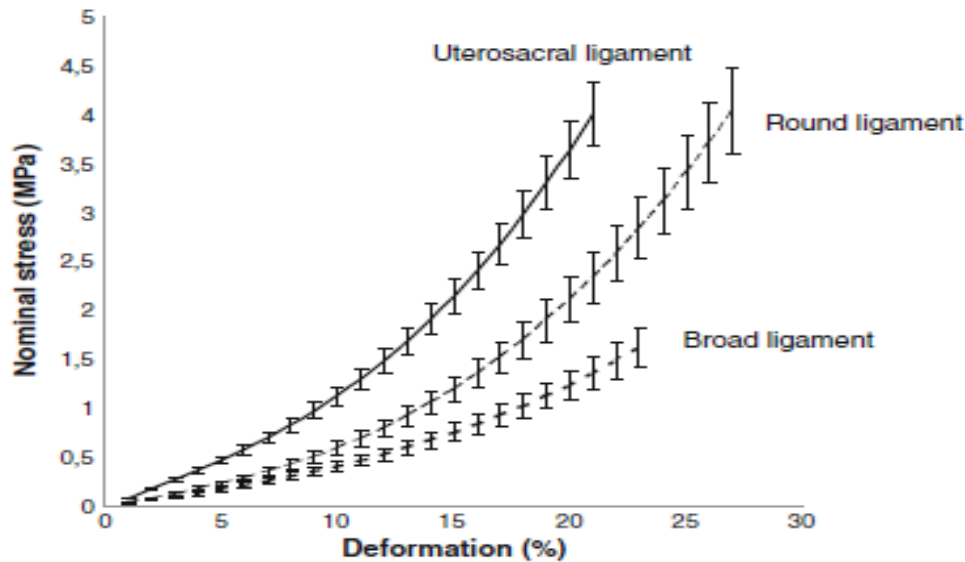


Figure 36 - Biomechanical properties of pelvic ligaments studied by Rivaux et al. Mechanical response of uterosacral, round and broad ligaments to tension loading. Representative stress-deformation curves show the non-linear and hyperelastic behaviour of the tissues [53].

In 2007, Lei et al. studied the relationship between biomechanical properties and the occurrence of POP through analysis on biomechanical properties of vaginal tissue. It was used biopsy specimens from patients undergoing transvaginal hysterectomy into premenopausal POP, postmenopausal POP, premenopausal control and postmenopausal control groups. It was confirmed that the Young's modulus and Poisson's ratio were 12.10 ± 1.10 MPa and 0.39 ± 0.01 in postmenopausal POP group and 10.26 ± 1.10 MPa and 0.42 ± 0.01 [169]. A few years after, Martins et al. performed similar tests in different vaginal tissue specimens of postmenopausal women, during prolapse-correcting surgeries. The vaginal tissue was assumed to behave as a transversely isotropic hyperelastic material, confirming the findings of Lei et al. On the other hand, comparing Young's modulus values obtained for the average data, ≈ 9.7 MPa, with those reported by the last authors for post-menopausal women with prolapse, 12.1 MPa, it was seen that they deform with the same magnitude (Figure 37) [59]. Both findings corroborate differences found by Epstein et al. regarding prolapsed vaginal tissue. Furthermore Epstein et al. found that the vaginal extensibility was related to POP-Q stage [60].

In 2011, Martins et al. presented an experimental study concerning the tensile biomechanical properties of female bladder tissues without previous observable clinical pelvic floor conditions. Interestingly they found that bladder tissue from younger women was stiffer than older subjects. Results of different bladder tissues demonstrated a stiffness ranging from 1 to 4.1 MPa (mean of 1.9 ± 0.2 MPa) and maximum stress ranging from 0.5 to 2.6 MPa (mean of 0.9 ± 0.1) [51].

In 2012, Rubod et al. studied the biomechanical characteristics of the pelvic organs: vagina, uterus and rectum. In the study it was verified a nonlinear and hyperelastic behaviour

during stress-deformation uniaxial tests (Figure 38). The ultimate strain level before tissue rupture for the vagina, rectum, and the bladder was 20%, 30% and 80%, respectively. These data confirmed the weak rigidity of bladder and rectum which is a key factor to allow these organs to fulfill deformation without rupture, in accordance with their filling (urine and stool) function and organ mobility [52].

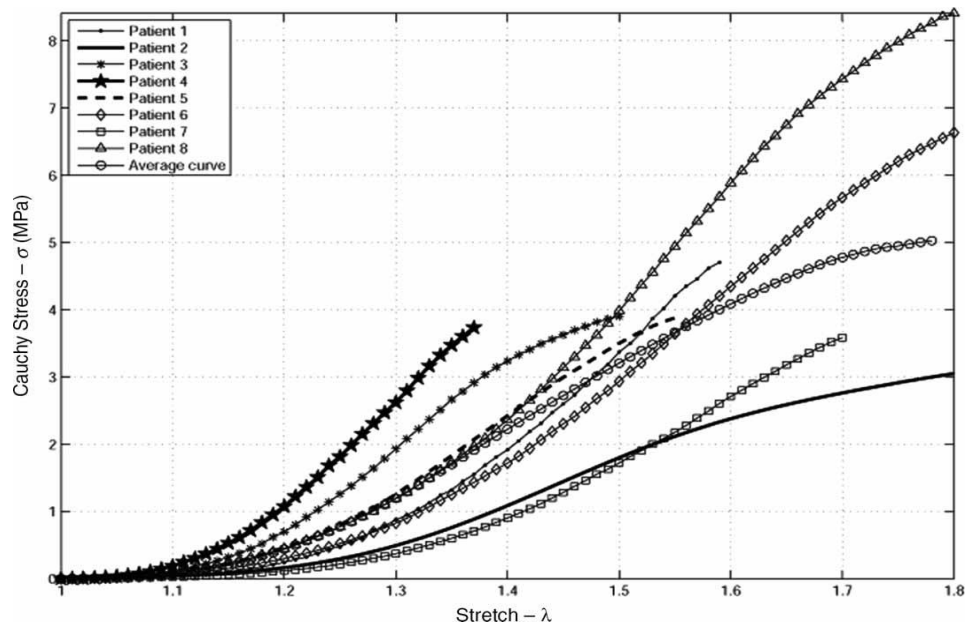


Figure 37 - Experimental data acquired in [59]. Biomechanical testing stress-deformation curves of 8 specimens of vaginal prolapsed tissue. Bold line represents the average data.

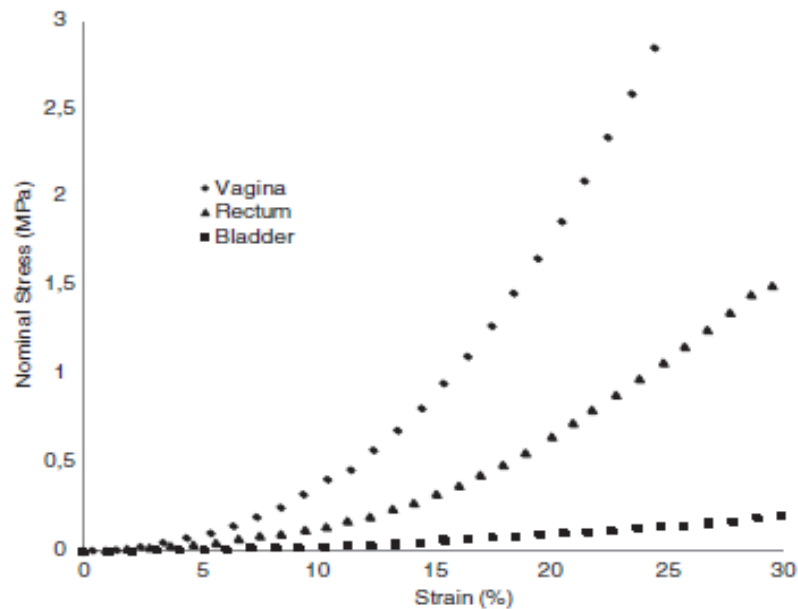


Figure 38 - Experimental data acquired in [52]. Biomechanical stress-deformation behaviour of vaginal, rectal and bladder tissues. Vaginal tissue is clearly the most rigid tissue followed by rectum and bladder.

5.3 Mechanical Properties of Urogynecologic Surgical Meshes

Surgical meshes have become an integral element of corrective and reconstructive surgery when native tissues are weakened. As it was mentioned in 3.2.2, there are a wide variety of absorbable and non-absorbable biomaterials available for the construction of surgical meshes [170].

However in gynecologic and urological repair polypropylene-like mesh is considered the strongest non-absorbable prosthetic. Usually surgeons opt for monofilament and macroporous implantable material which is highly elastic and more able to withstand infection. To date, the core of research into surgical meshes has been focused on improving the biocompatibility and biomechanical properties of the surgical meshes [15].

In 1985, Chu et al. studied mechanical properties of three different types of urogynecologic meshes. It was found that polypropylene mesh (Marlex) had the highest stiffness behavior when compared to polyethylene terephthalate (Mersilene) and Teflon. This rigidity confers higher support to fascial tissues but can be associated to high rates postoperative complications such as mesh extrusion and enteric fistula formation [171].

In 2003, Dietz et al. examined the static uniaxial tensile stiffness and ultimate load of eight commonly used non-resorbable meshes, including some specifically designed for suburethral sling placement. Authors found that TVT™, Sparc and Prolene® mesh biomaterials verified a nonlinear behavior with well-defined low stiffness followed by a rise in stiffness and linear behavior (Figure 42). The elastic limit of mesh-like implants was reached at an elongation of almost 50% (standard) of their initial length. TVT had the lowest initial stiffness whereas the stiffest implant tested was a nylon tape, 0.23 N/mm vs 6.83 N/mm, respectively. In the study, it was concluded that TVT™ and wide-weave Prolene® tapes had the most interesting results showing unique biomechanical characteristics [19].

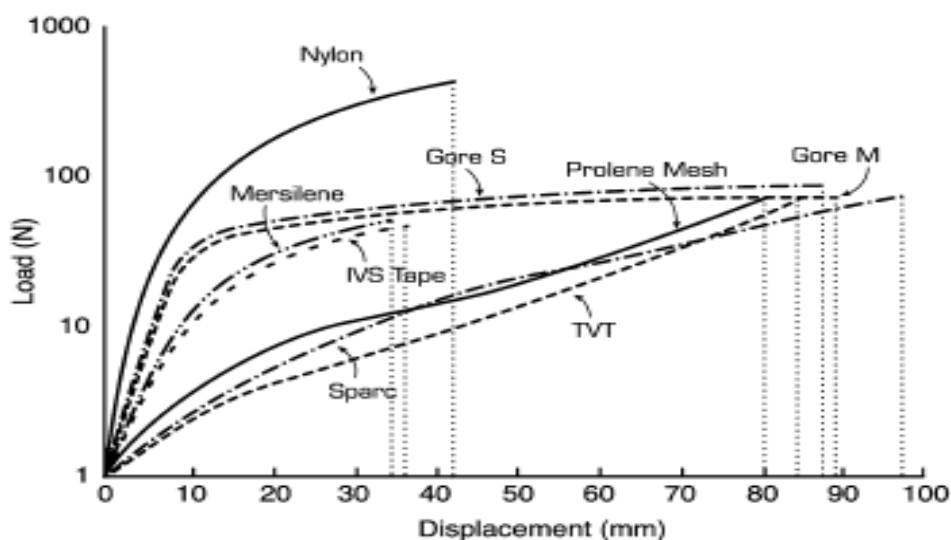


Figure 39 - Experimental data acquired in [19]. Representation of typical load-deformation curves for eight tested non-absorbable mesh-like materials (white dotted lines indicate the displacement at which failure occurred).

In 2008, Afonso et al. tested the tensile and flexural stiffness of five different mesh types. Tensile stiffness was evaluated through uniaxial tests and two stiffness parameters E_I and E_{II} were extracted given the fact that the load displacement curves presented two distinct mechanical behaviors (Figure 40). Among the tested suburethral slings group (ArisTM, TVTOTM and UretexTM), used SUI treatment, TVTOTM showed the lowest stiffer behavior ($E_I = 942,8$ N/mm and $E_{II} = 13083$ N/mm) and ArisTM showed the highest stiffer behavior ($E_I = 23898$ N/mm and $E_{II} = 53705$ N/mm). Flexure properties of implant materials were tested through the tape ring compression test. In compressive tests TVTOTM presented the best results followed by UretexTM and AvaultaTM. The presented results for TVTOTM behavior are consistent to those performed by Dietz et al. These findings can be explained by fundamental knitted porous structure of TVTOTM presenting the highest fiber diameter (0,179 mm) in comparison to the other four implants [172].

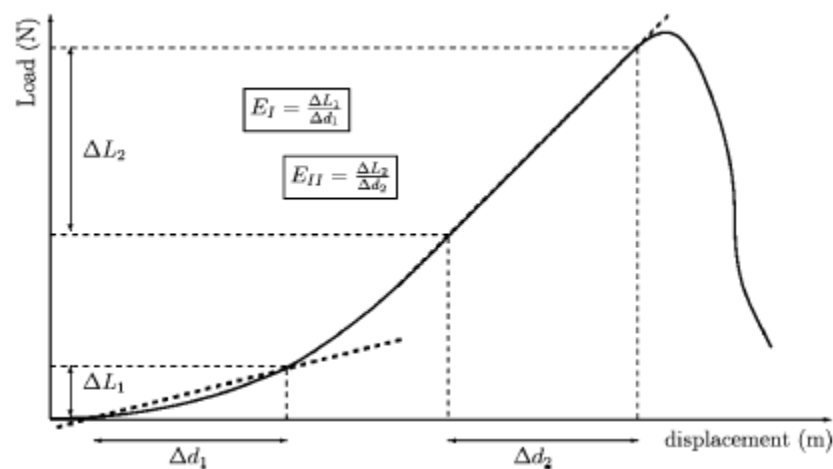


Figure 40 - Representation of the load-displacement curve postulated in [172]. The curve shows the definitions of stiffness quantities E_I and E_{II} .

Hollinsky et al. developed a biomechanical study concerning tensile tests to determine the ultimate tensile strength and modulus of elasticity of six lightweight meshes and six heavyweight meshes for inguinal hernia repair. In the study it was proved a significantly lower ultimate tensile strength and modulus of elasticity in the lightweight mesh group than in heavyweight mesh group. The mean friction coefficient was 0.4 for all meshes. At opening of 5 cm the lightweight and heavyweight meshes flexed on the average of 10.40 ± 2.5 mm and 3.97 ± 0.7 mm. This revealed a significantly less flexible behavior by heavyweight meshes [173].

Moalli et al. characterized, in 2008, the tensile properties of five mid-urethral slings relative to the Gynecare TVTTM. As in [172] two bilinear regions were characterized in the study and slings had elongated 90–110% greater than their initial length. The most important finding of the paper was that Gynecare TVTTM mesh had an unique tensile behavior which was characterized by an initial region of very low stiffness in which the mesh easily elongates in response to small changes in force. This is followed by a transition period (inflection point) and an area of high stiffness. As a result of this behavior, after cyclical loading at low loads (0.5 to 5 N or 0.1 to 1.1 lbs), Gynecare mesh permanently elongated by more than 10% of its initial length, confirming the easy permanent deformability of this surgical mesh that is

observed clinically during placement. The mesh with mechanical behavior more similar to Gynecare was that supplied by AMS [174].

In 2009, Velayudhan et al. examined the dynamic creep behavior of four commercial surgical meshes and found that Prolene®, Ultrapro®, Vypro® and Vypro® II were biochemical and -mechanical overengineered compared to physiological-loading criteria and displayed good load-carrying performance. Except to Ultrapro®, all meshes survived to 100,000 cycles of sinusoidal loading without fracture (at 37°C in physiological saline conditions). Besides, authors also found that meshes underwent strain-hardening and permanent plastic deformation which suggested that this could be a possible cause for complications related to abdominal mobility during long-term implantations [175].

In 2011, Saeberski et al. tested the anisotropic potential of six different synthetic meshes. Elastic modulus in each axis was determined during uniaxial tensile tests. The degree of anisotropy was calculated as a logarithmic expression of the ration between longitudinal and transverse mesh orientation. In Figure 41 it is possible to compare transverse and longitudinal orientations of knitted Ulltrapro™ configuration. Striking differences were noticed between elastic properties of perpendicular axes for commonly used synthetic meshes. Infinit and Ultrapro™ presented the best anisotropic behavior exhibiting approximately 20- and 12-fold differences between perpendicular axes, respectively. Dualmesh® was the least anisotropic mesh with anisotropy close to 1. This could be an important discovery to understand mesh failure implications during tissue native repair or reinforcement since there are significant differences concerning implants orthogonal orientations [176].

In 2012, Sheperd et al. studied the mechanical properties of exclusive type I macrosporous polypropylene vaginal meshes. In all uniaxial tests bilinear behavior was proved with Ascend™ revealing the hardest elastic behavior in the first and second regions of elongation, 0.72 N/mm and 1.66 N/mm, respectively, and offering the lowest transition to higher stiffness, 13.4%. Polyform™ showed the highest failure load while Ultrapro™ had the lowest, 53.8 N and 7.83 N, respectively. On the other hand, the highest relative elongations at failure corresponded to Novasilk™ and Ultrapro™, 89.4% and 87.9%, respectively. Ulltrapro™ was considered the less stiff mesh and demonstrated the greatest permanent deformation with cyclic loading. This mesh had similar behavior of prototypical pelvic mesh of the same brand, Gynemesh PS™. These findings can highlight the feasibility, exceptional strength, surgical adaptability and potential reconstructive of urogynecologic meshes designed and engineered by ETHICON [177].

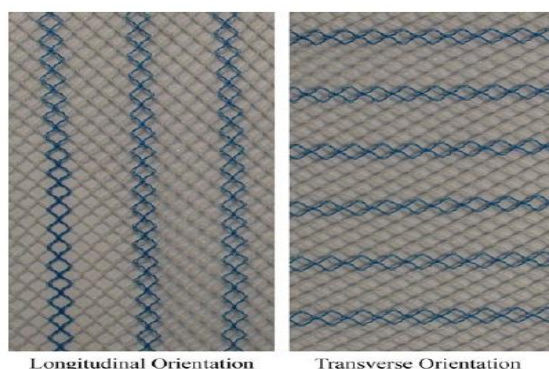


Figure 41 - Ultrapro™ (lightweight type I macrosporous) mesh in longitudinal (left) and transverse (right) orientations [176].

5.4 Three-Dimensional Modeling of the Pelvic Floor

Computer three-dimensional reconstruction of pelvic tissues and supportive actions (i.e. hammock), based on theoretical mathematical models (i.e. finite elements) predict the invasiveness effect of surgical interventions. Besides, it provides insight into accurate geometrical simulated anatomic data and morphologic parameters of all different structures of pelvic floor (bones, ligaments, tendons, muscles and organs).

A wide range of realistic pelvic floor disorders and surgical invasive procedures can be simulated and controlled by precise numerical software applications, with a low-cost and high efficiency.

Furthermore, to obtain a complex anatomic three-dimensional model, several parameters should be accounted, such as structures physical properties, boundaries conditions and mechanical behaviour during different scenarios [178].

When a finite element method is developed for a living patient, healthy subject or specific biomaterial, the only way to obtain accurate morphological parameters is using previous three-dimensional model through: cadaveric study; magnetic resonance image MRI; 3D ultrasound (US) and/or Computer-aided design (CAD) [178, 37 - 38].

In specific application of the pelvic floor system, FEM may allow the creation of anatomical and physiological pelvic support. It may help to understand the mechanism that could explain the occurrence of a genital prolapse. The model can be developed for a single patient with her own anatomy, vaginal forces and pelvic tissues for a generalized global approach.

Nowadays, ABAQUS is a well-known and complex software used for FEM application in generated models. It achieves a wide range 3D-geometrical numerical different deformable stages and tension scenarios of pelvic floor muscles (i.e levator ani muscle; anal canal; etc) due to specific movements (i.e. Valsalva maneuver; extreme loading; childbirth; etc) [42, 37].

In the future, the use of precise numerical models of the female pelvic cavity, will provide the tools to simulate, in a realistic manner, pelvic floor function and the effects of physiopathological conditions.

5.4.1 Finite Element Model

FEM is a mathematical system that meshes precisely geometric structures in different type of elements (i.e. triangular, tetrahedric, cubic, etc), depending on function and problem dimension (uni, bi or tri-dimensional).

The FEM has three distinct methods. During displacement method several parameters are taken into account; degrees of freedom, rigidity matrix, number of nodes, boundary conditions [36].

Generally in FEM, deformation and tension stages analysis involves stepped phases:

- Mesh generation;
- Tension stages determination;
- Mesh element deformability;
- Assembling - finite elements of the structure;
- Forces application to respective nodes;

- Support conditions - nodal liberty degrees;
- Algebraic linear equation resolution to determine nodal displacement;
- Nodal deformation calculation and displacements by interpolation;

5.4.2 ABAQUS

ABAQUS is a powerful engineering simulation program, based on the FEM that can solve problems ranging from relatively simple linear analyses to the most challenging nonlinear simulations. This software possesses an extensive library of elements and material models.

It is a versatile tool, which can determine stress problems in static structures as well as in dynamic systems. *ABAQUS* offers a wide range of capabilities for simulation of linear and nonlinear applications.

Furthermore, it has automatic functions which choose appropriate load increments and convergence tolerances, continually adjusting them during the analysis to ensure that an accurate solution is obtained efficiently.

It consists in a vast product set: *ABAQUS/CAE* (Complete *ABAQUS* Environment) an interactive, graphical environment which allows models to be created quickly and easily by producing or importing geometry of the structure to be analyzed and decomposing geometry into meshable regions; *ABAQUS/STANDARD* is a general-purpose analysis product that can solve a wide range of linear and nonlinear problems; *ABAQUS/EXPLICIT* is a special-purpose analysis product that uses an explicit dynamic finite element formulation. It is suitable for transient dynamic events or changing contact conditions; *ABAQUS/CFD* is a computational fluid dynamics analysis product which can solve deforming mesh and incompressible low problems [179].

5.4.2 Three-Dimensional Numerical Models of the Pelvic Floor

It has been stated that pathophysiology of pelvic support tissue is complex and computer-based applications can offer precise tools to understand the mechanisms under the occurrence of genital prolapse. Therefore, several studies have been performed in FEM-based simulations to understand the evolution of PFD mechanisms and to offer individual optimized therapeutic strategies.

Martins et al developed, in 1997, their first motion and deformation skeletal muscles representative FEM, using *ABAQUS* to analyze large numerical deformations of elbow joint and bones respecting biceps brachialis [178].

In 2003, Janda et al. started to obtain data set to study the complex biomechanical behavior of the pelvic floor muscles using a computer model based on the finite element (FE) theory. Apart from other techniques, to develop a building FE model for a living patient or healthy subject, the only way found to obtain morphological parameters was using MRI scans. Important parameter of LA muscle, like the optimum muscle length and fiber orientation, could not be obtained from MRI scans so cadaveric study by palpator measurements allowed importation of such parameters (Figure 42). Data obtained about geometry of muscle fibers could be directly used as an input for building a mathematic model [37]. MRI can also be used to identify morphologic changes in the LA muscle, in different grades of prolapsed women, by systems of classification, like POP-Q.

Sigh et al. found four well-defined patterns in women with different stages of uterovaginal prolapse. Both levator III and IV showed indubitably an abnormal levator ani [38].

In 2005, Aulignac et al. used the dataset developed by Janda et al. [37] and have reconstructed the geometry of LA using NURB surfaces. The elements of the modeled muscle were shelled. Connections were established in an easy manner, to be helpful to use some special 8-node birck elements, which behave well in the thin-structure limit. The modeled muscle presented transversal isotropic and hyperelastic behaviour with activation of the fibers. Studies proved that simulation damaging of pelvic floor could occur after childbirth [40].

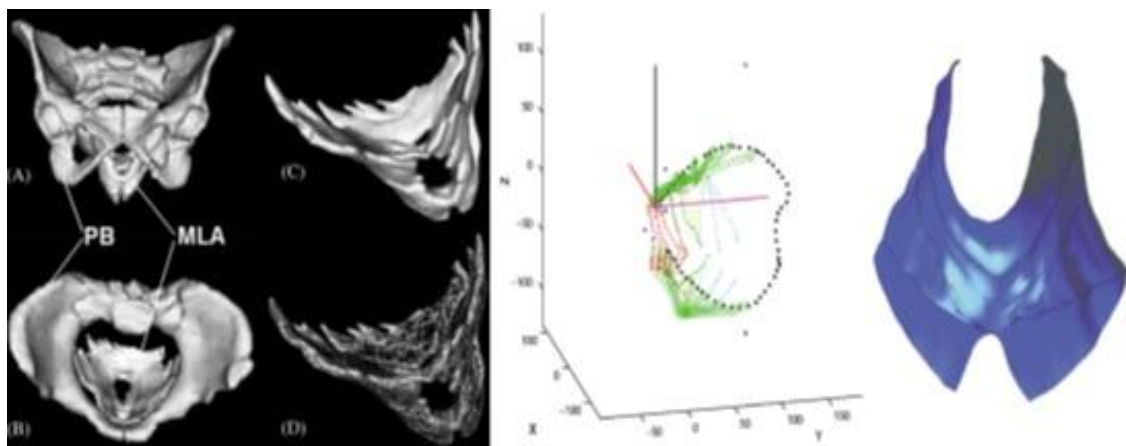


Figure 42 - On the left, is exposed the 3D geometrical experimental data set from MRI measurements, with representations of pelvic bone in images (A) and (B) and muscle levator ani in images (C) and (D). On the right, is exposed the 3D geometrical model of pelvic floor muscles based on the experimental data set from the palpator measurements: on the left are the points measured during palpator approach and on the right is presented the final rendered surface muscular floor [37].

In 2007, Martins et al used again, the cadaveric simulated model developed by Janda et al [37] and constructed the surface in two consecutive steps: firstly the edges of the muscles were defined using splines and then nonuniform rational B-splines (NURBS) surfaces were created. The final result showed a three-dimensional mesh of 8 node hexahedral elements. For posterior childbirth simulations, the FEM of pelvic floor was connected to a model of pelvic skeletal structure (Figure 43). Besides, connections were established between muscles of pelvic floor and the coccyx. To the finite element model was also added new muscles; arcus tendineus, oturator fascia and obturator internus. The final modeled sample showed great pelvic tissue improvements: relevant model contractions occurred in intervals of time of the same order of magnitude of muscle activation and deactivation times; preventing UI in coughing or sneezing [42].

In 2008, Parente et al. constructed a FEM model using geometrical data obtained from cadaver measurements by Janda et al. The FEM used was composed by modeled pelvic bones attached LA muscles and a fetus, in order to study the effects of vaginal delivery. The authors simulated several biomechanical assays: engagement, descent, flexion, internal roatation, and extension of the fetal head. It was found that the maximum stretch ratio of 1.63 exceeded the maximum noninjurious stretch, 1.5 stretch ratio, of previous studies. The authors concluded that, throughout childbirth simulation, there is evidence of risk of injury during second stage of labor [44].

Noakes et al., also used the same cadaveric pelvic floor data [37] to produce two cadaveric-based meshes, using Visible Human Project (male - VM and female - VW) and a third mesh was produced based on MRI. VW and MRI meshes contained 14 and 13 structures, respectively. Each image set was digitized and then finite element meshes were created using an iterative fitting procedure with smoothing constraints calculated from 'L'-curves. The VW mesh included: puborectalis, levator ani, internal/external sphincter, transverse perinea, pubis, coccyx, rectum, vagina, uterus, bladder, bulbospongiosus group and urethra (Figure 44) [43]. However, it should be noted that as this mesh was based upon a cadaver specimen and the soft tissue components of this mesh may not be representative of live subjects.

In 2009, the same group trimmed the computational MRI mesh developed in the previous study [43] and obtained only the LA muscle.

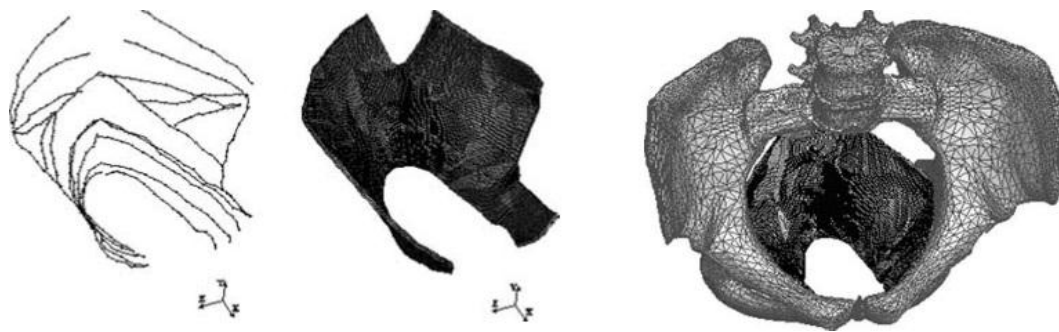


Figure 33 - From left to right: The first presents mesh FEM generation and the last is a representation of pelvic bone fused with pelvic floor mesh [42].

It was used as a framework to examine the mechanics of normal function of levator ani group during valsalva maneuver deformation, with an applied pressure of 4KPa, causing the 'seagull-like' shape to deform into a concave, 'bowl' shape with an average, experimentally consistent, downwards displacement of 27.2mm measured at nodes. Pelvic simulated musculature produced promising results, consistent with those found in literature. Besides, anisotropic material laws enabled improvement of the simulation accuracy [45].

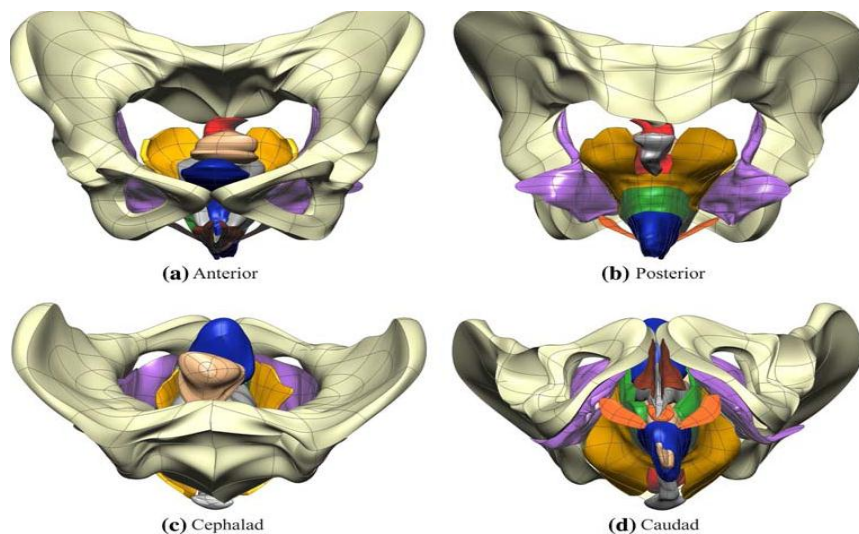


Figure 44 - Final fitted meshes from Visible Woman data set [43].

In 2009, Zhang et al. conducted a fluid-structure interaction analysis by using a FEM of a female pelvic of a younger woman, in order to investigate the urine leakage in female during jumping (Figure 45). The dynamic computer-based simulation results revealed that jumping heights have a significant influence on the volume of urine leakage caused by the landing impact of jumping. Additionally, the computer simulation results showed that the deformation difference between the anterior and posterior portion of female pelvis causes opening of the urethra and consequent urine leakage [46].

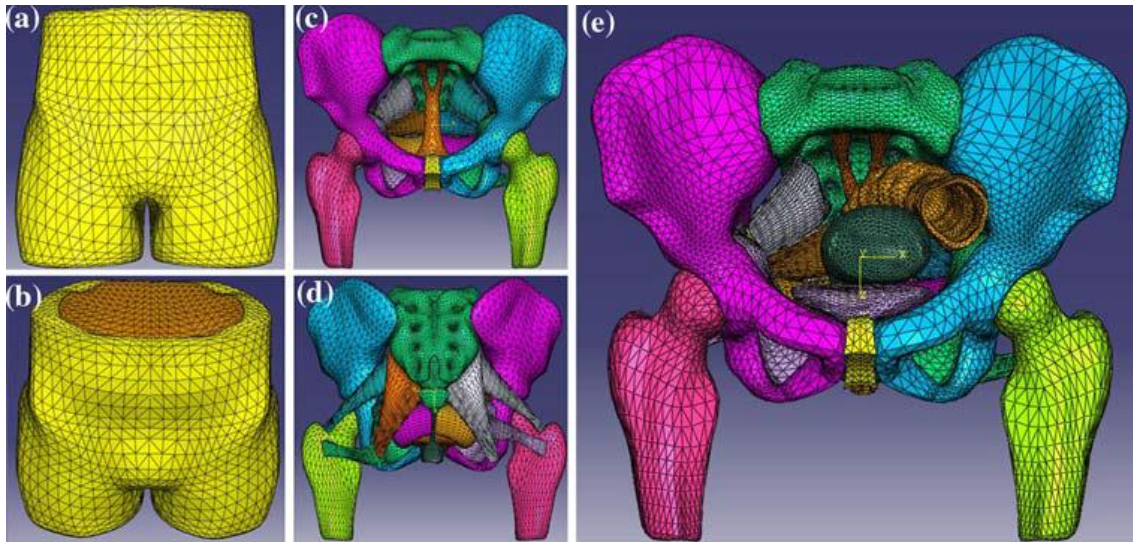


Figure 45 - Generated realistic geometry of a 20-year-old female subject's pelvis. The model consisted in 35 anatomical parts including 10 pelvic muscles, 10 pelvic ligaments, 6 pelvic bone, skin, fat tissues, bladder, urethra, uterus, vagina and colon, rectum and anus. The ambulatory model was used on the participants to characterize their specific landing impact parameters [46].

In 2010, CAD models were developed individually for vagina, bladder, uterus, rectum, pubic and sacrum bones from MRI data. Rao et al. designed a complete 3D FEM of pelvic floor system, including the bladder, vagina, and rectum as well as ligaments. The model helped to understand the biomechanical influence of anterior cystoceles in the pelvic floor [49].

Chapter 6

Biomechanical Simulation of Pelvic Floor Impairment and Repair

This biomechanical study consisted in the analysis and adjustment of the 3D FEM developed in [69] for consistent simulation of defective connective tissue (PCF and USL) under different fault scenarios. At the same time support reinforcement of pelvic organs (vagina and uterus) was obtained through well anatomically designed anterior and posterior polypropylene-like grafted implants. Therefore, geometry of the pelvic cavity and pelvic floor support structures (LA, PUL, USL, ATFP, PCF and Posterolateral Rectal Ligament) were kept. Besides, the respective hyperelastic material properties obtained by constitutive models, in *ABAQUS*, were not modified for all tissues. Generated finite element model, in *FEMAP*, of each pelvic structure was assessed without adjustments except for pelvic organs (bladder, vagina/uterus and rectum).

Given the fact that it was pretended to develop urogynecologic soft meshes for reconstructive surgery of the anterior and posterior uterine/vaginal wall support, pelvic organs were remodeled and refined for a suitable interaction between meshed implants. Pelvic organs surfaces were re-designed using CAD software - *Rhinoceros* and meshed in *ABAQUS* using anatomical and biomechanical information presented in [69] and literature.

Regarding surgical implants procedures there were designed (in *Rhinoceros*) two different non-absorbable urogynecologic surgical meshes and both sacrospinous ligaments (for suspension of posterior vaginal wall through mesh support). Surgical meshes placement under vesicovaginal and rectovaginal space of the 3D anatomical model followed the procedure of Prolift® system for anterior and posterior repair of the vaginal wall, respecting uterine preservation [30]. The material isotropic properties of three different polypropylene-like meshes (Ultrapro™, Prolite™ and Trelex®) were added to the simulations and constitutive models were associated to each mesh material. These properties consisted in longitudinal tensile strength behavior found in [176].

6.1 Construction of 3D pelvic structures

Firstly, the FEM model developed in [69] was assessed and acutely examined (Figure 46). Both *ABAQUS* and *FEMAP* software were used to investigate whole pelvic structure and meshed geometries of pelvic organs, muscles and connective tissue. Concerning anatomic and material properties of the structures, it was considered that every component was well

defined. Despite this, the FE mesh generated for bladder, uterus-vagina and rectum presented 3D solid elements (C3D4H) with high distance between nodes: $\approx 3,0$ mm. Besides, organs surfaces smoothness was irregular not reproducing ideal morphology of pelvic tissue walls. Therefore, to study biomechanical behavior of pelvic organs tied with propylene-like meshed structures it was required a smaller distance between nodes and implementation of smoother contact surfaces of the organs and shell-based urogenital meshes.

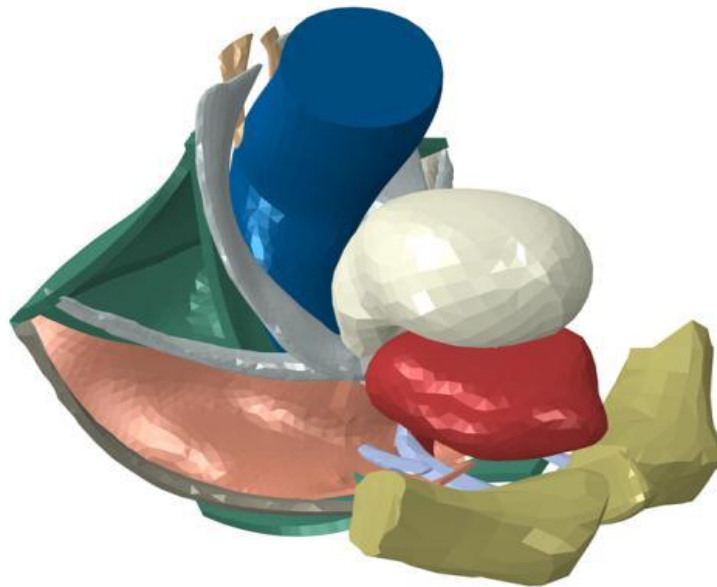


Figure 46 - Final 3D FEM developed in [69] containing the pelvic organs (bladder, uterus and rectum), levator ani main musculature, key pelvic support ligaments (uterosacral, pubourethral, arcus tendineus and posterolateral retal), pubocervical fascia and pubic bone.

6.1.1 Pelvic Organs

In the beginning of the study it was established that geometrical reconstruction was preferable instead of a new theoretical construction. In [69] the pelvic organs were based on *VisibleBody 3D Human Anatomy* (tool containing precise and sophisticated 3D anatomic models) and recreated in *SolidWorks* (CAD-based software containing design tools based on splines and lofts to create engineered surfaces). The geometrical pelvic organ models created in *SolidWorks* were imported to *Rhino* to rebuild each organ separately in a similar way.

Rhino (v. 5.0) is a commercial NURBS-based 3D modeling software. This program is more intuitive and preferred by designers than *SolidWorks*. It has the advantage of presenting a graphic interface spitted in four planes (top, front, right and 3D perspective) with no need to choose planes to create detailed surfaces. Basically, after importing the organs geometries their configuration was kept and new organ construction was started. Two main well-known commands were manually used in *Rhino*: free-form rational B-spline (*NURBS*) modeling and network crossing surfaces (allowing application of interior and edge curves values of tolerance).

In Figure 47, it is represented the design process involved to generate 3D surfaces envelope of the smoothed organs. Each organs was re-designed separately in order to reproduce in a suitable way the anatomical parameters, length and width, found in [69].

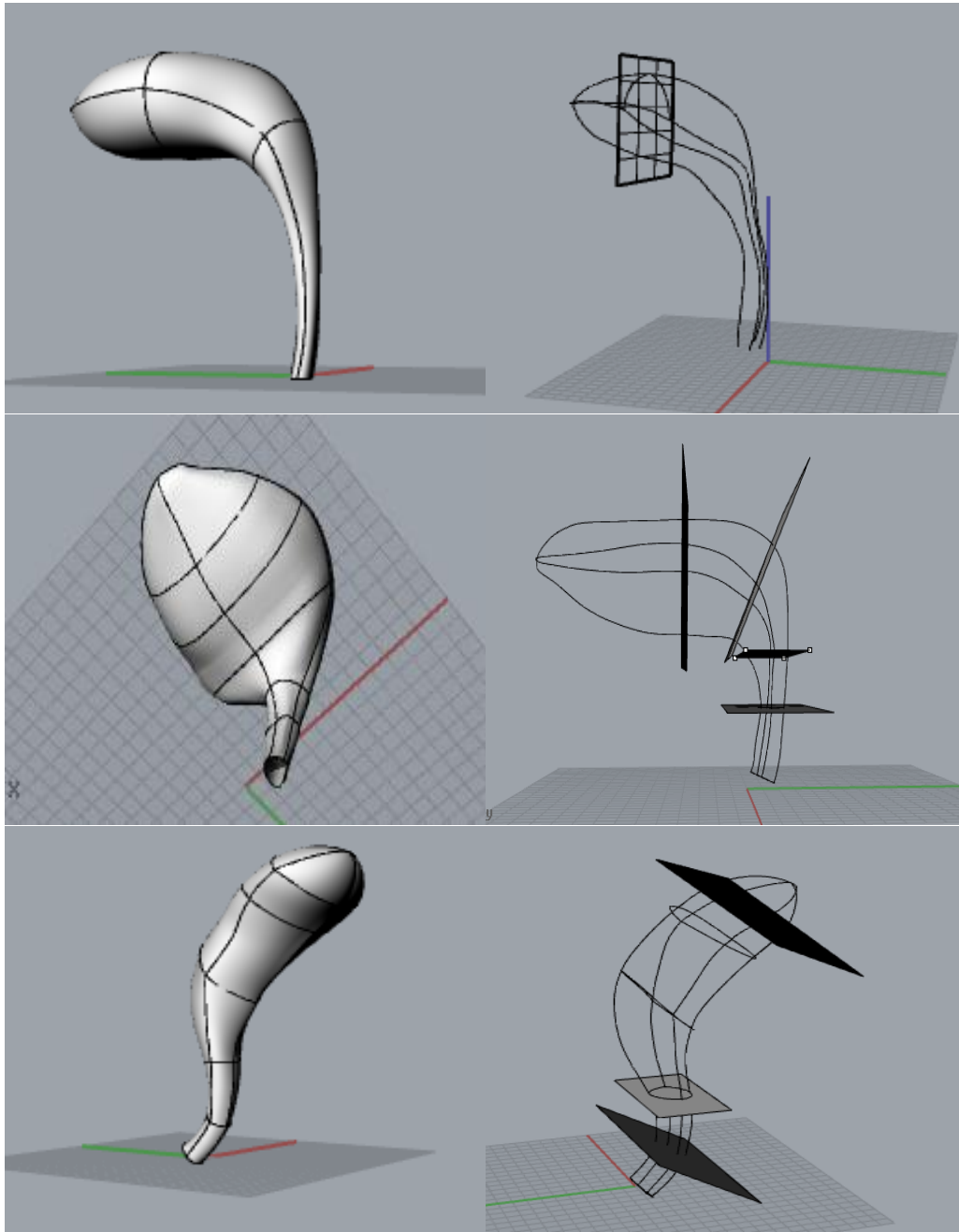


Figure 47 - Representation of uterus (top), bladder (center) and rectum (bottom) obtained in *Rhino*. B-splines and surfaces network used in the design process are shown.

6.1.2 Sacrospinous Ligament

The sacrospinous ligament, as mentioned in 3.2, has been used as a convenient structure for treating vaginal vault and uterine prolapse [74-75, 180]. More recently, this ligament has been used in minimally invasive transvaginal procedures for treatment of pelvic floor defects. It is a reliable anatomic site for passage of surgical mesh arms and subsequent tension-free technique adjustment [22, 30].

Anatomically, as described in 2.2.1.1, the SPL extends from the ischial spine, to the lateral margin of the sacrum and coccyx. Its anterior surface is muscular and forms the

coccygeus muscle [180]. Roshanravan et al. characterized the anatomy of the coccygeus muscle-sacrospinous ligament complex and correlated the findings with sacrospinous ligament fixations, on female cadavers, and found that the mean length of the right and left SPL were 53.7 mm (range, 44-60 mm) and 53.6 mm (range, 44-62 mm) [181]. In 2008, Lazarou et al. described the variations in the location and/or proximity of pelvic nerves in relation to the SPL, on female cadavers, and found that the mean SPL width was 3 mm [182].

Despite this information, the geometry and length of the SPL were precisely fitted to geometric properties of coccygeus muscle and anatomical relations to specific insertion sites - sacrum and ischial spine - developed in [69]. In figure 48 it is possible to observe the right and left sacrospinous ligament surfaces developed in *Rhino*, for posterior mesh extrusion with 3,0 mm of thickness.

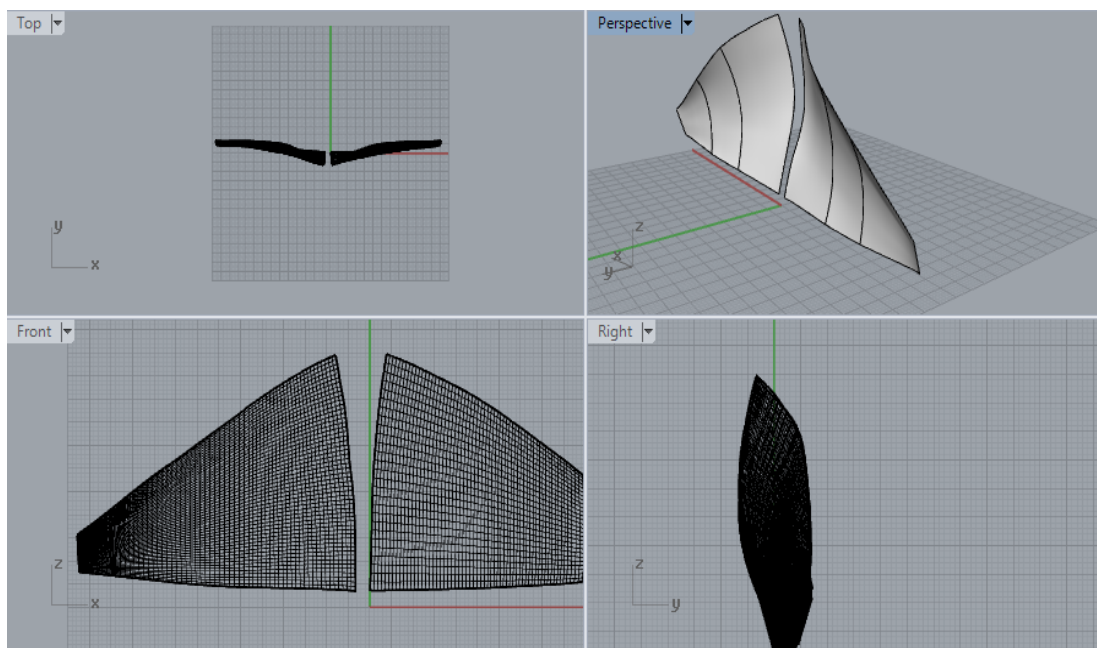


Figure 48 - Sacrospinous ligaments obtained in *Rhino* with designed B-splines and respective network surfaces. The program provides four different perspectives which can be simultaneously manipulated during the design perspective.

6.1.3 Urogynecologic Surgical Meshes

To design commercial Gynecare Prolift® surgical meshes for the anterior and posterior vaginal-uterine wall mechanical support, several data of standardized surgical procedures were evaluated since there was no previous 3D geometric model or simulation performed with this new TVM system [23, 29, 30, 155-156, 160].

The estimated geometrical size, shape and dimensions for both anterior and posterior systems followed information and surgical description found in ETHICON product reports [156] and in the surgical proposal of Reisenauer et al [23]:

- **Prolift Anterior System:**
 - 2 bilateral arms for ATRP fixation/suspension
 - Height \approx 13 cm
 - Maximal width \approx 10 cm

- Straps width \approx 2 cm
- Thickness \approx 0.5 mm
- **Prolift Posterior System:**
 - 2 arms for SPL fixation/suspension
 - Height \approx 16 cm
 - Maximal width \approx 7 cm
 - Straps width \approx 2 cm
 - Thickness \approx 0.5 mm

However, as in the case of sacrospinous ligament design, dimensions of the surgical meshes were adapted to the unique 3D geometry pelvic structure developed in [69] and new modeled pelvic organs and SPL.

Furthermore, fundamental standardized surgical information for placement of Prolift TVM systems, with uterus preservation, was available in Gynecare Surgical Technique brochure [30] and two procedures practiced in [23] and [27]. Therefore the following surgical methodology was carefully considered and applied:

- **Anterior System Placement and Reinforcement:**
 - Placed within the vesicovaginal space
 - Inserted as a hammock under the bladder
 - Anterior arms: fixated 1 - 2 cm from the proximal part of the ATFP
 - Posterior arms: fixated 2 cm from the distal part of the ATFP
 - Reinforcement of anterior vaginal-uterine wall mechanical support
 - Replacement of PCF defects
- **Posterior System Placement and Reinforcement:**
 - Placed within the rectovaginal space
 - Retained by 2 lateral arms through the medial part of the SPL
 - Reinforcement of posterior vaginal-uterine wall mechanical support
 - Replacement of USL defects

Several

anterior and posterior meshes were designed and re-designed until obtain the most similar mesh comparing to those finding in the literature. In Figures 49 and 50 there is represented, in more than one plane, the final size and shape of USM surfaces obtained through *Rhino* software.

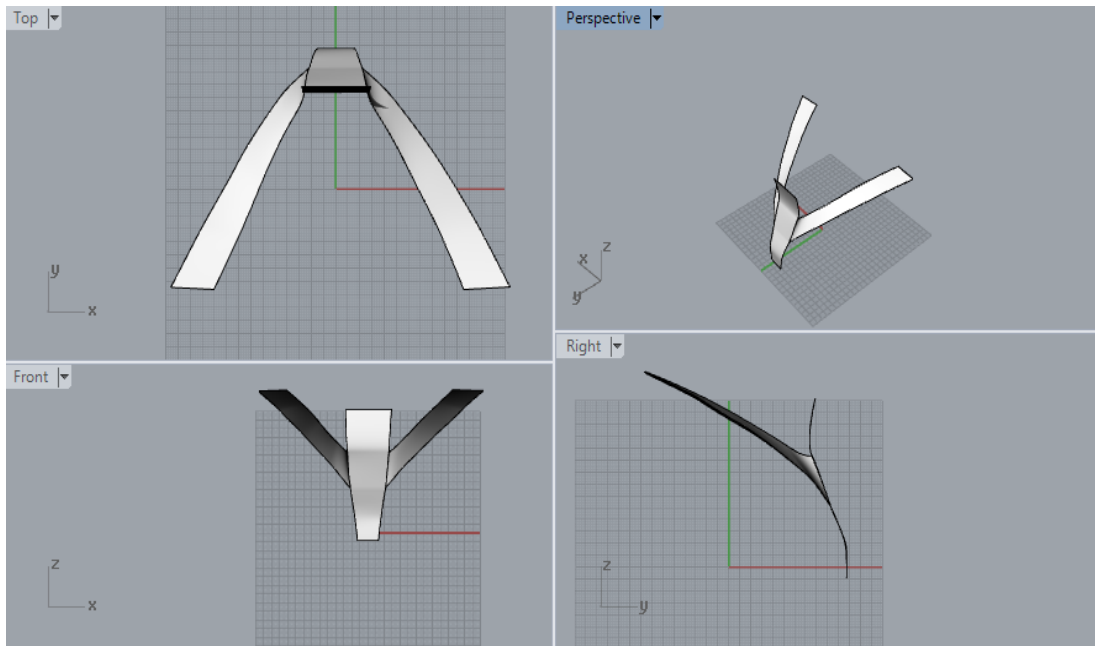


Figure 49 - Four perspectives of the final job of the posterior surgical mesh design. The mesh arms were carefully aimed to reproduce their real design. The top segment has an approximate shape and width for suitable attachment to the posterior face of the uterine isthmus (about 2cm above the cervix).

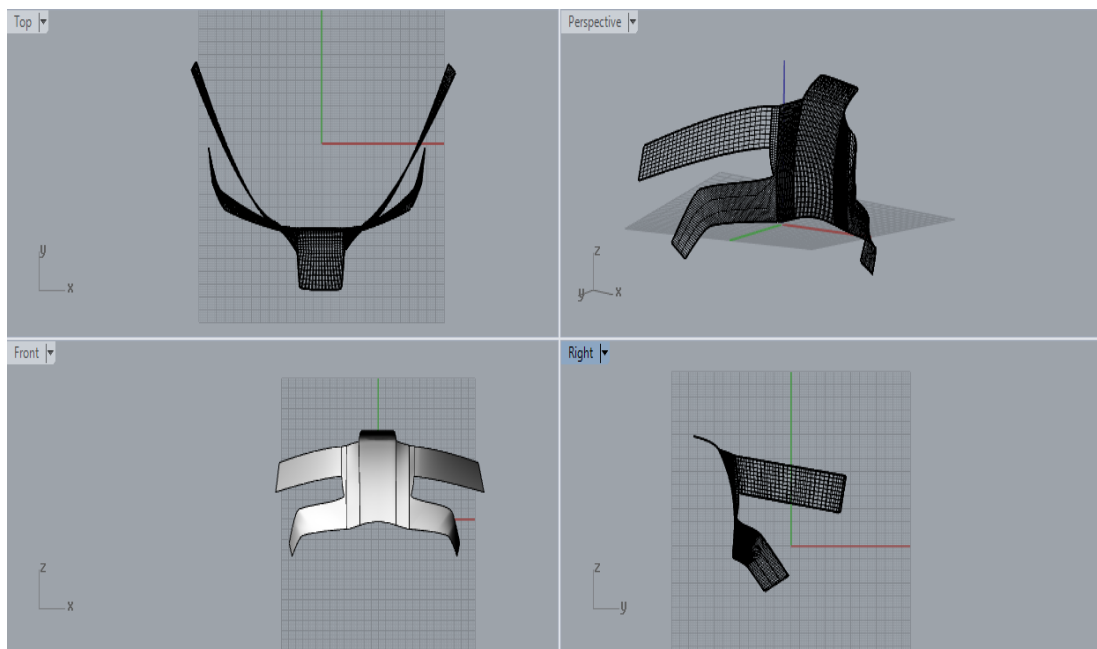


Figure 50 - Four perspectives of the design complexity of the 2 bilateral arms and top segment of the anterior surgical mesh. It is possible to observe that the top surface presents a suitable size and shape for suitable attachment of the anterior face of the uterine isthmus (about 2 cm above the cervix).

6.2 Construction of Finite Element Model

Once created the 3D geometrical structures, assigned in *Rhino*, it was necessary to implement a finite element model to use the biomechanical assays. Regarding the FEM of the pelvic floor structures, created in [69], they were not-modified or refined (excepting for

pelvic organs), maintaining all element types generated and numeration of the nodes and elements, as they were defined in the assay. Instead of using *FEMAP*, as in [69], it was used *ABAQUS*.

Given the fact that the 3D pelvic arrangements were based on surfaces, *ABAQUS* was the most suitable software to allow the construction of meshed structures based on posterior thickness extrusion concerning the normal direction to the surface. On the other hand, for Prolift® surfaces *ABAQUS* was considered very precise to generate automatically a shell- and membrane-based meshing.

6.2.1 Pelvic Organs and Sacrospinous Ligament

Given the high morphological complexity and exclusive hyperelastic behavior of pelvic organs, mentioned in 5.2, it was obtained a double-layer mesh extrusion for bladder, vagina and rectum with tetrahedral elements. The true wall thickness of the organs could only be implemented using 3D solid elements - tetrahedrons. On the other hand, sacrospinous ligament were meshed using the same 3D solid elements but with just one layer of elements for the reason that this structure would serve only for surgical mesh fixation during mechanical simulations.

In the table 6 are presented the main characteristics of the meshes generated, in *ABAQUS*, for bladder/urethra, vagina/uterus, rectum and sacrospinous ligament.

Table 6 - Main characteristics of meshed pelvic surfaces based on extrusion (single or double).

<i>Mesh</i>	<i>Number of nodes</i>	<i>Number of elements</i>	<i>Distance between nodes</i>	<i>Thickness</i>	<i>Type of elements</i>
Bladder/Urethra	111663	111588	0,6 mm	0,96 mm	C3D6H
Vagina/Uterus	54292	54220	1 mm	2,10 mm	C3D6H
Rectum	61164	61090	1 mm	1,68 mm	C3D6H
Sacrospinous Ligaments R/L	12395	11973	1,5 mm	3,0 mm	C3D6H

6.2.2 Urogynecologic Surgical Meshes

The urogynecological implants can be considered as thin hyperelastic membranes with complex knitted macroporous interconnectivity. Thus, membrane or shell meshing were considered the best options for mild shearing and/or large-strain solicitations. On the other hand, shell-based meshes have been used in several studies concerning pelvic floor modeling. The main advantages relay in the reduced computation costs, easy implementation, and it is possible to vary thickness during 3D simulations [45].

Given the fact that simulations performed with membrane or shell-based mesh did not converge conveniently, the implants surfaces were meshed together, mixing the reliable deformable properties of membrane elements and firmness conferred by shell-based elements. The thickness of membrane meshes was established to be the double of the shell elements.

Table 7 - Main characteristics of triangular shell and membrane meshed surfaces of urogynecologic surgical meshes.

<i>Mesh</i>	<i>Number of nodes</i>	<i>Number of elements</i>	<i>Distance between nodes</i>	<i>Thickness</i>	<i>Type of elements</i>
Prolift Anterior	6977	26392	1,0 mm	1,0 mm and 0,5 mm	M3D3 and S3R
Prolift Posterior	5420	20449	1,0 mm	1,0 mm and 0,5 mm	M3D3 and S3R

Finally, *FEMAP* software was requested for the adjustment of the new meshed geometries. All 3D meshed bodies were spatially placed in their anatomy sites respecting to pelvic floor disposition and interaction between the pelvic viscera. The pelvic organs anatomic expended more time, since they had more associations with whole pelvic floor components. Meanwhile, to adjust the surgical meshes ‘pre-simulations’ were done to deform them under the pelvic organs. In figure 51 is displayed the final 3D FEM with all new structures and both the Prolift Anterior and the Prolift Posterior synthetic reinforcements.

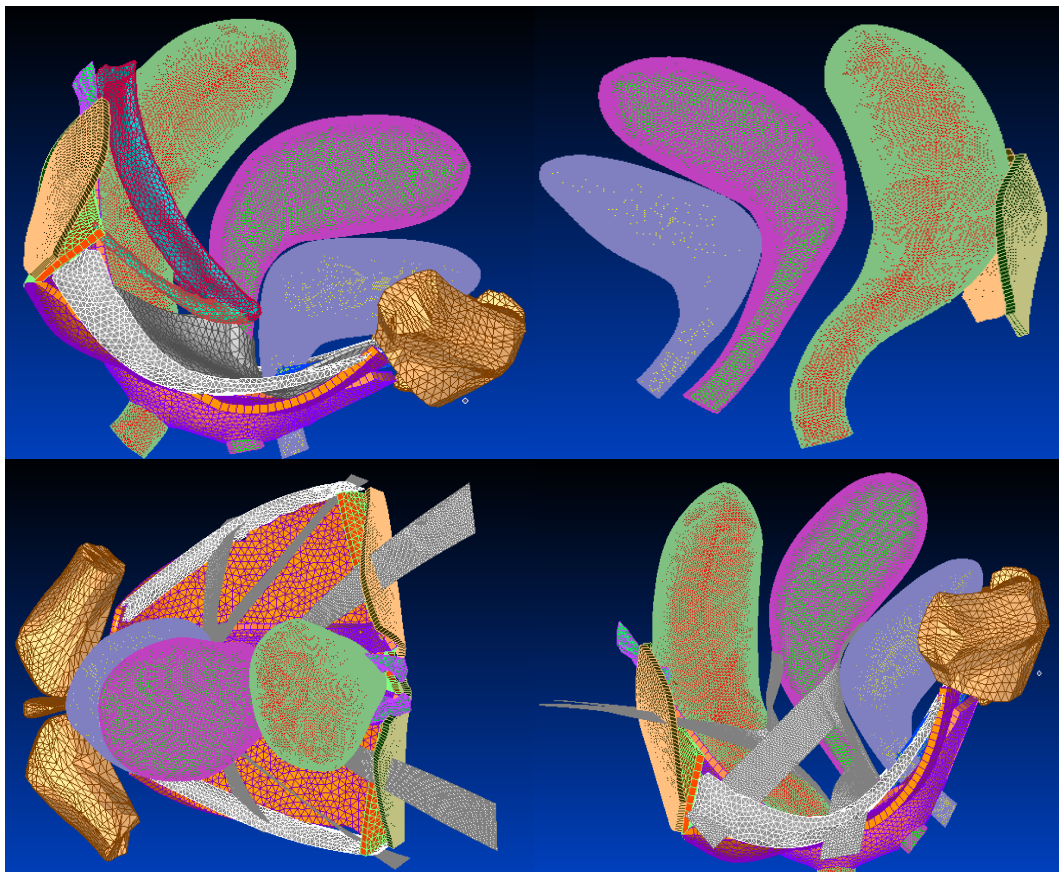


Figure 51 - Final 3D FEM of the pelvic floor containing the new organs and sacrospinous ligaments. It is possible to observe new smoothed organs with precise elements definition (top) and placement of the meshes within vesicovaginal and rectovaginal space (bottom).

6.3 Simulation of the 3D FEM

The simulation of the previous biomechanical 3D model refined with the new pelvic structures was the most time-consuming part of this work.

This work was based in two different numerical simulation experiments. As no surgical experimental characterization is available in the literature and no researcher has yet performed such a mechanical assay at the moment, easy and simple approaches were tested.

The first tests consisted in studying biomechanically the progressive failure of bilateral suspension of the uterosacral ligaments under subsequent analyzes of the uterine cervix displacement and support of pubocervical fascia under subsequent analyzes of cervical ring displacement. Both fault scenarios were under application of specific intrabdominal loads.

The second tests consisted in the study of the success of mechanical reinforcement of impaired support of the anterior and posterior vaginal wall placing the surgical meshes, respectively, in pubovesical and rectovaginal space. In order to study the success of mesh reinforcement, it was removed the uterosacral ligament. In these assays were implemented loads above intrabdominal values.

The major challenge in this assay comprehended the interaction sets as well as interaction properties between the novel surgical shell-based meshes and 3D anatomic surfaces of organs and fixation sites (ligament-like and structures).

In order to understand all the processes executed to run the simulations by the *ABAQUS* software, this section is segmented in: 1) materials properties modeling, 2) boundary conditions, 3) constraints, 4) contact pairs, and 5) loads set.

6.3.1 Materials Mechanical Properties

The mechanical properties of modeled tissues were settled in [69] and they were applied even for the refined pelvic organs. However, to study the effectiveness of USM support the use of one type of propylene material was not clearly enough. Therefore, detailed research work, of found in 5.3, was crucial to identify the exclusive mechanical behavior of different meshes made of propylene. It was observed that nowadays propylene-like urogynecologic macroporous meshes and tapes assume a non-linear hyperelastic behavior. From Saberski et al study, it was chosen three different mechanical properties of surgical polypropylene meshes: Ultrapro™, ProLite™ and Trelex® [176]. Throughout a precise tool available in *ABAQUS*, data obtained from uniaxial can be submitted and precise hyperelastic stability of the materials can be simulated, using different constitutive models.

The constitutive models are widely used in theoretical and practical applications, especially in finite element calculations. The identification of the material parameters, is usually carried out by means of experiments for homogeneous stress-strain states (simple tension, simple or pure shear, biaxial tension) or inhomogeneous deformations (tension-torsion tests) for which analytical solutions exist. These solutions depend linearly on the material parameters which, in the case of their identification, lead to a linear least-square problem. To date, the most well-known elasticity relations are the Neo-Hooke model and the Mooney-Rivlin model. The underlying strain-energy function depends on the first and second invariant of the left Cauchy-Green tensor in the form of a polynomial. Each model is represented by a specific strain energy density function [183-185].

In (1) it is represented the polynomial-standard strain-stress function, developed by Mooney-Rivlin, for hyperelastic materials [185]:

$$W = C_{10}(I_1 - 3) + C_{01}(I_2 - 3) \quad (1)$$

Where W is the strain energy function and C_{10} and C_{01} are material parameters which have dimensions of stress but no physical interpretation, and must be determined from experiments on the particular material being modeled, and I_1 and I_2 are principal strain invariants of the right Cauchy-Green tensor.

In Figure 52, it is represented stress-strain curves of the experimental data obtained for Trelex® polypropylene mesh and respective constitutive models curves.

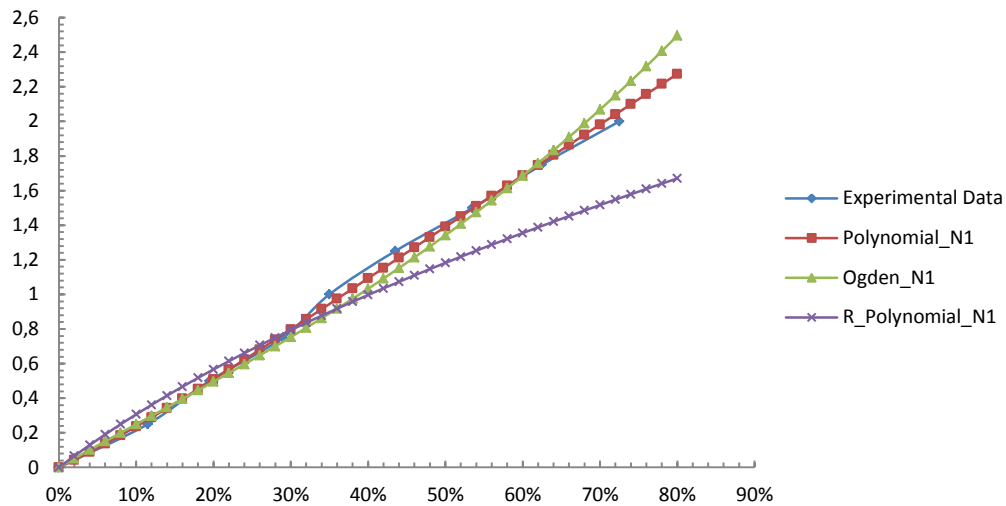


Figure 52 - Representation of the stress-strain graphical curves of uniaxial experimental data obtained for Trelex® and respective representation of three constitutive models.

The model chosen for Trelex® material was the Mooney-Rivlin, obtaining the following information: $D1 = 0,000$; $C10 = 1,281$; $C01 = -0.933$.

In Figure 53, it is represented stress-strain curves of the experimental data obtained for ProLite™ polypropylene mesh and respective constitutive models curves.

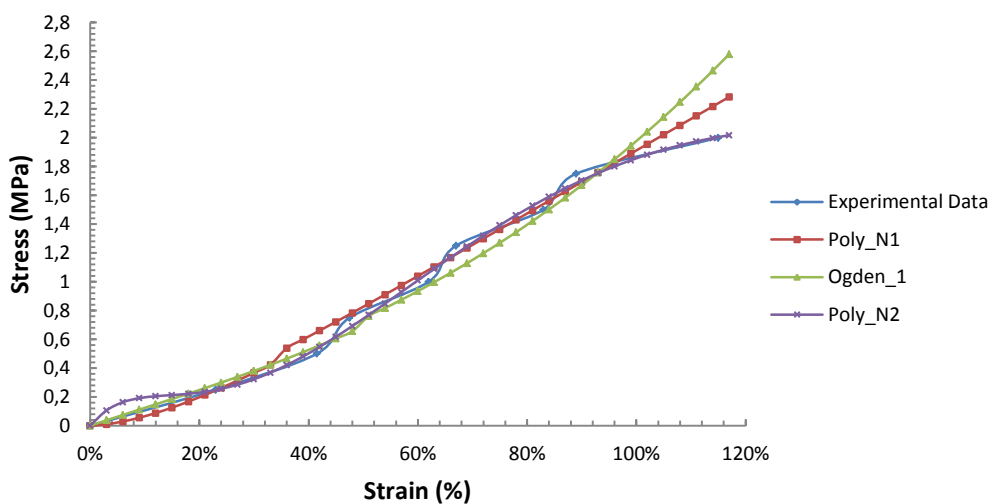


Figure 53 - Representation of the stress-strain graphical curves of uniaxial experimental data obtained for ProLite™ and respective representation of three constitutive models.

The model chosen for ProLite™ material was the Polynomial N=2, obtaining the following information: D1 = 0,000; C10 = -5,643; C01 = 6,419; D2 = 0,000; C20=0,653; C11=-3,370; C02=6,349.

In Figure 54, it is represented stress-strain curves of the experimental data obtained for Ultrapro™ polypropylene mesh and respective constitutive models curves.

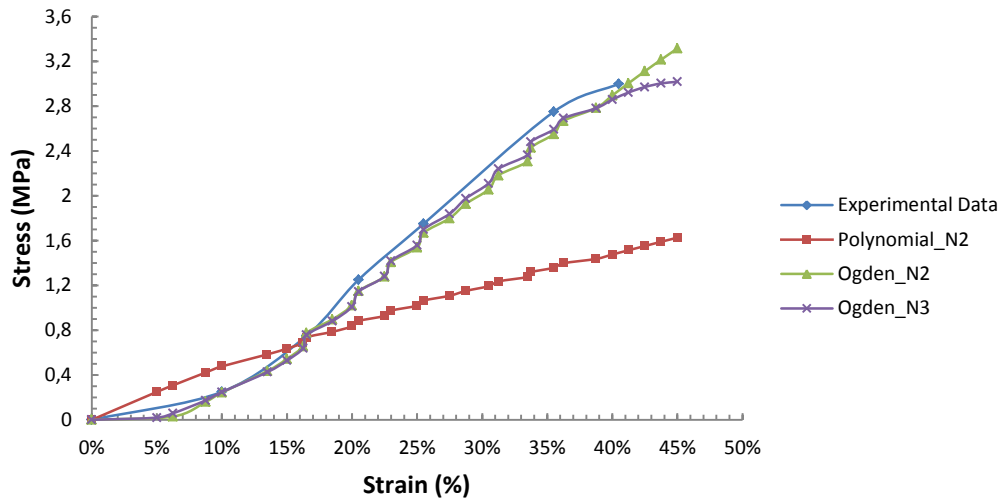


Figure 54 - Representation of the stress-strain graphical curves of uniaxial experimental data obtained for Ultrapro™ and respective representation of three constitutive models.

The model chosen for ProLite™ material was the Ogden N=3. The energy function of the strain is represented as:

$$W = \sum_{k=1}^N \frac{\mu_k}{\alpha_k} (\lambda_1^{\alpha_k} + \lambda_2^{\alpha_k} + \lambda_3^{\alpha_k} - 3) \quad (2)$$

Where λ_k represent the main tensions, μ_k and α_k are the material constants and N is the number of the terms of the function.

The constants of Ogden N=3 model obtained by the experimental data are respectively: K=1; $\mu_k=44,420$; $\alpha_k=4,146$; $D_k=0$; K=2; $\mu_k=-13,599$; $\alpha_k=6,595$; $D_k=0$; K=3; $\mu_k=-31,474$; $\alpha_k=1,038$; $D_k=0$.

6.3.2 Boundary Conditions

To achieve a better understanding of the deformations and movements of the pelvic viscera during specific loadings it is imperative to determine precisely the boundary conditions of the modeled structures. Besides, the main problems rely on the fact that all the pelvic tissues present a non-linear behavior incrementing difficulties to know what nodes are better suitable to fixate. The means to fix pelvic organs in the cavity are multiple in nature and are poorly defined anatomically [135].

The boundary conditions considered were imported from the previous model [69] and then modified. In this case all the pelvic floor bony insertions were selected to implement boundary conditions. Thus, certain nodes of LA and pelvic ligaments were designated to be conditioned. Additionally the sacrospinous ligaments insertion nodes for ischial spine and sacrum were picked. On the other hand, in this study the pubis was considered as a rigid body

and all of their respective degrees of freedom were conditioned. All the nodes selected were fully constrained - all translations (U_x , U_y and U_z) and rotations (R_x , R_y and R_z) with respect to x, y and z-axis are zero.

6.3.3 Constraints

The tie constraints are basically identified as the relation between two meshed structures where certain nodes from a 'slave' surface are tied to the most proximal nodes of a 'master' surface. In this case, degrees of freedom of both surfaces were constrained and subsequently the degrees of freedom (translation and/or rotation) were limited. Generally the master surface should be the surface corresponding to the stiffer structure, or the one which the meshed surface presents the most significant distance between nodes. The user can manipulate these surfaces freely by picking slave/master surfaces in the viewport and then tests can be performed to adjust the action of 'fused' surfaces [179].

This process is the key to define the non-linear complex behaviour of all pelvic floor structure under certain pathophysiological conditions. As an example, in the case of the user pretend to simulate the disruption of musculo-fascial associations, generating subsequent pelvic floor defects, in *ABAQUS* that is simply done by decreasing the number of constrained nodes between LA muscles and connective tissue.

Concerning the constraints of the 3D model, all pelvic ties between the different pelvic tissues were maintained. In the case, of new pelvic organs - pelvic tissues ties, they were redefined. Tie associations between synthetic meshes and pelvic tissues were carefully implemented considering the supporting function designated for these structures. The propylene meshes were requested to provide support and functional interaction with sacrospinous ligament, arcus tendineus and uterus/vagina mimetizing as possible surgical scenarios. The types of ties chosen were analogous to those provided by uterosacral ligament and pubocervical fascia. In Table 8 it is possible to analyze the kind of ties that were preferably used.

Table 8 - New constraints (added or redefined) considering master and slave surfaces and correspondent type of ties defined in the simulation

<i>Master Surface</i>	<i>Slave Surface</i>	<i>Type of Tie</i>
Uterosacral and cardinal ligaments	Uterus	Translation and Rotation
Uterus	Pubourethral ligament	Translation
Uterus	Pubocervical fascia	Translation and Rotation
Bladder	Pubourethral ligament	Translation
Bladder	Pubocervical Fascia	Translation and Rotation
Arcus tendineus fascia pelvis	Prolift Anterior	Translation
Prolift Anterior	Uterus	Translation and Rotation
Prolift Posterior	Uterus	Translation and Rotation
Sacrospinous ligament	Prolift Posterior	Translation
Puborectal muscle	Rectum	Translation and Rotation

Lateroposterior rectal ligament	Rectum	Translation
---------------------------------	--------	-------------

6.3.4 Contact Pairs

The contact pair definition is an important part of the mode definition. Generally, contact is generated when there are two surfaces that may interact with each other. *ABAQUS* enforces contact conditions by forming equations involving groups of nearby nodes from the respective surfaces or, in the case of self-contact, from separate regions of the same surface.

For contact pairs consisting of two deformable surfaces, as in this case (rectum-uterus; uterus-bladder; bladder-pubic bone and fascia; and pubocervical fascia-iliooccygeus muscle and puborectal muscle), the larger of the two surfaces should act as the master surface. If the surfaces are of comparable size, the surface on the stiffer body should act as the master surface. If the surfaces are of comparable size and stiffness, the surface with the coarser mesh should act as the master surface.

ABAQUS consents the set of two main types of interaction: finite-sliding and small-sliding. In the first case, surface nodes between the pair can slide and rotate with a wide amplitude which can also increase or decrease during the process of interaction. In the second case, surface nodes slide within smaller spaces and computational costs are lower than in the finite-sliding. However in both the finite- and small-sliding, arbitrary rotation can occur considering an unrestricted mode [69, 179].

In this work, to avoid high complexity inherent to finite-sliding interaction, the small-sliding was defined for all contact pairs interactions. New contact surfaces were established between new pelvic organs (Table 9). Concerning other pelvic tissues contacts, available contacts of the previous model [69] were imported to the simulation general folder.

Table 9 - New contact pairs surfaces defined between pelvic floor, bony tissue and refined pelvic organs.

<i>Master Surface</i>	<i>Slave Surface</i>
Anterior well of the rectum	Posterior wall of the uterus
Anterior wall of the uterus	Posterior wall of the bladder
Anterior wall of the bladder	Pubic bone and pubocervical fascia

6.3.5 Loads Set

Usually the female intrapelvic organs and inherent tissues are subjected to several pressure magnitudes in different dynamic directions. Generally these pressures are associated to normal abdominal pressures exerted during daily actions such as standing, resting, supine and sitting positions. Additionally, Valsalva maneuver is a specific exercise usually performed in current medical examination as a test to analyze several human physiological conditions. In the urogynecology medical field this test is performed to analyze hypermobility of the bladder neck and normal sphincter as well as normal or abnormal pelvic organ descent [67, 69]. Therefore, the magnitude values for abdominopelvic pressures were considered very important to study pathophysiological evolution of the pelvic structures and respective support defects (Table 10).

Concerning the direction and surface load, considered to study the progressive loss of rigid properties of uterosacral and cardinal complex and pubocervical ligaments, it was assumed that pressures applied in the normal direction of the posterior surface of the vaginal vault and uterine isthmus were appropriated to perform the simulation in a reliable way.

The second study contained new shell-based geometries which were never modelled in computer-based FEM programs. Therefore relative lower pressures were applied in posterior surfaces of vaginal vault and uterine isthmus. However the highest pressure load tested in the second study corresponded to the lowest pressure used in the first one (Table 11).

Table 10 - Intraabdominal pressure values for each type of maneuver. Magnitude of four pressures submitted in the first study [67].

<i>Maneuver</i>	<i>Pressure</i>
Supine	0,00024
Sitting	0,00223
Standing	0,00267
Valsalva	0,00529

Table 11 - Magnitude of four pressures submitted in the second study.

<i>Maneuver</i>	<i>Pressure</i>
Pressure 1	0,00005
Pressure 2	0,0001
Pressure 3	0,00015
Pressure 4	0,00024

6.4 Results and Discussion

6.4.1 Analyzes of vaginal and uterine wall displacements during normal and clinical conditions

In order to understand the physiopathological evolution of clinical conditions of uterine/vaginal wall the material properties of the USL and PCF were proportionally modelled to obtain a progressive decrease of connective tissue. Therefore PCF was modelled applying the following approach: normal material properties (100% PCF), 75% (75% PCF), 50% (50% PCF), and 25% (25% PCF) of the initial stiffness and no inclusion of the pubocervical fascia in the simulation (0% PCF). The same was done to USL: 100% USL, 75% USL, 50% USL, 25% USL and 0% USL.

The injury of the anterior and posterior pelvic walls support was studied through two different perspectives: displacements of sagittal cut approximately symmetric to the pelvic structures, and nodal displacement of the cervical ring and uterine cervix. The sagittal plan,

imported from ABAQUS viewport, allowed the visual characterization of the displacement and contact behaviour of big nodal groups, obtained in the simulations. This characterization was performed analyzing a continuous scale of colours - red and dark blue, representing, respectively, the highest and lowest displacements in positive direction. Concerning negative directions, dark blue corresponds to the highest displacements and red to highest displacements. Both the XX and YY axis were analyzed separately using these colour scales.

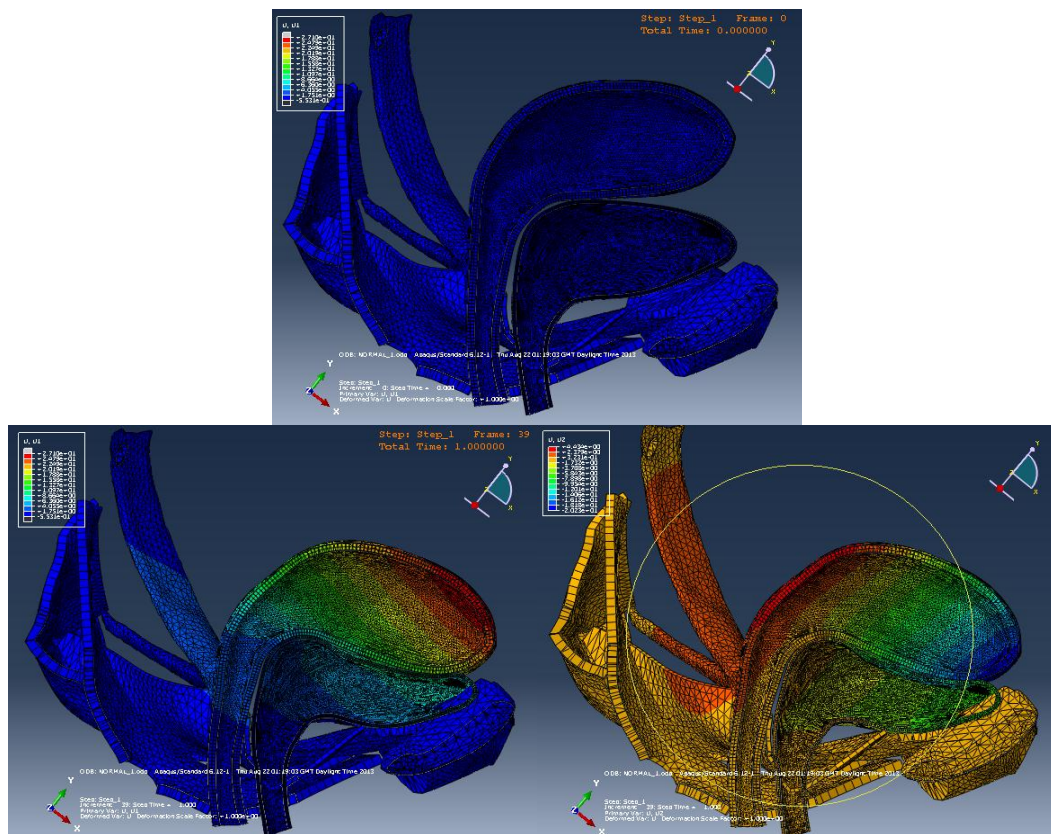


Figure 55 - Schematic representation of static non-pathologic pelvic structure (top) and nodal displacements in the XX (bottom left) and YY (bottom right) axis after valsalva pressures.

In Figure 55, it is characterized the pelvic floor, pubic bone and respective organs movements in normal conditions for applied valsalva pressures. As it was expected the uterus forced the bladder down and main nodes were displaced in an anterior and/or inferior direction. In this case, displacement in XX axis direction (anterior) was markedly higher in the upper body of the uterus with magnitudes ranging approximately 25 mm. In the YY axis (anterior) positive direction it was observed a displacement of the posterior uterine/vaginal wall of ≈ 4.30 mm. The anterior uterine/vaginal wall had a displacement of ≈ -1.70 mm in the YY axis (posterior).

In pathologic conditions, for 50% PCF and 50% USL, (Figure 56 and 57) the same pressures led to higher and complex contact between anterior surface of the vagina/uterus and posterior surface of the bladder.

In the case of 50% USL (Figure 56), comparing to non-pathologic conditions (Figure 55), it was observed a higher displacement of the upper body of the uterus in XX axis, almost 29 mm. There was also a greater displacement of the posterior and anterior uterine/vaginal

wall, in the YY axis, ≈ 4.70 mm and ≈ -3.20 mm, respectively. Besides, comparing to Figure 55, the central part of the ligaments of 50% USL presented a higher anterior displacement in the XX axis due to lowered restiveness to stretch.

In the case of 50% PCF (Figure 57), comparing to non-impaired fascia (Figure 52), there were no significant differences of uterus' upper body displacement in XX axis. This might be explained due to a continuous support of healthy USL which is the most superior support of the vaginal wall, preventing accentuated displacements of the uterus in the anterior direction. Moreover, for the same fault scenario (50% PCF), this exclusive support provided by USL prevented significant movements of the posterior vaginal wall, in the YY axis, ≈ 4.70 mm. Interestingly, displacements of the anterior vaginal wall, in the same axis, were two times higher, - 7.47 mm. This is explained by the increase of 50% of fascial elasticity.

In figure 58, in the absence of fascial support (0% PCF), comparing to 50% PCF, it was identified a higher visual displacement of the uterus fundus in the direction of pubic bone, compressing consistently the external surface of the bladder. The uterus fundus tends to expand while the USL exhibits an exclusive behavior during posterior wall suspension. Additionally, it was observed a total contact between the cervical ring and the posterior bladder wall, as it was expected.

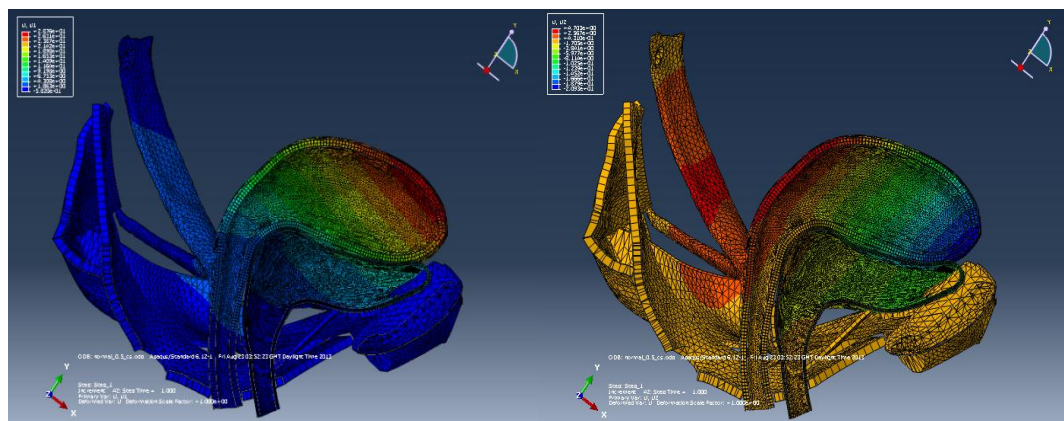


Figure 56 - Schematic representation of pathologic pelvic structure 50% USL. There are presented nodal displacements in the XX (bottom left) and YY (bottom right) axis after valsalva pressures.

Therefore, nodes of the anterior and posterior uterine/vaginal wall presented a displacement in YY axis of approximately 5,00 mm and - 7,85 mm.

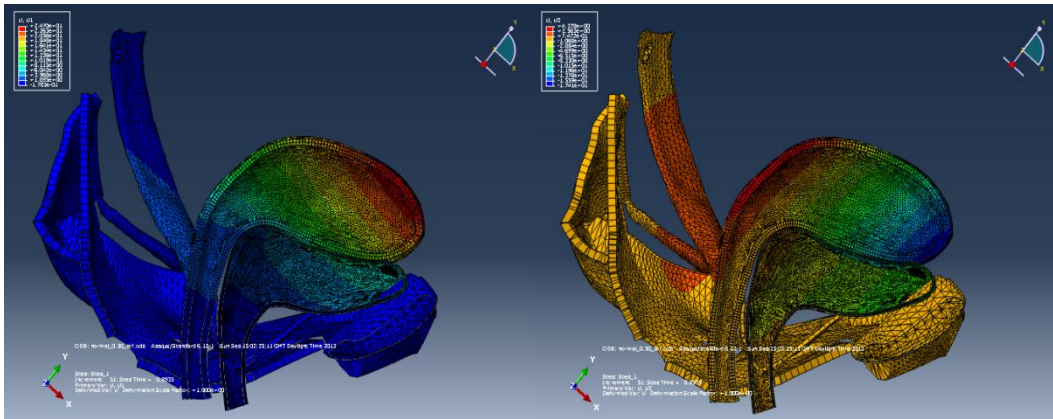


Figure 57 - Schematic representation of pathologic pelvic structure 50% PCF. There are presented nodal displacements in the XX (bottom left) and YY (bottom right) axis after valsalva pressures.

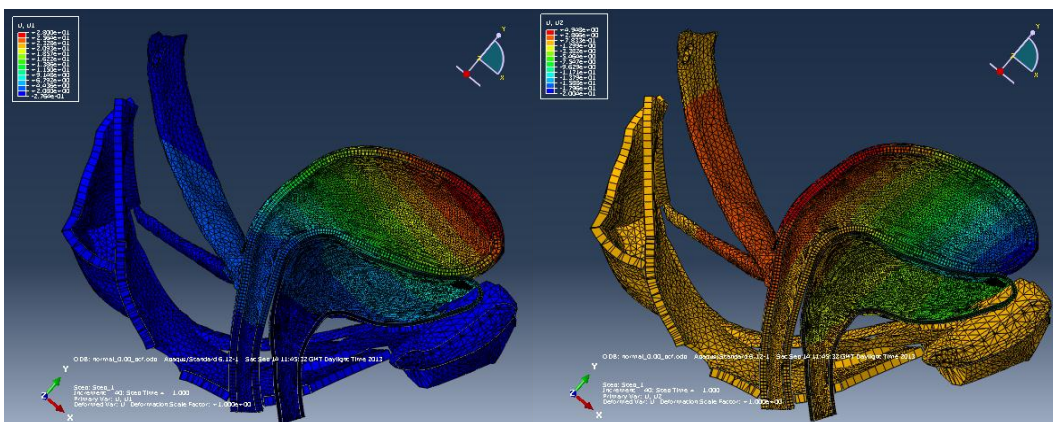


Figure 58 - Schematic representation of pathologic pelvic structure 0% PCF. There are presented nodal displacements in the XX (bottom left) and YY (bottom right) axis after valsalva pressures.

Furthermore, the second part of analyzes consisted in specific nodes selection for posterior numerical evaluation. In order to obtain precise measurements of nodal displacement of the cervical ring (by lowering the PCF stiffness) and the uterine cervix (lowering the USL stiffness), 4 nodes of each uterine region were carefully selected for posterior numerical analysis, represented in Figures 59 and 60. The effect of modelled injuries is well presented in both figures.

In figure 59 the graphical interface assumes a proportional association between increase of elasticity and increase of nodal displacement of the cervical ring. More precisely, from 50% PCF to 0% PCF there is a successive displacement increase of approximately 0,25 mm in XX axis, for the same applied pressure (0.00024 MPa). Furthermore, comparing 0% PCF and 100% PCF, there was a total increase of nodal displacement of 0,6737 mm in XX axis (anteroinferior direction). Interestingly, during the simulations the nodal displacement direction from 100% PCF to 25% PCF was mainly negative, posterior, but when there was not presence of fascia tissue, 0% PCF, direction turned positive, anterior (towards the bladder), with a value of 0,0979 mm. This reinforces theoretical information stating that loss of pubocervical fascial support leads to anterior vaginal wall prolapse [63].

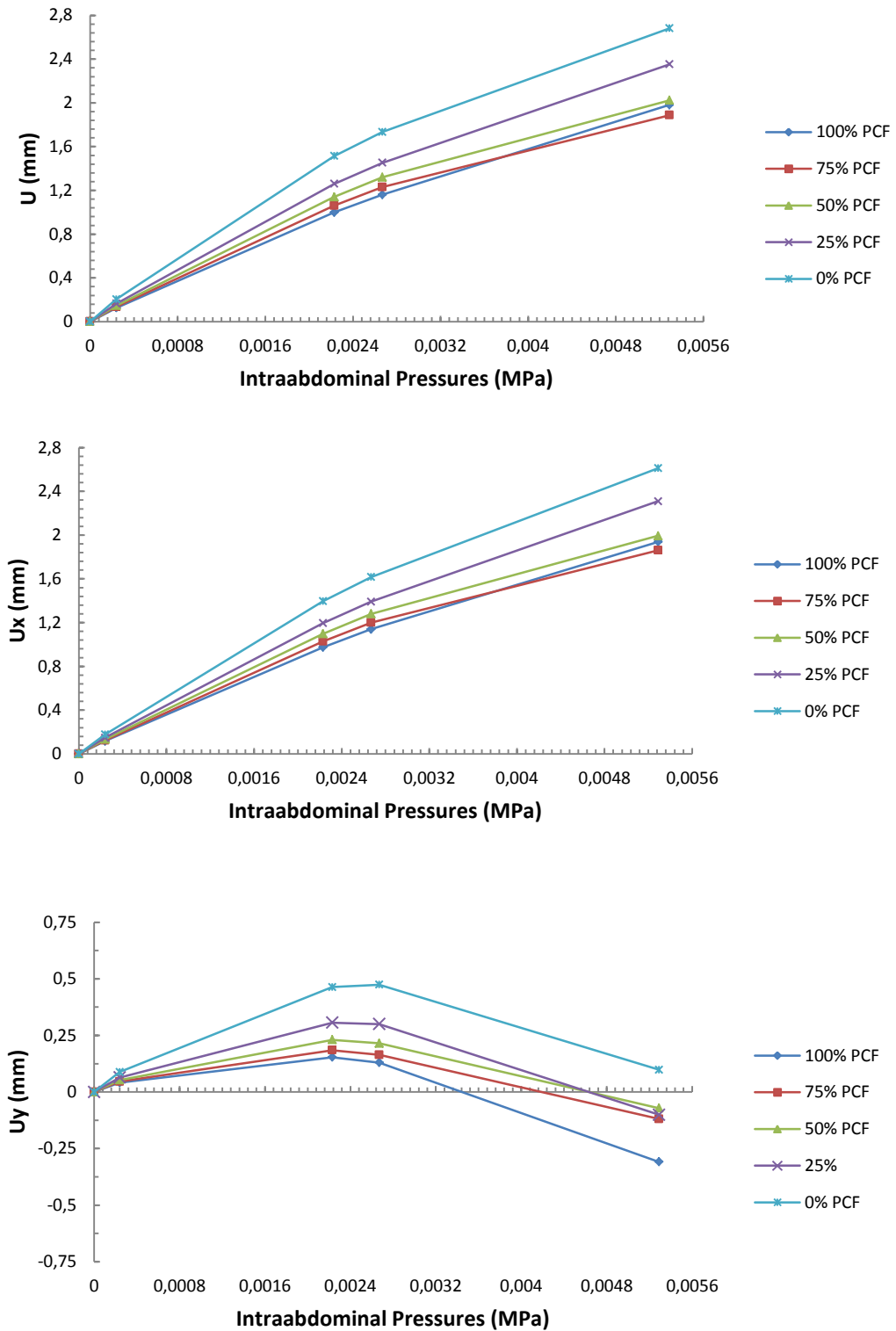


Figure 59 - Graphical representation of the cervical ring displacement (U, Ux, and U, respectively) regarding the stiffness variation (0% PCF to 100% PCF).

In Figure 60, 0% USL, was not plotted because simulations did not converge properly for the following loads: 0,00529, 0,00267 and 0,00223 MPa. In the case of 25% USL model failed for the last pressure (0,00529 MPa). In these results it is possible to observe that USL

injury is associated to higher displacement on the XX axis anterior direction, towards the posterior bladder wall. This displacement increase was significant with a value of 3,233 mm.

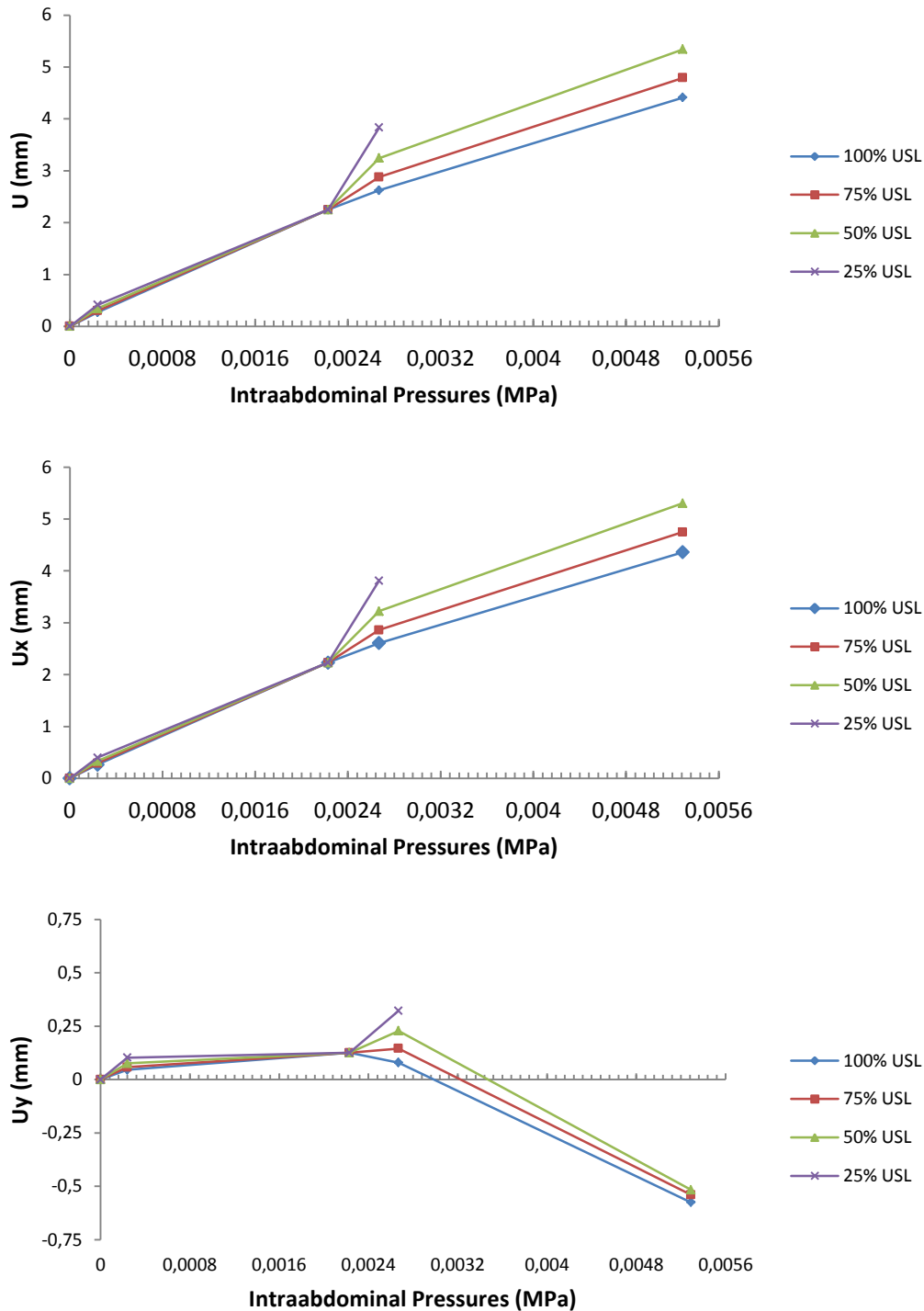


Figure 60 - Graphical representation of the cervix uterine displacement (U, Ux, and Uy, respectively) regarding the stiffness variation (0% USL to 100% USL).

Concerning the nodal displacement in YY axis, there were not observed relevant differences between the different states of defective USL. Thus, it can be concluded that PCF

fascia is an important anteromedial support of vaginal wall which also prevents great displacements of uterine cervix.

6.4.2 Analyzes of vaginal and uterine wall displacements during clinical conditions after urogynecologic surgical mesh placement

Clinical conditions after implantation of Prolift-like anterior or posterior repair were analyzed in a similar way of 6.4.1., in order to observe differences between impaired tissues and reinforced compartments. The simulations of clinical conditions were performed for 0% PCF and 0% USL to verify if there was some tissue reinforcement and pelvic organs stabilization under defined pressures.

In Figure 61, it is possible to observe that Prolift Posterior mesh lowered anterior and posterior vaginal displacement towards the uterus (anterior direction). The range of displacements, in the XX axis, without fascial support (0% USL), was between 0,765 mm and 1,75 mm. On the other hand, the range of displacements, in the XX axis, with tension-free Prolift Posterior reinforcement, was between 0,340 mm and 1,41 mm. Concerning the YY axis displacements, there were not evidences of support with mesh presence, without prevention of uterine movement towards the bladder. The 0% USL presented vaginal wall displacements, in the YY axis, ranging from - 0,805 mm to 0,150 mm. Additional support with Prolift Posterior presented displacements ranging from - 0,433 mm to 0,821 mm.

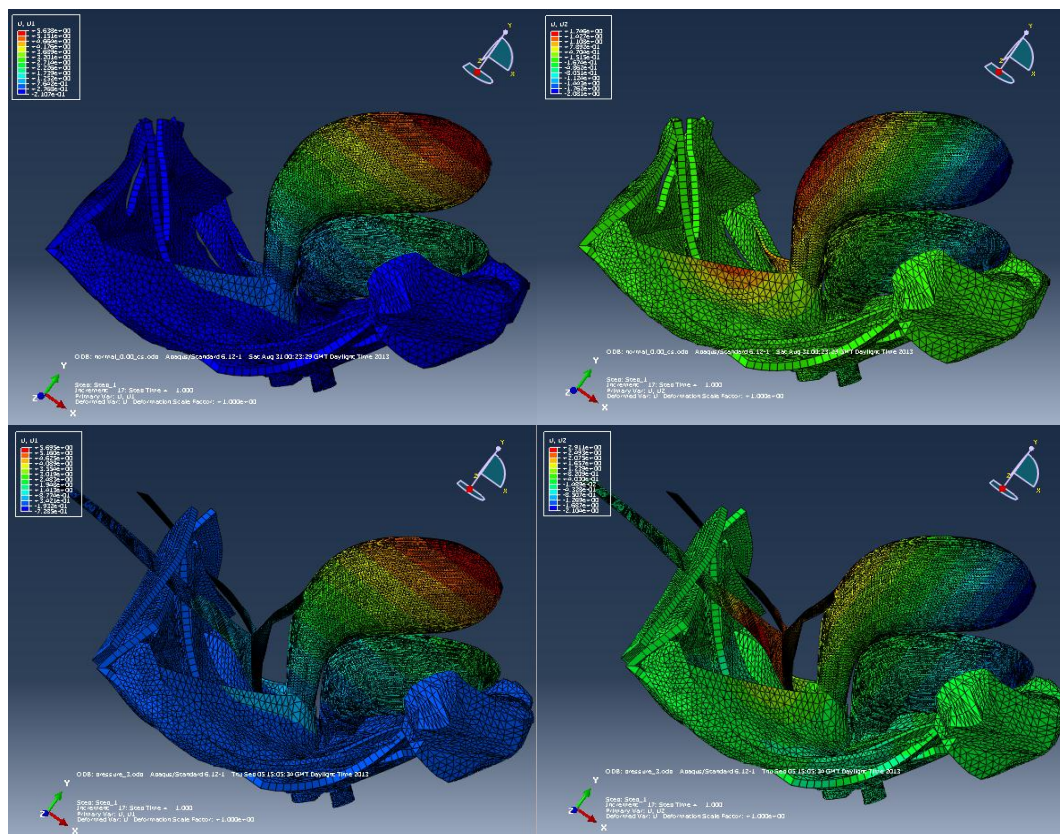


Figure 61 - Schematic representation of nodal displacement, in XX (left) and YY (right) axis, for pathological 0% USL condition (top) and Prolift-like posterior support (bottom), under pressures of 0,00024 MPa. Ultrapro was the surgical mesh's material used in this simulation.

However, it is apparent that pubocervical fascia and uterine isthmus presented significant lower displacements, in the anterior direction, with synthetic reinforcement.

It is possible to infer that, even if there were used low intraabdominal pressures, the shell-based mesh for the posterior reinforcement revealed suitable sacrospinous ligament and uterine isthmus fixation. While the uterus is supported, the mesh lateral arms suffer displacement, in positive YY axis, preventing great vaginal wall displacements.

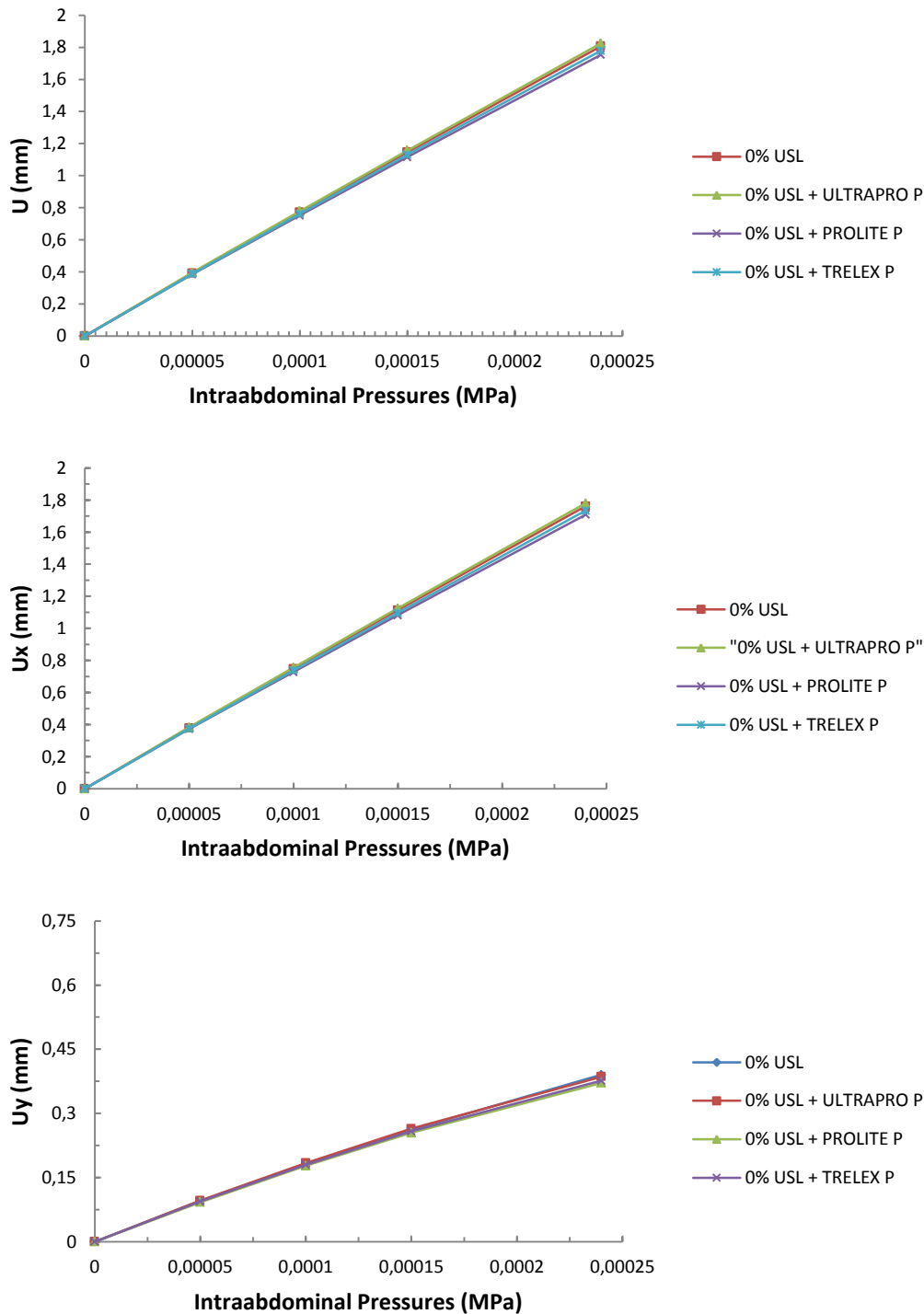


Figure 62 - Graphical representation of the cervix uterine displacement (U, Ux, and U, respectively) for 0% USL with and without different polypropylene-like meshes reinforcement.

In the study of numerical analyses of uterine cervix displacement (Figure 62) there were not evidences of support when it was placed Prolift Posterior within the rectovaginal space. Ultrapro, Prolene and Trelex had the same behaviour for all applied pressures.

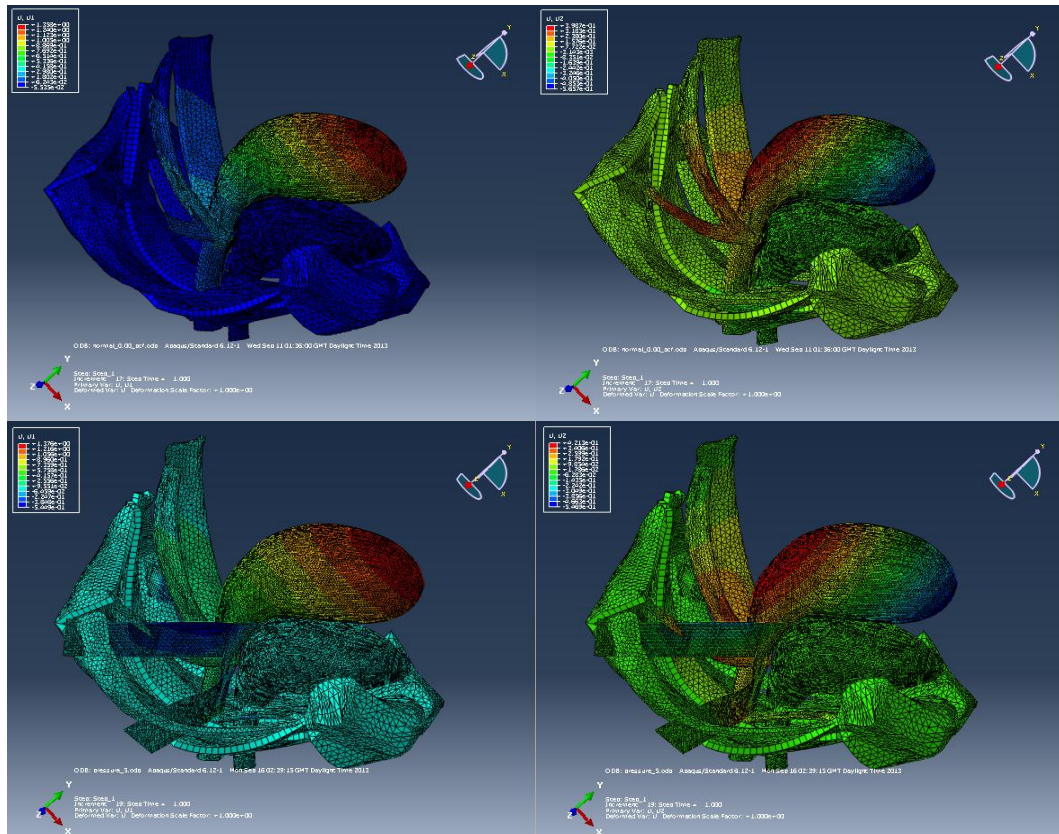


Figure 63 - Schematic representation of nodal displacement, in XX (left) and YY (right) axis, for pathological 0% PCF condition (top) and Prolift-like anterior support (bottom), under pressures of 0,00024 MPa. Ultrapro was the surgical mesh's material used in this simulation.

In Figure 63, for the pathologic scenario (0% PCF) it was observed a nodal displacement of the vaginal wall ranging from 0,180 mm and 0,415 mm, the XX axis. After the reinforcement with Prolift Anterior the range of displacements, in the same axis, was approximately 0,096 mm. The displacement of vaginal wall with mesh reinforcement was a half of the displacement without presence of the mesh. In YY axis, the range of displacements of vaginal impaired tissue was 0,077 - 0,158 mm. In the case of additional reinforcement with Prolift using Ultrapro material, the nodal displacements of vaginal wall ranged from 0,098 mm to 0,179 mm. The anterior mesh placement in vesicovaginal space presented considerable preventive movements of the vaginal/uterine walls towards the bladder.

Contrarily to Prolift Posterior, the anterior support with Prolift-like mesh revealed to be significantly effective, even if for prevention of cervical ring displacement, Figure 64. Remarkably, midweight and heavyweight (stiffer than Ultrapro) prevented more reliably cervical ring displacements. Prolite (midweight) presented the best results, lowering anterior displacement of cervical ring in 0,0220 mm and 0,0302 mm, respecting XX and YY axis,

respectively. Trelex present the second best results and Ultrapro did not show evidences of additional support for the cervical ring.

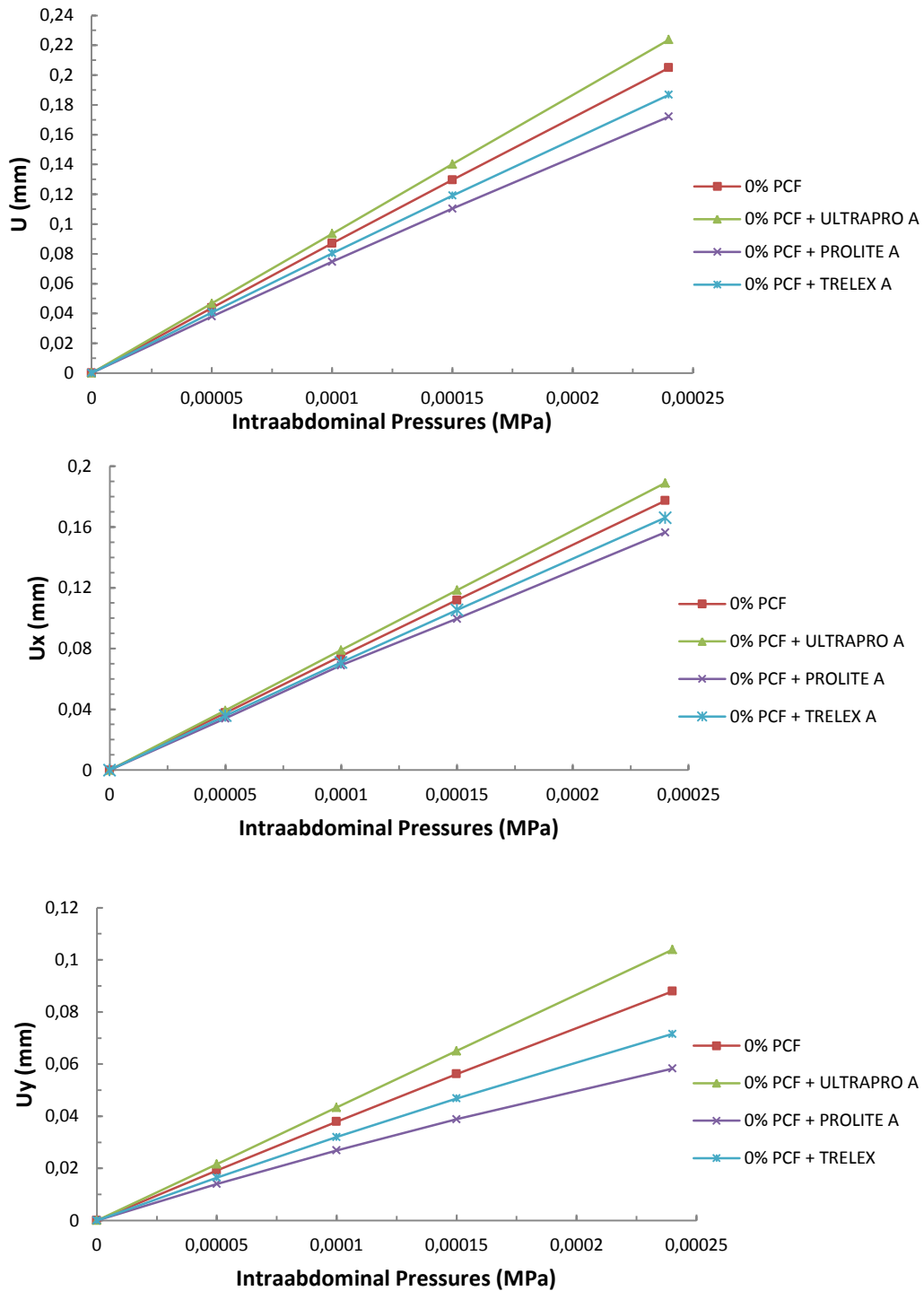


Figure 64 - Graphical representation of the cervical ring displacement (U, Ux, and U, respectively) for 0% PCF with and without different polypropylene-like meshes reinforcement.

Chapter 7

Conclusion and Future Perspectives

7.1 Conclusion

Nowadays, mathematical investigation models of 3D structures are considered desirable and complex tools to obtain and reproduce detailed information about specific real-life problems, more precisely pathologic biomedical scenarios. Several studies, analyzed in this work, proved that is possible to achieve similar and reliable approximation of normal and clinical situations.

More specifically, in the urogynecological field it is possible to simulate anatomically realistic computational models of the main structures of the pelvic floor: levator ani muscles, endopelvic connective tissue and pelvic organs. These are important components to develop mechanical studies of the normal function of whole pelvic floor.

Moreover, in the few currently available geometric pelvic floor models, suitable for finite element analysis, there was not developed surgical approximations or simulations. Therefore, in this work, a previous pelvic floor model was carefully analyzed and refined to introduce failures in the system of support and suspension of the pelvic floor organs, more precisely vagina and uterus.

The simulation of fault scenarios, of the generated model, exclusively through the decrease of strength and rigidity of the pubocervical fascia and uterosacral ligaments, were key factors to understand how the injured pelvic tissues responded during applied intraabdominal loads. In order to analyze the biomechanical behavior of impaired connective tissue, it was compared vaginal and/or uterine nodal displacements during vasalva pressures (0,00529 MPa) applied in the posterior wall of the uterus for normal and weakened structures. Concerning non-pathological scenarios, uterus fundus displacement, in XX axis, and anterior and posterior vaginal wall displacement, in YY axis, was: 25 mm, -1,70 mm, and 4,30 mm, respectively. For 50% of the initial uterosacral ligaments stiffness, the same sequence of displacements was: 29 mm, -3,20 mm, and 4,70 mm. For 50% of the initial pubocervical fascia stiffness this sequence was: 28 mm, -7,85 mm and 5 mm. On the other hand, about cervical ring nodal displacement, absence of pubocervical fascia lead to an increase of 0,6737 mm, in XX axis, comparing to healthy fascia.

These results confirmed that existence of connective tissue weakening lead to higher magnitude of displacements in inferior direction of pelvic organs in a sagittal view. During the analysis, uterosacral ligaments were considered the most supportive structures for both the anterior and posterior vaginal wall support, although they remained more effective

preventing great displacements of the posterior vaginal wall. These findings can be crucial to understand how vaginal and uterine wall are mechanically affected after impairment of specific pelvic floor tissues. In this study, pelvic floor damage revealed a tendency to introduce higher mechanical instability of the vaginal and uterine pelvic walls.

Nevertheless, it was inevitable to study the relevance of surgical interventions based on minimally invasive placement of polypropylene-like urogynecologic meshes within both the vesicovaginal and rectovaginal space. Geometrical and mechanical properties of Prolift-like meshes were carefully developed for this type of modeled pathology. The sacrospinous suspension of the posterior uterine wall with Prolift Posterior as well as anterior uterine wall reinforcement with Prolift Anterior mesh, followed meticulous surgical information found in the literature for a consistent reconstruction of the uterine/vaginal wall support. Similarities between real and modeled repair were confirmed. Hyperelastic properties of different polypropylene meshes were also modeled precisely with application of specific stress-strain constitutive models.

Therefore, applied pressures of 0,00024 MPa on the posterior uterine surface established that, in the absence of uterosacral ligaments support, the magnitude of displacements of the anterior/posterior vaginal wall, in the XX axis, ranged between 0,765 - 1,75 mm. After vaginal reinforcement, with Prolift Posterior, this range was lowered to 0,34 - 1,41 mm. Concerning, uterine cervix there were no evidences of pronounced displacements before and after Prolift Posterior placement, even if it was used three different polypropylene materials. In the absence of pubocervical fascia the displacements of the anterior and posterior vaginal wall, in the XX axis, ranged between 0,180 - 0,415 mm and after Prolift Anterior placement this range was lowered to 0,096 mm. Regarding YY axis, this range was initially 0,077 - 0,158 mm and after anterior vaginal wall reinforcement with Prolift Posterior the range was 0,098 - 0,179 mm. Therefore, both the anterior and the posterior modelled meshes presented reliable biomechanical support with interesting results for future surgical applications.

On the other hand, surgical simulation with application of polypropylene-like meshes with different hyperelastic behaviors can be really useful to understand how pelvic organs are re-supported and how effective is the restoration of the expected support. In this case, midweight polypropylene mesh, ProLite™, presented the best results, lowering the displacement of the cervical ring, in the XX and YY axis, in magnitudes of 0,0220 mm and 0,0302 mm, respectively. Trelex also presented a great supportive behaviour, although magnitude of displacements was half of the presented by ProLite™.

Hence, in this study, it was conducted a novel simulated hypothesis about the pathophysiological evolution of vaginal and uterine supporting system. The present study demonstrated the feasibility of using computer-based research to study specific female pelvic organ prolapse by correlating dynamic mechanical behavior of the impaired connective tissue with the dynamic biomechanical response of pelvic organs. The FEM system used and remodelled, presented considerable variances between injured pelvic organs with and without repair employing polypropylene-like mesh. The simulations presented reliable data to continue developing unique 3D surgical models for genital prolapse treatment. It is vital to continue optimizing new therapeutic strategies for injured pelvic tissues in order to develop standardized global approaches.

7.2 Future Perspectives

Given the fact that, this was a pioneer study based on 3D finite element modeling for genital reinforcement, using novel simulated urogynecologic meshes, there are considerable limitations associated to this approach.

First of all, in this study it was noticed the necessity of refining some structural aspects of the general finite element model, more precisely contacts pairs between viscera from the middle compartment. In this case, endopelvic fascia and pelvic bone presented could be remodelled and re-meshed, in order to obtain surfaces with high contact definition with the bladder. The usual convergence problems for considerable high intraabdominal pressures would be eliminated from the 3D model. Additionally, contact pairs between internal surfaces of the uterus could produce interesting results, regarding its deformable behavior during high pressure loads.

On the other hand, the Mooney-Rivlin and Ogden $N=3$ stress-strain energy functions used to model the mechanical properties of polypropylene meshes, were found to be unstable for determined uniaxial strains. Therefore, other constitutive models such as Reduced Polynomial $N=1$ and Ogden $N=1$ were found to be great possibilities to obtain stable hyperelastic materials and evaluative associations between new surgical meshes and female pelvic floor.

As mentioned before, no research work was published or done concerning simulation of injured pelvic floor with subsequent urogynecologic mesh repair. Therefore, there is a lack of validation models in this field, even for uterine cervix and/or cervical ring. The data presented in this work was only compared between normal, abnormal and/or post-implantation of the mesh. Comparison of modeled results with those obtained during diagnostic techniques could be a powerful tool to analyse dynamically each pelvic floor structure, injury or reinforcement, with high rate of feasibility. Researchers could develop a new validation model concerning specifications of each simulation.

Quite a few techniques can be employed and tested to study biomechanical impairment of endopelvic connective tissue, because in the study it was used a simple approach to introduce fault scenarios in the system.

Concerning surgical meshes, new prosthetics with new geometries and property material, could be included in the model to obtain the best possible relation between mesh placement - tissue healing and reinforcement.

Several modifications and improvements can be employed in this finite element model. Every evaluation of the model will lead to develop precise numerical analysis of genital prolapse and develop knowledge about pelvic floor impairment.

References

- [1] Subramanian, D., et al. **Rate, type, and cost of pelvic organ prolapse surgery in Germany, France, and England.** *European Journal of Obstetrics & Gynecology and Reproductive Biology* (2009) 144: 177-181.
- [2] Krissi, H., et al. **The role of primary physicians in the diagnostic delay of lower urinary tract and pelvic organ prolapse symptoms.** *European Journal of Obstetrics & Gynecology and Reproductive Biology* (2012) 161: 102-104.
- [3] Luber, K., et al. **The Demographics of Pelvic Floor Disorders: Current observations and future projections.** *American Journal of Obstetrics & Gynecology* (2001) 184: 1496 -1503.
- [4] Thakar, R., et al. **Regular Review: Management of genital prolapse.** *British Medical Journal* (2002) 324: 1258-1262.
- [5] Ghetti, C., et al. **Pelvic organ descent and symptoms of pelvic floor disorders.** *American Journal of Obstetrics & Gynecology* (2005) 193: 53-7.
- [6] Kim, C., et al. **Risk factors for pelvic organ prolapse.** *International Journal of Gynecology & Obstetrics* (2007) 98: 248-251.
- [7] Brækken, I., et al. **Can pelvic floor muscle training reverse pelvic organ prolapse and reduce prolapse symptoms? An assessor-blinded, randomized, controlled trial.** *American Journal of Obstetrics & Gynecology* (2010) 170: 1-7.
- [8] Castelo-Branco, C., et al. **Management of post-menopausal vaginal atrophy and atrophic vaginitis.** *Maturitas* (2005) 52: 46-52.
- [9] Hanson, L-A., et al. **Vaginal pessaries in managing women with pelvic organ prolapse and urinary incontinence: patient characteristics and factors contributing to success.** *International Urogynecology Journal* (2006) 17: 155-159.
- [10] Beer, M., et al. **Surgical techniques for vault prolapse: a review of the literature.** *European Journal of Obstetrics & Gynecology and Reproductive Biology* (2005) 119: 144-155.
- [11] Olsen, A., et al. **Epidemiology of surgically managed pelvic organ prolapse and urinary incontinence.** *Obstetrics & Gynecology* (1997) 89: 501-506.
- [12] Cvach, K., et al. **Surgical management of pelvic organ prolapse: abdominal and vaginal approaches.** *World Journal of Urology* (2011) 345.
- [13] Fukuda, T., et al. **Outcomes of traditional prolapse surgery for pelvic organ prolapse repair at a single center.** *International Journal of Gynecology & Obstetrics* (2012) 119: 277-280.
- [14] Huebner, M., et al. **The use of graft materials in vaginal pelvic floor surgery.** *International Journal of Gynecology & Obstetrics* (2006) 92: 279–288.
- [15] Iglesia, C., et al. **The use of mesh in Gynecologic Surgery.** *International Urogynecology Journal* (1997) 8: 105-115.

- [16] Hogston, P., et al. **Management of recurrent vaginal prolapse.** *Reviews in Gynaecological Practice* (2003) 3: 109-113.
- [17] Deprest, J., et al. **Synthetic and biodegradable prostheses in pelvic floor surgery.** *International Congress Series* (2005) 1279: 387- 397.
- [18] Theobald, P., et al. **Place of mesh in vaginal surgery, including its removal and revision.** *Best Practice & Research Clinical Obstetrics and Gynaecology* (2011) 25: 197-203.
- [19] Dietz, H., et al. **Mechanical properties of urogynecologic implant materials.** *International Urogynecology Journal* (2003) 14: 239-243.
- [20] Birch, C., et al. **The use of prosthetics in pelvic reconstructive surgery.** *Best Practice & Research Clinical Obstetrics & Gynaecology* (2005) 19: 979-991.
- [21] Jones, K., et al. **Tensile properties of commonly used proplapse meshes.** *International Urogynecology Journal* (2009) 20: 847-853.
- [22] Walter, J-E., et al. **Transvaginal Mesh Procedures for Pelvic Organ Prolapse.** *Journal of Obstetrics & Gynaecology Canada* (2011) 33: 168-174.
- [23] Reisenauer, C., et al. **Anatomical conditions for pelvicfloor reconstruction with polypropylene implant and its application for the treatment of vaginal prolapse.** *European Journal of Obstetrics & Gynecology and Reproductive Biology* (2007) 131: 214-225.
- [24] Lensen, E., et al. **The use of synthetic mesh in vaginal prolapse surgery: a survey of Dutch urogynaecologists.** *European Journal of Obstetrics & Gynecology and Reproductive Biology* (2012) 162: 113-115.
- [25] Sung, V., et al. **Graft Use in Transvaginal Pelvic Organ Prolapse repair, A systematic review.** *Obstetrics & Gynecology* (2008) 112: 1131-1142.
- [26] Sola, V., et al. **Tension free monofilament macropore polypropylene mesh (Gynemesh PS) in female genital prolapse repair.** *International Brazilian Journal of Urology* (2006) 32: 410-415.
- [27] Fatton, B., et al. **Transvaginal repair of genital prolapse: preliminary results of a new tension-free vaginal mesh (Prolift™ technique) - a case series multicentric study.** *International Urogynecology Journal* (2007) 18: 743-752.
- [28] De Vita, D., et al. **Vaginal reconstructive surgery for severe pelvic organ prolapses: A 'uterine-sparing' technique using polypropylene prostheses.** *European Journal of Obstetrics & Gynecology and Reproductive Biology* (2008) 139: 245-251.
- [29] Moore, R., et al. **Vaginal Mesh Kits for Pelvic Organ Prolapse, Friend or Foe: A Comprehensive Review.** *The Scientific World Journal* (2009) 9: 163-189.
- [30] Gynacera Prolift Pelvic Floor Repair System. *Surgical Technique.*
- [31] Food and Drug Administration (FDA). **Urogynecologic Surgical Mesh: Update on the Safety and Effectiveness of Transvaginal Placement for Pelvic Organ Prolapse.** *Center for Devices and Radiological Health* (2011).
- [32] Altman, D., et al. **Short-term outcome after transvaginal mesh repair of pelvic organ prolapse.** *International Urogynecology Journal* (2008) 19: 787-793.
- [33] Sokol, A., et al. **One-year objective and functional outcomes of a randomizedclinical trial of vaginal mesh for prolapse.** *American Journal of Obstetrics & Gynecology* (2012) 86: e1-e9.
- [34] Long, C-Y., et al. **Three-year outcome of transvaginal mesh repair for the treatment of pelvic organ prolapse.** *European Journal of Obstetrics & Gynecology and Reproductive Biology* (2012) 161: 105-108.
- [35] Deffieux, X., et al. **Prevention of complications related to the use of prosthetic meshes in prolapse surgery: guidelines for clinical practice.** *European Journal of Obstetrics & Gynecology and Reproductive Biology* (2012) 1-11.
- [36] Fung, Y.; Tong, P. **Classic and computational solid mechanics.** (2001) World Scientific, Singapore.

- [37] Janda, S., et al. **Measuring morphological parameters of the pelvic floor for finite element modelling purposes.** *Journal of Biomechanics* (2003) 36: 749-757.
- [38] Singh, K., et al. **Three-dimensional magnetic resonance imaging assessment of levator ani morphologic features in different grades of prolapse.** *American Journal of Obstetrics & Gynecology* (2003) 188: 910-915.
- [39] Boukerrou, M., et al. **Etude préliminaire d'un modèle mécanique de cavité vaginale.** *ITBM-RBM* (2004) 25: 3-14.
- [40] D'Aulignac, D., et al. **A shell finite element model of the pelvic floor muscles.** *Computer Methods in Biomechanics and Biomedical Engineering* (2005) 8: 339-347.
- [41] Rubod, C., et al. **A biomechanical model of the pelvic cavity: first steps.** *EMBS Annual International Conference* (2006) 968-971.
- [42] Martins, J., et al. **Finite Element Studies of the Deformation of the Pelvic Floor.** *New York Academy of Science* (2007) 1101: 316-334.
- [43] Noakes, K., et al. **Anatomically Realistic Three-Dimensional Meshes of the Pelvic Floor & Anal Canal for Finite Element Analysis.** *Annals of Biomedical Engineering* (2008) 36: 1060-1071.
- [44] Parente, M., et al. **Deformation of the pelvic floor muscles during a vaginal delivery.** *International Urogynecology Journal* (2008) 19: 65-71.
- [45] Noakes, K., et al. **Subject specific finite elasticity simulations of the pelvic floor.** *Journal of Biomechanics* (2008) 41: 3060-3065.
- [46] Zhang, Y., et al. **Feasibility of Using a Computer Modeling Approach to Study SUI Induced by Landing a Jump.** *Annals of Biomedical Engineering* (2009) 37: 1425-1433.
- [47] Hoyte, L., et al. **Measurements from Image-Based Three Dimensional Pelvic Floor Reconstruction: A Study of Inter- and Intra-observer Reliability.** *Journal of Magnetic Resonance Imaging* (2009) 30: 344-350.
- [48] Ma, Z., et al. **A review of algorithms for medical image segmentation and their applications to the female pelvic cavity.** *Computer Methods in Biomechanics and Biomedical Engineering* (2010) 13: 235-246.
- [49] Rao, G., et al. **Experiments and finite element modelling for the study of prolapse in the pelvic floor system.** *Computer Methods in Biomechanics and Biomedical Engineering* (2010) 13: 349-357.
- [50] Janda, S. **Biomechanics of the pelvic floor musculature.** (2006) PhD Thesis, Netherlands.
- [51] Martins, P., et al. **Uniaxial mechanical behavior of the human female bladder.** *International Urogynecology Journal* (2011) 22: 991-995.
- [52] Rubod, C., et al. **Biomechanical Properties of Human Pelvic Organs.** *Urology* (2012) 79: 968.e17-968.e22.
- [53] Rivaux, G., et al. **Comparative analysis of pelvic ligaments: a biomechanics study.** *International Urogynecology Journal* (2013) 24: 135-139.
- [54] Kirilova, M., et al. **Experimental study of the mechanical properties of human abdominal fascia.** *Medical Engineering & Physics* (2011) 33: 1-6.
- [55] Cosson, M., et al. **A study of pelvic ligament strength.** *European Journal of Obstetrics & Gynecology and Reproductive Biology* (2003) 109: 80-87.
- [56] Dalstra, M., et al. **Mechanical and textural properties of pelvic trabecular bone.** *Journal of Biomechanics* (1993) 26: 523-535.
- [57] Cosson, M., et al. **A biomechanical study of the strength of vaginal tissues. Results on 16 post-menopausal patients presenting with genital prolapse.** *European Journal of Obstetrics & Gynecology and Reproductive Biology* (2004) 112: 201-205.
- [58] Rubod, C., et al. **Biomechanical Properties of Vaginal Tissue. Part 1: New Experimental Protocol.** *The Journal of Urology* (2007) 178: 320-325.

- [59] Martins, P., et al. **Prediction of nonlinear elastic behaviour of vaginal tissue: experimental results and model formulation.** *Computer Methods in Biomechanics and Biomedical Engineering* (2010) 13: 327-337.
- [60] Epstein, L., et al. **Systemic and vaginal biomechanical properties of women with normal vaginal support and pelvic organ prolapse.** *American Journal of Obstetrics & Gynecology* (2007) 165: e1-e6.
- [61] Drake, R.; Vogl, W. **Gray's Anatomy for Students.** (2005) 1st Edition - Elsevier.
- [62] Ashton-Miller, J., et al. **On the Biomechanics of Vaginal Birth and Common Sequelae.** *Annual Review of Biomedical Engineering* (2009) 11: 163-176.
- [63] Ashton-Miller, J., et al. **Functional Anatomy of the Female Pelvic Floor.** New York Academy of Sciences (2007) 1101: 266-296.
- [64] Bharucha, A. **Pelvic floor: anatomy and function.** *Neurogastroenterology & Motility* (2006) 18: 507-519.
- [65] Barber, M., et al. **Contemporary views on female pelvic anatomy.** *Cleveland Clinic Journal of Medicine* (2005) 72: 1-11.
- [66] Petros, P. **The Pubourethral Ligaments - an Anatomical and Histological Study in the Live Patient.** *International Urogynecology Journal* (1998) 9: 154-157.
- [67] Cobb, W., et al. **Normal Intraabdominal Pressure in Healthy Adults.** *Journal of Surgical Research* (2005) 129: 231-235.
- [68] Alrteiro, M., et al. **Construção de um modelo 3D dos órgãos da cavidade pélvica feminina.** (2009).
- [69] Silva, A. **Estudo Biomecânico da Cavidade Pélvica da Mulher.** Unpublished Master Thesis. Faculdade de Engenharia da Universidade do Porto, Portugal (2012).
- [70] Herschorn, S., et al. **Female Pelvic Floor Anatomy: The Pelvic Floor, Supporting Structures, and Pelvic Organs.** *Reviews in Urology* (2004) 6: 2-10.
- [71] Moore, K.; Dalley A. **Oriented Anatomy.** (2006) 5th Edition - Lippincott Williams & Wilkins.
- [72] Seeley, R.; Stephens, T.; Tate, P. **Anatomy and Physiology.** (2003) 6th Edition - McGraw-Hill Higher Education.
- [73] Williams, P.; Warmick, R.; Dyson, M.; Bannister, L. **Gray's Anatomy.** (1995) 37th Edition - Guaranaabara Koogan.
- [74] International Urogynecological Association (IUGA). **Sacrospinous Fixation/ Ileococcygeus Suspension. A Guide for Women.** (2011).
- [75] Lantzsch, T., et al. **Sacrospinous ligament fixation for vaginal vault prolapse.** *Archieve of Gynecology and Obstetrics* (2001) 265: 21-25.
- [76] Bonnet, P., et al. **Transobturator vaginal tape inside out for the surgical treatment of female stress urinary incontinence: anatomical considerations.** *The Journal of Urology* (2006) 173: 1223-1228.
- [77] Prather, H., et al. **Review of Anatomy, Evaluation, and Treatment of Musculoskeletal Pelvic Floor Pain in Women.** *American Academy of Physical Medicine and Rehabilitation* (2009) 1: 346-358.
- [78] Petros, P. **The female pelvic floor: function, dysfunction and management according to the integral theory.** (2007) Springer.
- [79] Netter, M., et al. **Atlas Of Human Anatomy** (2006) 4th Edition - Elsevier.
- [80] Elneil, S., et al. **Complex pelvic floor failure and associated problems.** *Best Practice & Research Clinical Gastroenterology* (2009) 23: 555-573.
- [81] Davis, K., et al. **Pelvic floor dysfunction: a conceptual framework for collaborative patient-centred care.** *Journal of Advanced Nursing* (2003) 43: 555-568.
- [82] Persu, C., et al. **Pelvic Organ Prolapse Quantification System (POP-Q) - a new era in pelvic prolapse staging.** *Journal of Medicine and Life* (2011) 4: 75-81.
- [83] Chen, G-D., et al. **Updated Definition of Female Pelvic Organ Prolapse.** *Incont Pelvic Floor Dysfunct* (2007) 1: 121-124.

- [84] Bump, R., et al. **The standardization of terminology of female pelvic organ prolapse and pelvic floor dysfunction.** American Journal of Obstetrics & Gynecology (1995) 175: 10-17.
- [85] The Harvard Medical School. Family Health Guide <http://www.health.harvard.edu>
- [86] Kerkhof, M., et al. **Changes in connective tissue in patients with pelvic organ prolapse—a review of the current literature.** International Urogynecology Journal (2009) 20:461-474.
- [87] Hilton, P., et al. **Pathophysiology of urinary incontinence and pelvic organ prolapse.** International Journal of Obstetrics and Gynaecology (2004) 1: 115-119.
- [88] Gabriel, B., et al. **Uterosacral ligament in postmenopausal women with or without pelvic organ prolapse.** International Urogynecology Journal (2005) 16: 475-479.
- [89] Jackson, S., et al. **Changes in metabolism of collagen in genitourinary prolapse.** Lancet (1996) 347: 58-61.
- [90] Brubaker, L., et al. **Pelvic Organ Prolapse.** International Incontinence Society Committee. International Incontinence Society Committee 5 Chapter 5: 243-264.
- [91] Lukacz, E., et al. **Parity, Mode of Delivery, and Pelvic Floor Disorders.** Obstetrics & Gynecology (2006) 107: 1253-1260.
- [92] Kapoor, D., et al. **Pelvic Floor Dysfunction in Morbidly Obese Women: Pilot Study.** Obesity Research (2004) 12: 1104-1107.
- [93] Nygaard, I., et al. **Pelvic Organ Prolapse in Older Women: Prevalence and Risk Factors.** The American College of Obstetricians and Gynecologists (2004) 104: 489-497.
- [94] Mostwin, J., et al. **Pathophysiology of Urinary Incontinence, Fecal Incontinence and Pelvic Organ Prolapse.** International Incontinence Society Committee 4 Chapter 8: 423-484.
- [95] Samuelsson, E., et al. **Signs of genital prolapse in a Swedish population of women 20 to 59 years of age and possible related factors.** American Journal Obstetrics & Gynecology (1999) 180: 300-305.
- [96] Morrill, M., et al. **Seeking healthcare for pelvic floor disorders: a population-based study.** American Journal of Obstetrics & Gynecology (2007) 197: 1-6.
- [97] Wang, C-L., et al. **Impact of total vaginal mesh surgery for pelvic organ prolapse on female sexual function.** International Journal of Gynecology and Obstetrics (2011) 115: 167-170.
- [98] Ramirez, M., et al. **Obesity as a risk factor in surgery for urinary incontinence.** Ginecología y Obstetricia de Mexico (1997) 65: 58-60.
- [99] Reid, R., et al. **Repair of recurrent prolapse.** Best Practice & Research Clinical Obstetrics and Gynaecology (2011) 25: 175-196.
- [100] Myers, D., et al. **The Role of Urogynecology In Women's Pelvic Floor Disorders.** Medicine & Health/Rhode Island.
- [101] Moalli, P., et al. **Risk Factors Associated With Pelvic Floor Disorders in Women Undergoing Surgical Repair.** The American College of Obstetricians and Gynecologists (2003) 101: 869-874.
- [102] Huang, A., et al. **Urinary incontinence and pelvic floor dysfunction in Asian-American women.** American Journal of Obstetrics & Gynecology (2006) 195: 1331-1337.
- [103] McGuire, E., et al. **Pathophysiology of Stress Urinary Incontinence.** Reviews in Urology (2004) 6; 11-17.
- [104] Jorge, J., et al. **Etiology and Management of Fecal Incontinence.** Diseases of the Colon Rectum (1993) 36: 77-82.
- [105] Nelson, R., et al. **Epidemiology of Fecal Incontinence.** Gastroenterology (2004) 126: 3-7.

- [106] Rao, S., et al. **Pathophysiology of Adult Fecal Incontinence**. *Gastroenterology* (2004)126: 14-22.
- [107] Hunskaar, S., et al. **Epidemiology of Urinary (UI) and Faecal (FI) Incontinence and Pelvic Organ Prolapse (POP)**. *International Incontinence Society Committee 1 - Chapter 5*: 255-312.
- [108] Swift, S., et al. **Correlation of symptoms with degree of pelvic organ support in a general population of women: What is pelvic organ prolapse?** *American Journal of Obstetrics & Gynecology* (2003)189: 372-379.
- [109] Shah, A., et al. **Racial characteristics of women undergoing surgery for pelvic organ prolapse in the United States**. *American Journal of Obstetrics & Gynecology* (2007) 197: 70-78.
- [110] Pannu, H., et al. **Dynamic MR Imaging of Pelvic Organ Prolapse: Spectrum of Abnormalities**. *RadioGraphics* (2000) 20:1567-1582.
- [111] Chaliha, C., et al. **Management of vault prolapse**. *Reviews in Gynaecological Practice* (2005) 5: 89-94.
- [112] Dain, L., et al. **Urodynamic findings in women with pelvic organ prolapse and obstructive voiding symptoms**. *International Journal of Gynecology and Obstetrics* (2010) 111: 119-121.
- [113] Kuncharapu, I., et al. **Pelvic organ prolapse**. *American Family Physician* (2010) 81: 1111-1117.
- [114] Taylor, S., et al. **Imaging pelvic floor dysfunction**. *Best Practice & Research Clinical Gastroenterology* (2009) 23: 487-503.
- [115] Dietz, H., et al. **Pelvic floor ultrasound: a review**. *American Journal of Obstetrics & Gynecology* (2010) 230-334.
- [116] Barry ,C., et al. **The use of ultrasound in the evaluation of pelvic organ prolapse**. *Reviews in Gynaecological Practice* (2005) 5: 182-195.
- [117] Nilsson, C., et al. **Eleven years prospective follow-up of the tension-free vaginal tape procedure for treatment of stress urinary incontinence**. *The International Urogynecological Association* (2008) 19: 1043-1047.
- [118] Ulmsten, U., et al. **A Multicenter Study of Tension-Free Vaginal Tape (TVT) for Surgical Treatment of Stress Urinary Incontinence**. *International Urogynecology Journal* (1998) 9: 210-213.
- [119] Maher, C., et al. **Abdominal sacral colpopexy or vaginal sacrospinous colpopexy for vaginal vault prolapse: A prospective randomized study**. *American Journal of Obstetrics & Gynecology* (2004) 190: 20-26.
- [120] Dorsey, J., et al. **Laparoscopic sacral colpopexy and other procedures for prolapse**. *Baillikre' s Clinical Obstetrics and Gynaecology* (1995) 9: 749-756.
- [121] Shalom, D., et al. **Effect of prior hysterectomy on the anterior and posterior vaginal compartments of women presenting with pelvic organ prolapse**. *International Journal of Gynecology and Obstetrics* (2012) 119: 274-276.
- [122] Hogston, P., et al. **Is hysterectomy necessary for the treatment of utero-vaginal prolapse?** *Reviews in Gynaecological Practice* (2005) 5: 95-101.
- [123] Prodigalidad, L., et al. **Long-term results of prolapse recurrence and functional outcome after vaginal hysterectomy**. *International Journal of Gynecology and Obstetrics* (2013) 120: 57-60.
- [124] Reid, F, et al. **Uterine prolapse e preservation or excision?** *Obstetrics, Gynaecology and Reproductive Medicine* (2011) 21: 165-179.
- [125] Roovers, J-P., et al. **A randomised controlled trial comparing abdominal and vaginal prolapse surgery: effects on urogenital function**. *International Journal of Obstetrics and Gynaecology* (2004) 111: 50-56.

- [126] Barranger, E., et al. **Abdominal sacrohysteropexy in young women with uterovaginal prolapse: Long-term follow-up.** American Journal of Obstetrics & Gynecology (2003) 189:1245-1250.
- [127] Nygaard, I., et al. **Abdominal Sacrocolpopexy: A Comprehensive Review.** The American College of Obstetricians and Gynecologists (2004) 104: 805-823.
- [128] Blanchard, K. et al. **Recurrent Pelvic Floor Defects After Abdominal Sacral Colpopexy.** The Journal of Urology (2003) 175: 1010-1013.
- [129] Ganatra, A., et al. **The Current Status of Laparoscopic Sacrocolpopexy: A Review.** European Urology (2009) 55: 1089-1105.
- [130] Higgs, P., et al. **Long term review of laparoscopic sacrocolpopexy.** International Journal of Obstetrics and Gynaecology (2005) 112: 1134-1138.
- [131] Richter, K., et al. **Long-term results following fixation of the vagina on the sacrospinal ligament by the vaginal route (vaginaefixatio sacrospinalis vaginalis).** American Journal of Obstetrics & Gynecology (1981) 141: 811-816.
- [132] Benson, J., et al. **Vaginal versus abdominal reconstructive surgery for the treatment of pelvic support defects: A prospective randomized study with long-term outcome evaluation.** American Journal of Obstetrics & Gynecology (1996) 175: 1418-1422.
- [133] Jelovsek, J. E., et al. **Women seeking treatment for advanced pelvic organ prolapse have decreased body image and quality of life.** American Journal of Obstetrics & Gynecology (2006) 194: 55-61.
- [134] Amid, P., et al. **Classification of biomaterials and their related complication in abdominal wall surgery.** Hernia (1997) 1: 15-21.
- [135] Deffieux, X., et al. **Prevention of complications related to the use of prosthetic meshes in prolapse surgery: guidelines for clinical practice.** European Journal of Obstetrics & Gynecology and Reproductive Biology (2012).
- [136] Abed, H., et al. **Incidence and management of graft erosion, wound granulation, and dyspareunia following vaginal prolapse repair with graft materials: a systematic review.** International Urogynecology Journal (2011) 22: 789-798.
- [137] Bellon, J., et al. **Tissue response to polypropylene meshes used in the repair of abdominal wall defects.** Biomaterials (1998) 19: 669-675.
- [138] Lin, L., et al. **Dyspareunia and chronic pelvic pain after polypropylene mesh augmentation for transvaginal repair of anterior vaginal wall prolapse.** International Urogynecology Journal (2007) 18: 675-678.
- [139] Meschia, M., et al. **Porcine Skin Collagen Implants to Prevent Anterior Vaginal Wall Prolapse Recurrence: A Multicenter, Randomized Study.** The Journal of Urology (2007) 177: 192-195.
- [140] Dell, J., et al. **PelviSoft BioMesh augmentation of rectocele repair: the initial clinical experience in 35 patients.** International Urogynecology Journal (2005) 16: 44-47.
- [141] Rice, R., et al. **Comparison of Surgisis, AlloDerm, and Vicryl Woven Mesh Grafts for Abdominal Wall Defect Repair in an Animal Model.** Aesthetic Plastic Surgery (2010) 34: 290-296.
- [142] Pierce, L., et al. **Biomechanical properties of synthetic and biologic graft materials following long-term implantation in the rabbit abdomen and vagina.** American Journal of Obstetrics & Gynecology (2009) 200: 549-557.
- [143] Winters, J., et al. **InteXen tissue processing and laboratory study.** International Urogynecology Journal (2006) 17: 34-38.
- [144] Brown, S., et al. **Cadaveric versus autologous fascia lata for the pubovaginal sling: Surgical outcome and patient satisfaction.** American Urological Association (2000) 164: 1633-1637.

- [145] Dora, C., et al. **Time dependent variations in biomechanical properties of cadaveric fascia, porcine dermis, porcine small intestine submusosa, polypropylene mesh and autologous fascia in the rabbit model: implications for sling surgery.** American Urological Association (2004) 171: 1970-1973.
- [146] Groutz, A., et al. **Use of cadaveric solvent-dehydrated fascia lata for cystocele repair - Preliminary results.** Adult Urology (2001) 58: 179-183,
- [147] FitzGerald, M., et al. **Functional failure of fascia lata allografts.** American Journal of Obstetrics & Gynecology (1999) 181: 1339-1346.
- [148] Cervigni, M., et al. **Collagen-coated polypropylene mesh in vaginal prolapse surgery: an observational study.** European Journal of Obstetrics & Gynecology and Reproductive Biology (2011) 156: 223-227.
- [149] Tayrac, R., et al. **Prolapse repair by vaginal route using a new protected low-weight polypropylene mesh: 1-year functional and anatomical outcome in a prospective multicentre study.** International Urogynecology Journal (2007) 18: 251-256.
- [150] Tayrac, R., et al. **Collagen-coated vs noncoated low-weight polypropylene meshes in a sheep model for vaginal surgery. A pilot study.** International Urogynecology Journal (2007) 18: 513-520.
- [151] Hilger, W., et al. **Histological and biomechanical evaluation of implanted graft materials in a rabbit vaginal and abdominal model.** American Journal of Obstetrics & Gynecology (2006) 195: 1826-1831.
- [152] Huffaker, R., et al. **Histologic response of porcine collagen-coated and uncoated polypropylene grafts in a rabbit vagina model.** American Journal of Obstetrics & Gynecology (2008) 198: 582-589.
- [153] Leanza, V., et al. **Tension-free techniques in Urogynaecological Surgery.** Urogynaecologia International Journal (2005) 19: 5.45.
- [154] Rafii, A., et al. **Tension-Free Vaginal Tape and Associated Procedures: A Case Control Study.** European Urology (2004) 45: 356-361.
- [155] Takeyama, M. **Basic procedures in tension-free vaginal mesh operation for pelvic organ prolapse.** International Journal of Urology (2011) 18: 555-556.
- [156] ETHICON Women's Health & Urology. **GynCare Prolift - Pelvic Floor Repair Systems.** (2006).
- [157] Park, H-K., et al. **Initial Experience with Concomitant Prolift™ System and Tension-Free Vaginal Tape Procedures in Patients with Stress Urinary Incontinence and Cystocele.** International NonWovens Journal (2010) 14: 43-47.
- [158] Jacquetin, B. , et al. **Total transvaginal mesh (TVM) technique for treatment of pelvic organ prolapse: a 3-year prospective follow-up study.** International Urogynecology Journal (2010) 21: 1455-1462.
- [159] Ek, M., et al. **Clinical efficacy of a trocar-guided mesh kit for repairing lateral defects.** International Urogynecology Journal (2013) 24: 249-254.
- [160] Milani, A., et al. **Trocar-guided total tension-free vaginal mesh repair of post-hysterectomy vaginal vault prolapse.** International Urogynecology Journal (2009) 20: 1203-1211.
- [161] Nguyen, J., et al. **Outcome After Anterior Vaginal Prolapse Repair.** Obstetrics & Gynecology (2008) 111: 891-898.
- [162] Salomon, L., et al. **Treatment of Anterior Vaginal Wall Prolapse with Porcine Skin Collagen Implant by the Transobturator Route: Preliminary Results.** European Urology (2004) 45: 219-225.
- [163] Schwertner-Tiepelmann, N., et al. **Obstetric levator ani muscle injuries: current status.** Ultrasound Obstetrics Gynecology (2012) 39: 372-383.

- [164] Abramowitch, S., et al. **Tissue mechanics, animal models, and pelvic organ prolapse: A review.** European Journal of Obstetrics & Gynecology and Reproductive Biology (2009) 144: 146-158.
- [165] Ulmsten, U., et al. **Different biomechanical composition of connective tissue in continence in stress incontinence.** Acta Obstet Gynecol Scand (1987) 66: 455.
- [166] Facolner, C., et al. **Paraurethral Connective Tissue in Stress-Incontinence Women After Menopause.** Acta Obstet Gynecol Scand (1998) 77: 95-100.
- [167] Liapis, A., et al. **Changes of Collagen Type II In Female Patients With Genuine Stress Incontinence And Pelvic Floor Prolapse.** European Journal of Obstetrics & Gynecology and Reproductive Biology (2001) 97: 76-79.
- [168] DeLancey, J., et al. **Comparison of Levator Ani Muscle Defects and Function in Women With and Without Pelvic Organ Prolapse.** Obstetrics & Gynecology (2007) 109: 295-302.
- [169] Lei, L., et al. **Biomechanical properties of prolapsed vaginal tissue in pre- and postmenopausal women.** International Urogynecology Journal (2007) 18: 603-607.
- [170] Pandi, A. et al. **Design of surgical meshes - an engineering perspective.** Technology and Health Care(2004) 12: 51-65.
- [171] Chu, C., et al. **Characterization of morphologic and mechanical properties of surgical mesh fabrics.** Journal of Biomedical Materials Research (1985) 19:903-916.
- [172] Afonso, J., et al. **Mechanical properties of polypropylene mesh used in pelvic floor repair.** International Urogynecology Journal (2008) 19: 375-380.
- [173] Hollinsky, C., et al. **Biomechanical properties of lightweight versus heavyweight meshes for laparoscopic inguinal hernia repair and their impact on recurrence rates.** Surgical Endoscopy (2008) 22: 2679-2685.
- [174] Moalli, P., et al. **Tensile properties of five commonly used mid-urethral slings relative to the TVT™.** International Urogynecology Journal (2008) 19: 655-663.
- [175] Velayudhan, S., et al. **Evaluation of Dynamic Creep Properties of Surgical Mesh Prostheses—Uniaxial Fatigue.** Journal of Biomedical Materials Research (2009) Part B: Applied Biomaterials: 287-296.
- [176] Saberski, E., et al. **Anisotropic evaluation of synthetic surgical meshes.** Hernia (2011) 15: 47-52.
- [177] Shepherd, J., et al. **Uniaxial biomechanical properties of seven different vaginally implanted meshes for pelvic organ prolapse.** International Urogynecology Journal (2012) 23: 613-620.
- [178] Martins, J., et al. **A numerical model of passive and active behavior of skeletal.** Computer Methods in Applied Mechanics and Engineering (1998) 151: 419-433.
- [179] **Finite Elements:** <http://127.0.0.1:2080/v6.12/books/gsa/default.html>.
- [180] Rane, R., et al. **The sacrospinous ligament: Conveniently effective or effectively convenient?** Journal of Obstetrics and Gynaecology (2011) 31: 366-370.
- [181] Roshanvaran, S., et al. **Neovascular anatomy of the sacrospinous ligament region in female cadavers: Implications in sacrospinous ligament fixation.** American Journal of Obstetrics and Gynecology (2007) 197: 660.e1-660.e6.
- [182] Lazarou, G., et al. **Anatomic variations of the pelvic floor nerves adjacent to the sacrospinous ligament: a female cadaver study.** International Urogynecology Journal (2007) 19: 649-654.
- [183] Hartmann, S., et al. **Parameter estimation of hyperelasticity relations of generalized polynomial-type with constraint conditions.** International Journal of Solids and Structures (2001) 28: 7999-8018.
- [184] Ogden, R., **Large Deformation Isotropic Elasticity - On the Correlation of the Theory Experiment of Incompressible Rubberlike Solids.** Proceedings of the Royal Society Of London. Mathematical and Physical Sciences (1972) 326: 565-584.

- [185] Rivlin, R. et al. **Large Elastic Deformations of Isotropic Materials. Fundamental concepts.** Philosophical Transaction of the Royal Society of London Series A (1948) 240:459-490.